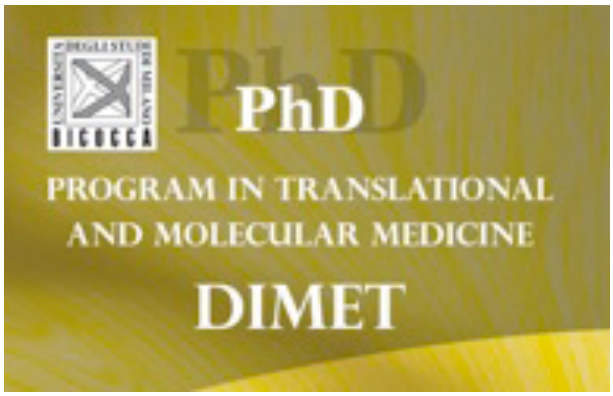

Characterization and comparison of muscle fibrosis in two mouse models and *In Vivo* test of an anti-fibrotic molecule

Coordinator: Prof. Andrea Biondi
Tutor: Dr. Renato Mantegazza
Co-Tutor: Dr. Marina Mora

Dr. Sara GIBERTINI
Matr. No. 775120

XXVIII CYCLE
ACADEMIC YEAR
2014-2015

Se sapessimo (esattamente)

quel che stiamo facendo,

non si chiamerebbe ricerca

ALBERT EINSTEIN

…AL MIO CIELO

Table of Contents:

Chapter 1:

GENERAL INTRODUCTION

Skeletal muscle

Muscle fibers are formed during myogenesis from the fusion of myoblasts, postmitotic, mononucleated cells. Myoblasts fuse into multinucleated (syncytial) cells, called myotubes. They have central nuclei and peripheral myofibrils. The muscle cells are termed myofibers when the myonuclei shift from the central to a sub-sarcolemmal position. The presence of central nuclei in normal adult muscle are usually indicative of muscle regeneration. (1)

The functional development of muscle includes the formation of basal lamina, innervation (neuromuscular junction) and anchorage to tendon. This process involves extra- and intracellular events that lead to fiber differentiation, distribution of integral membrane proteins and to correct anchoring of cytoskeletal proteins to the sarcolemma.

Myofibrils are the largest functional unit of muscle fiber. The principal components of myofibrils are actin (forming the thin filaments) and myosin (forming the thick filaments), together termed contractile proteins. In addition the regulatory proteins, troponin and tropomyosin, control interaction between the contractile proteins.

Altogether these proteins form filaments organized in repeated units called sarcomeres. Their interaction is responsible for muscle contraction.

The sarcomeres give to skeletal and cardiac muscles their striated appearance at electronic miscopy (EM).

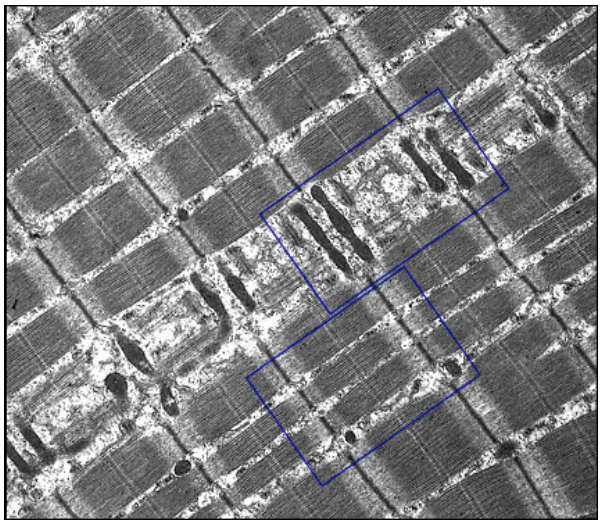

Fig. 1 Electron microscopy of a striated muscle section

Each sarcomere is bound by two Z-discs, the dark lines visible at EM mainly constituted by alpha-actinin, that anchor the actin thin filaments from adjacent units.

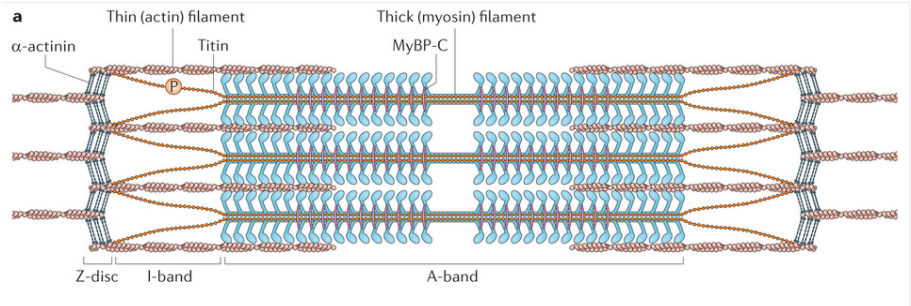

Fig. 2 Sarcomere's schematic representation

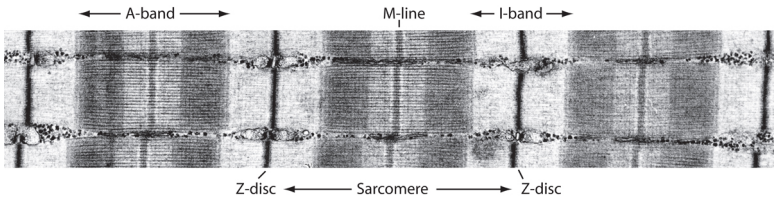

Fig. 3 Sarcomere's electron microscopy image

Thin filaments are contained in the I band, the zone where thin filaments are not superimposed by thick filaments, while in the A-band, the area that contains the entire length of a single thick filament, contains both thin and thick filaments.

Consecutive sarcomeres are also kept together across the Z-discs: the thin filaments are attached to the Z-disc on each end of the sarcomere, while the thick myosin filaments reside in the middle of the sarcomere. (2)

The muscle fiber contains the sarcoplasmic reticulum, that envelops the myofibrils and holds a reserve of the calcium ions required for muscle contraction. The calcium is stored into reservoirs called terminal cisternae, that run along the fiber.

In between two terminal cisternae are tubular invaginations named transverse tubules (T tubule). The T tubules are the pathways for action potentials to signal the sarcoplasmic reticulum to release calcium, causing the contraction of muscle. Together, two terminal cisternae and a transverse tubule form a triad. (3)

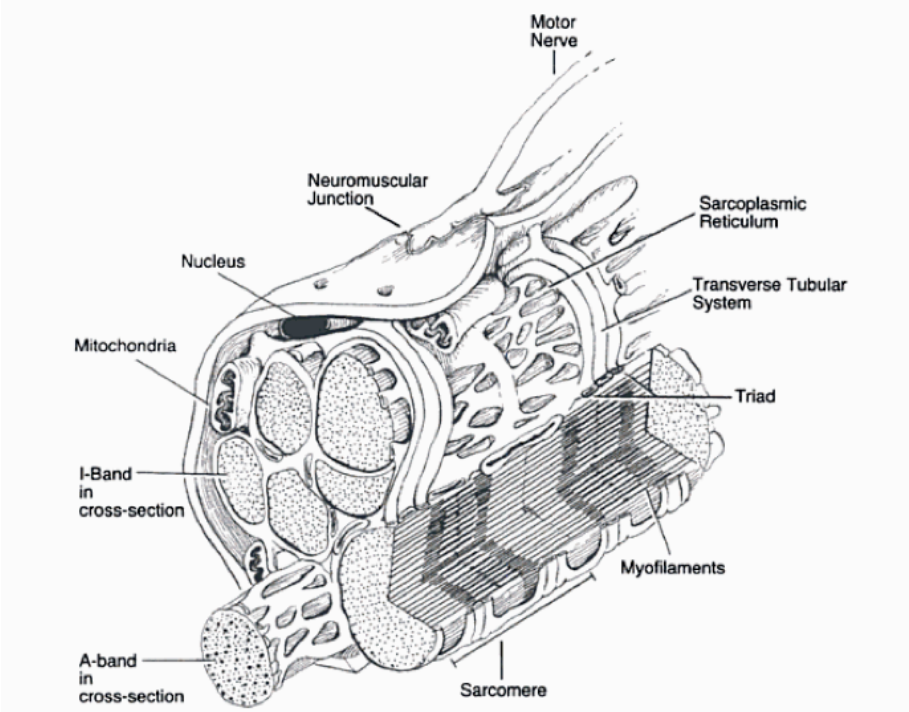

Fig. 4 A muscle cell' schematic representation
from Skeletal Muscle Structure, Function, and Plasticity (Richard L. Lieber)

Between the basal lamina and the sarcolemma there are the myosatellite cells, which are normally quiescent but can be activated by exercise or pathological conditions, to provide additional myonuclei for muscle growth or repair.

Dystrophin and Dystrophin-glycoprotein complex

The most important cytoskeletal protein is dystrophin, positioned at the inner surface of muscle fibers.

Dystrophin is a rod-shaped protein, constituted by 3685 amino acids with a molecular weight of 427 kDa. The dystrophin gene maps to chromosome X (Xp21.2).

Dystrophin can be divided into four domains:

- Actin binding domain (amino acids 14-240):
  domain probably responsible for cross-linking the dystrophin protein to the F-actin (a linear polymer microfilament composed of actin - filamentous actin) allowing the connection between filamentous elements and cell membrane.
- Central rod domain (amino acids 253-3040):
  a large central region composed of different spectrin-like repeats (R1–R24) interrupted by four proline-rich non-repeat segments called hinge regions (H1–H4). (Koenig and Kunkel 1990) (4)
- Cysteine-rich domain (amino acids 3080-3360):
  a cysteine-rich (CR) domain that binds β-dystroglycan.
- Carboxy-terminal domain (amino acids 3361-3685):

interacts with β-dystrobrevin and the syntrophins. This C-terminal domain consist of 324 amino acid residues. (5)

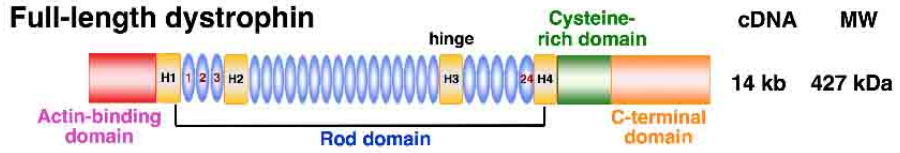

Fig. 5 Structure of full-length dystrophin
From: Progress and Challenges in AAV-Mediated Gene Therapy for Duchenne Muscular Dystrophy- (Takashi Okada)

The *DMD* gene produces different mRNA-transcripts encoding various dystrophin isoforms, differently expressed in various tissues. (i.e. Dystrophin protein full-length -Dp427- in brain, muscle, lymphoblastoid and Purkinje cells; shortest isoform Dp71 ubiquitous).

The different isoforms are generated by three strategies; (i) the use of different, unique and often tissue-specific promoters, (ii) alternative splicing, and (iii) the use of different polyA-addition signals.

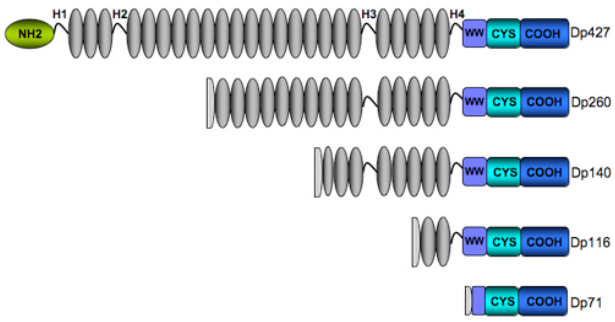

Fig. 6 Structure of dystrophin's isoforms

Dystrophin is associated with sarcolemmal proteins and glycoproteins, forming a large oligomeric complex, the dystrophin-glycoprotein complex (DGC).

The first to describe this complex and its proteins was the group of KP Campbell, who designated the components as dystrophin-associated proteins (DAPs) and dystrophin-associated glycoproteins (DAGs). (6)

They established that dystrophin is part of a large hetero-oligomeric complex, that forms a physical bridge between the cytoskeleton and the extracellular matrix. With this bridge dystrophin is able to protect membrane stability from mechanical stress caused by muscle contraction.

Because several constituents were glycosylated, this group was also named dystrophin-glycoprotein complex (DGC).

A key protein of the DGC is dystroglycan, (7, 8) encoded by *DAG1* and cleaved, by post-translational processing, into an extracellular α-dystroglycan protein and a transmembrane β-dystroglycan protein. Dystroglycan is also expressed in heart and smooth muscle, and in non-muscle tissues including brain and peripheral nerve. (9)

The β-dystroglycan binds intracellularly dystrophin, which in turn binds the actin cytoskeleton, and extracellularly is directly connected with α-dystroglycan. The link between cytoskeleton and basal lamina is completed by calcium-

dependent binding of α-dystroglycan to extracellular matrix proteins. (10, 11)

Dystroglycan undergoes a series of post-traslational glycosylations (*N*-linked and extensive *O*-linked) (8) which are fundamental for its function.

Glycosylation, one of the most common post-translational protein modification, is a process that leads to the addition of sugar chains to the proteins.

Glycosylation is important for controlling protein stability and conformation, for modulating interactions with other proteins, for differentiation and development.

Dystroglycan hypoglycosylation, in fact, causes complete loss of ligand binding activity, preventing the formation of the link between dystroglycan and extracellular matrix proteins, including laminin, neurexin, and agrin. (12)

Another sub-complex of the DGC is the sarcoglycan, which is composed of 5 known transmembrane sarcoglycan proteins (α, β, γ, δ, ε) and the sarcospan.

β- and δ- sarcoglycans are assembled first, followed by the inclusion of γ-sarcoglycan and α-sarcoglycan.

In the smooth muscle this complex includes the ε-sarcoglycan instead of α-sarcoglycan, while in the heart both types are present. (13)

The transmembrane localization of the complex is important for the proper preservation of DGC proteins in membrane.

α-SG. The human gene maps to chromosome 17 and encodes a protein of 387 amino acids (AAs). The native glycosylated molecule weight is about 50 kDa. It is only express in skeletal and cardiac muscle.

β-SG. The human gene maps to chromosome 4 and encodes a protein of 318 amino acids. The glycosylated protein weight is about 43 kDa. β-DG and β-SG directly bind to each other at their extracellular domains.

Mutations in the β-sarcoglycan gene result in the absence of the entire sarcoglycan-complex in the skeletal muscle membrane, suggesting that beta-sarcoglycan plays a critical role in the assembly and/or maintenance of the sarcoglycan complex. (14)

γ-SG. The human gene is located on chromosome 13. It is expressed only in skeletal and cardiac muscle and moderately in the lungs, skin, spinal cord, and olfactory bulb. The molecular mass of glycosylated γ-SG is 35 kDa.

δ-SG. The human gene is located on chromosome 5 and encodes a protein of 290 amino acids. The molecular mass of the native glycosylated δ-SG is about 35 kDa.

Protein	striated muscle (cardiac, skeletal)	smooth muscle	other tissues
SGCA	expressed	not expressed	not expressed
SGCB	selectively expressed	expressed (occurs post-nataly)	detectable
SGCG	expressed	not expressed	not expressed
SGCD	selectively expressed	expressed	detectable
SGCE	detectable (high in embryo)	expressed	widely expressed (early embryonic)
SGCZ			

Fig. 7 Sarcoglycans' expression in adult tissues

Sarcospan. The human gene maps to chromosome 12, encodes a major 6.5 kb transcript present exclusively in skeletal and cardiac muscle, and a 4.5 kb transcript in many other tissues. The presence of the sarcoglycan complex is required for its stability.

Sarcospan is tightly anchored in the lipid bilayer due to its multiple crossing of the sarcolemma thus aiding to keep in place the DGC. It is thought that these multiple transmembrane regions could form a pore in the sarcolemma, serving as a membrane channel as well.

The last peripheral cytoplasmic "subcomplex" is composed by syntrophins and dystrobrevins, which link to dystrophin at the sarcolemma.

A group of genes encodes for syntrophins, cytoplasmic phosphorylated adaptor proteins with a common domain structure. The complex is composed by five proteins; one alpha (alpha-1, acidic), two beta, (beta-1 and beta-2, basic) and two gamma (gamma-1 and gamma-2).

The alpha, beta1 and beta2 bind directly dystrophin, utrophin and α-dystrobrevin.

Two different genes encode for dystrobrevins α and β:

The human **alpha-dystrobrevin** gene is on chromosome 18, it undergoes many alternative splicing and poly-adenylation events in skeletal and cardiac muscle, but only the larger isoforms contain the syntrophin and dystrophin binding sites.

The human **beta-dystrobrevin** gene was identified thanks to its similarity to dystrobrevin alpha. (15)

The protein co-precipitates with the dystrophin isoforms Dp71 and Dp140.

In skeletal muscle, syntrophin isoforms have been shown to bind nNOS and voltage-gated sodium channels.

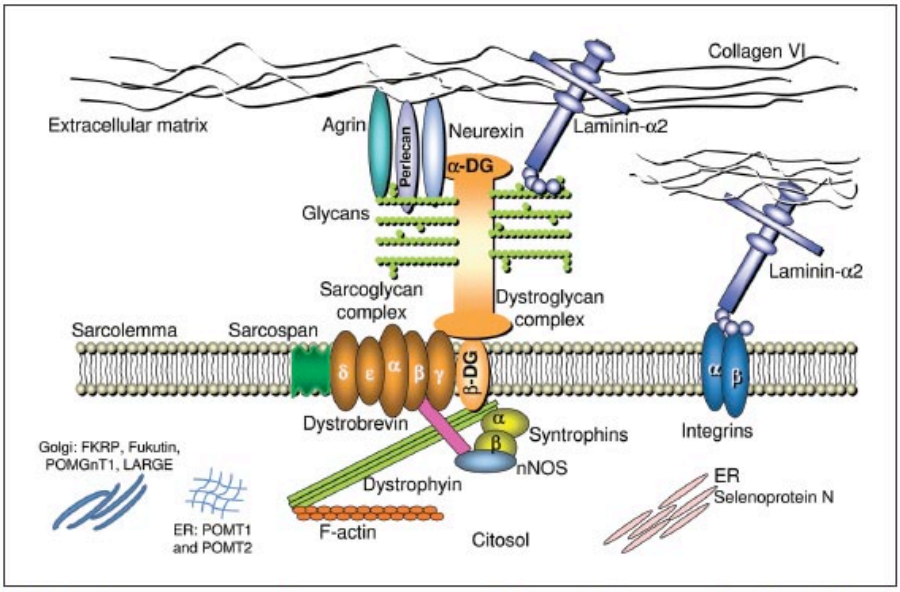

Fig. 8 Schematic representation of the main DGC's proteins
From Arq. Neuro-Psiquiatr. vol.67 no.2a São Paulo June 2009

The Extracellular Matrix

Like all the other cells, muscle fibers, are surrounded by an extracellular matrix (ECM), an amorphous tissue rich in carbohydrates and proteins, that constitutes the connective tissue of skeletal muscle.

The ECM is composed of different macromolecules including collagens, non collagenous glycoproteins, glycosaminoglycans (GAGs), and proteoglycans.

Skeletal muscle ECM is composed of two layers: the basal lamina, directly attached to the sarcolemma, and the interstitial matrix.

ECM provides mechanical support, organization and directional guidance for nerves, vessels, and also provides the overall anatomical organization of the muscle:

Thus to schematize the organization, three different compartiments of connective tissue can be observed:

endomysial (around the single fiber),

perimysial (around fiber bundles), and

epimysial (around the whole muscle)

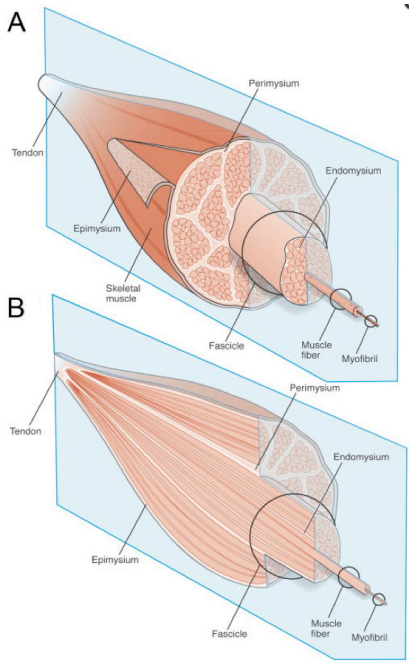

Fig. 9 Schematic organization of connective tissue in muscle

Collagens represent the most abundant ECM proteins, existing in about 26 different types in mammals. They are divided into subgroups:

fibrillar-forming (I, II, III, V, XI), representing the majority of collagens,

nonfibrillar-forming collagens (basement membrane collagen IV),

microfibrillar collagen (VI),

anchoring fibrils (VII),

hexagonal network-forming collagen (VIII, X),

fibril-associated collagens with interrupted triple helices (FACIT collagens) (IX, XII, XIV, XIX, XX, XXI) transmembrane collagens (XIII, XVII),
and multiplexins (XV, XVI, XVIII).

Despite the structural difference between various collagen types, all collagens have a right-handed triple helix, composed of three different α-chains. (16)

Fibroblasts, in skeletal muscle, are the major producers of collagen.

During biosynthesis, the collagen polypeptide chains go through extensive co- and post-translational modifications, which affect type and stability of collagen molecules. (17)

Procollagen molecules with their triple-helices (formed from polypeptide chains) are secreted into the extracellular space. After secretion the amino-terminal and carboxy-terminal extension peptides are cleaved by specific proteases. Thus the collagens self-assemble into fibrils or other supramolecular structures.

The same repeating amino acid sequences Gly-X-Y compose the α-chains.

Glycine residues prevent that two different triple α-chains would wrap to each other.

The position X- and Y- are mainly taken, respectively, by proline and 4-hydroxyproline residues. Those promote the formation of intermolecular cross-links. (18)

The various collagen types differ in their molecular organization: collagen type I is composed of a heterotrimer of two identical α1(I) chains and one α2(I) chain, collagen type III is a homotrimer of α1(III) chains. Type IV collagen exists in different form, the majority being composed of two α1(IV) chains and one α2(IV) chain. (19)

Table 1
Table showing the various collagen types as they belong to the major collagen families

Type	Molecular composition	Genes (genomic localization)	Tissue distribution
Fibril-forming collagens			
I	$[\alpha1(I)]_2\alpha2(I)$	COL1A1 (17q21.31–q22) COL1A2 (7q22.1)	bone, dermis, tendon, ligaments, cornea
II	$[\alpha1(II)]_3$	COL2A1 (12q13.11–q13.2)	cartilage, vitreous body, nucleus pulposus
III	$[\alpha1(III)]_3$	COL3A1 (2q31)	skin, vessel wall, reticular fibres of most tissues (lungs, liver, spleen, etc.)
V	α1(V),α2(V),α3(V)	COL5A1 (9q34.2–q34.3) COL5A2 (2q31) COL5A3 (19p13.2)	lung, cornea, bone, fetal membranes; together with type I collagen
XI	α1(XI)α2(XI)α3(XI)	COL11A1 (1p21) COL11A2 (6p21.3) COL11A3 = COL2A1	cartilage, vitreous body
Basement membrane collagens			
IV	$[\alpha1(IV)]_2\alpha2(IV)$; α1–α6	COL4A1 (13q34) COL4A2 (13q34) COL4A3 (2q36–q37) COL4A4 (2q36–q37) COL4A5 (Xq22.3) COL4A6 (Xp22.3)	basement membranes
Microfibrillar collagen			
VI	α1(VI),α2(VI),α3(VI)	COL6A1 (21q22.3) COL6A2 (21q22.3) COL6A3 (2q37)	widespread: dermis, cartilage, placenta, lungs, vessel wall, intervertebral disc
Anchoring fibrils			
VII	$[\alpha1(VII)]_3$	COL7A1 (3p21.3)	skin, dermal–epidermal junctions; oral mucosa, cervix,
Hexagonal network-forming collagens			
VIII	$[\alpha1(VIII)]_2\alpha2(VIII)$	COL8A1 (3q12–q13.1) COL8A2 (1p34.3–p32.3)	endothelial cells, Descemet's membrane
X	$[\alpha3(X)]_3$	COL10A1 (6q21–q22.3)	hypertrophic cartilage
FACIT collagens			
IX	α1(IX)α2(IX)α3(IX)	COL9A1 (6q13) COL9A2 (1p33–p32.2)	cartilage, vitreous humor, cornea
XII	$[\alpha1(XII)]_3$	COL12A1 (6q12–q13)	perichondrium, ligaments, tendon
XIV	$[\alpha1(XIV)]_3$	COL9A1 (8q23)	dermis, tendon, vessel wall, placenta, lungs, liver
XIX	$[\alpha1(XIX)]_3$	COL19A1 (6q12–q14)	human rhabdomyosarcoma
XX	$[\alpha1(XX)]_3$		corneal epithelium, embryonic skin, sternal cartilage, tendon
XXI	$[\alpha1(XXI)]_3$	COL21A1 (6p12.3–11.2)	blood vessel wall
Transmembrane collagens			
XIII	$[\alpha1(XIII)]_3$	COL13A1 (10q22)	epidermis, hair follicle, endomysium, intestine, chondrocytes, lungs, liver
XVII	$[\alpha1(XVII)]_3$	COL17A1 (10q24.3)	dermal–epidermal junctions
Multiplexins			
XV	$[\alpha1(XV)]_3$	COL15A1 (9q21–q22)	fibroblasts, smooth muscle cells, kidney, pancreas,
XVI	$[\alpha1(XVI)]_3$	COL16A1 (1p34)	fibroblasts, amnion, keratinocytes
XVIII	$[\alpha1(XVIII)]_3$	COL18A1 (21q22.3)	lungs, liver

Given are the molecular composition, the genomic localization of the different chains as well as the basic tissue distribution.

Fig. 10 Composition of collagens

Matrix metalloproteinases (MMPs) are a class of enzymes responsible for collagen and other ECM component degradation. MMPs are selectively inhibited by Tissue inhibitors of metalloproteinases (TIMPs), controlling local activities of MMPs in the tissues.

MMPs are finely regulated at transcriptional level to interact with specific ECM components.

In skeletal muscle the major fibrillar-forming collagens are types I, III and V (major constituent, with fibronectin and perlecan, of the interstitial matrix) while collagen type IV (major constituent of basement membrane together with laminin) is the most expressed type of one non fibrillar-forming collagen. (20, 21)

The collagen types are not uniformly expressed in the three different layers. This suggests a different role of each isoform in the composition of ECM.

In the epimysium and perimysium Type I and III collagens are present, type I is the most expressed in both layers, but in the endomysium of skeletal muscle all collagen types have been identified. (22, 23)

Furthermore the quantity of collagens in slow-twitch muscles is more than in fast-twitch muscles (24, 25), and in a study of rat skeletal muscle Kovanen and coworkers showed that in the endomysium, collagens are most aboundant around slow than around fast fibers. (26)

Other extracellular proteins, the laminins, are highly expressed in the basement membrane of most tissues and organs. By interacting with other extracellular matrix components they are involved in attachment, migration, and organization of cells during embryonic development.

Laminins are heterotrimeric proteins that contain an α-chain, a β-chain and a γ-chain, bound to each other by disulfide bonds. (27)

Each different chain is encoded by a different gene.

LAMA2 encodes the α–2 chain, one of the subunits of laminin-2 (also known as merosin) and laminin-4.

Laminin-2 and -4 are expressed in placenta, striated muscle and peripheral nerve. (28)

Mutations in the *LAMA2* gene are responsible for the congenital merosin-deficient muscular dystrophy MDC1A.

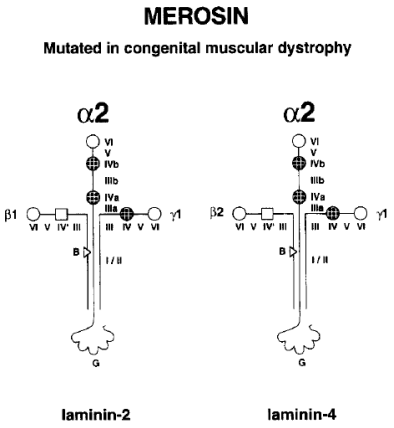

Fig.11 Merosin's schematic representation

Other important components of the ECM are

proteoglycans, present in all connective tissues including muscle. They also are present at the cell surface.

Proteoglycans exist in many different forms, many of whom are expressed in muscle ECM. Many of them belong to the small leucine-rich proteoglycan (SLRPs) family.

SLRPs are able to bind GAG chains, the majority of which are chondroitin sulphate and dermatan sulphate GAG chains. The most important SLRPs are biglycan and decorin. They are closely similar except that the first has two chondroitin or dermatan sulphate GAG chains, while the latter has only one chain. (29)

Biglycan and decorin have numerous functions including protein–protein interactions, cell adhesion, signal transduction, DNA repair and RNA processing (30, 31). Among the protein-protein interaction ability, of great importance is the binding to collagens and to transforming growth factor-β (TGF-β).

While in the past ECM was thought to exclusively have a structural role, more recently it has been shown to have multiple functions. Due to its very dynamic structure, it provides structural and biochemical support, and regulates cell behaviour via the interaction between ECM components with each other and with growth factors, and through cell-ECM mediated signal transduction pathways.

(32)

Moreover, by allowing to hold in place muscle stem cells and by constituting a scaffold for tissue structural integrity, ECM is able to strongly influence muscle function and its adaptive ability. (33)

Muscular Dystrophies

The muscular dystrophies are inherited disorders characterised by progressive muscle wasting and weakness, with a broad spectrum of symptoms and severity.

They can be subdivided into several groups depending on distribution of muscle involvement.

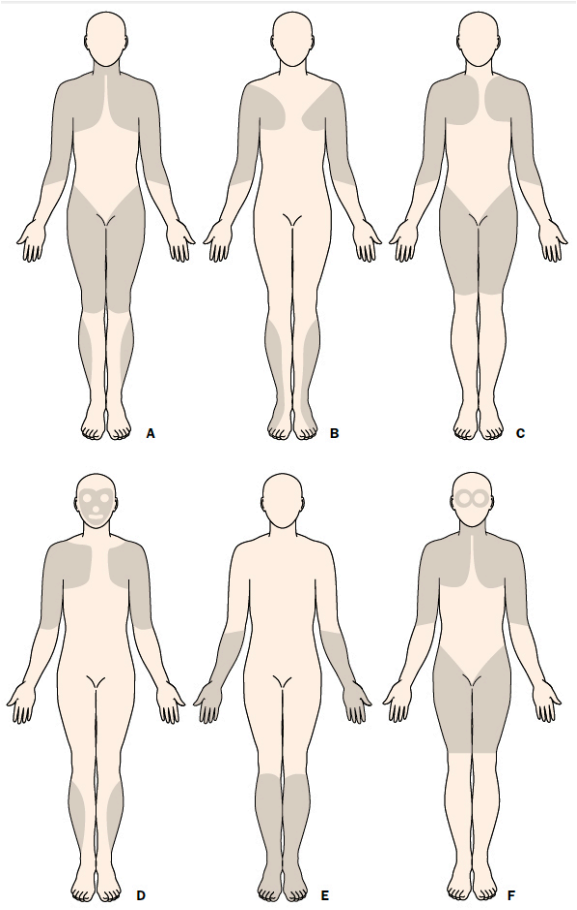

Figure 1: **Distribution of predominant muscle weakness in different types of dystrophy**
A, Duchenne-type and Becker-type; B, Emery-Dreifuss; C, limb-girdle; D, facioscapulohumeral; E, distal, F, oculopharyngeal. Shaded=affected areas. (Reproduced from *BMJ* 1998; **317:** 991–95 by permission of the BMJ Publishing Group).

Fig.12 Distribution of predominant muscle weakness in different types of dystrophy
Reproduced from *BMJ* 1998; 317: 991–95

Duchenne and Becker muscular dystrophy

Duchenne muscular dystrophy (DMD) is an X-linked genetic disease (OMIM#310200) with an incidence of about 1 in 3500 live male births. (34, 35)

DMD was described for the first time by Edward Meryon, an English doctor, in 1851 at the meeting of the Royal Medical and Chirurgical Society. (36) He presented a clinical description of this disorder, a familial progressive muscle wasting and weakness with onset in early childhood and death in late adolescence, that affected only boys.

Only a few years later, the disorder was named after a French doctor, Guillaume-Benjamin-Amand Duchenne, who described in detail the clinical and muscle histology. (37, 38)

DMD is caused by mutations in the dystrophin gene which generally lead to the complete absence of the protein. (39)

Although DMD phenotype is always severe, dystrophin mutations, like mutations in other dystrophin-associated protein complex components, result in variability of onset and progression of the disease, probably related to the degree of DGC complex disassembly and loss of the linkage between ECM and cytoskeleton.

In DMD patients blood creatine kinase levels are highly increased, and muscle biopsies show typical myopathic

changes with degeneration and regeneration of muscle fibers, hypercontracted fibers, nuclei centrally positioned, and, as end point of fiber loss, a progressive substitution of muscle by fibrotic and fatty tissue infiltration.

DMD patients exhibit symptoms in early childhood (around 3–5 years of age) with abnormal gait and difficulties in running and climbing stairs.

The patients need to use Gower's manoeuvre to get up from a sitting position. In addition they early show calf muscle pseudohypertrophy.

Patients are usually wheelchair bound by the age 10-12 years (35)

In the second decade most DMD patients show abnormal ECGs, due to variable severity of dilated cardiomyopathy, as well as respiratory complications. Cardiac and pulmonary involvements are the most frequent cause of death, which often happens in the second decade of life. (40)

Some DMD patients show variable signs of mental impairment.

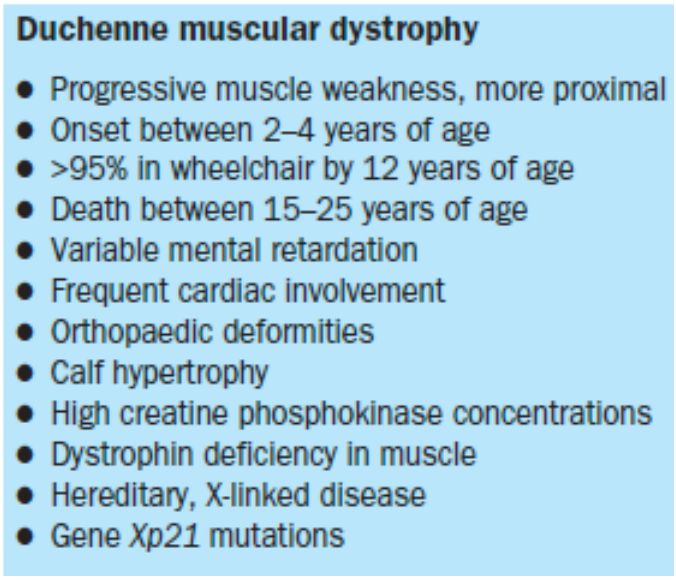

Fig. 13 main symptoms of DMD
from The dystrophy of Duchenne (Venita Jay, Jiri Vajsar)

Becker muscular dystrophy (BMD) (OMIM#300376) is a milder form of DMD. It is also caused by dystrophin gene mutations that lead to a reduced expression or shorter length of the dystrophin protein. (41, 42)

BMD patients show the same muscles involvement and weakness found in DMD but with a benign course of the disease. The age of onset is around 12 years (some patients have no symptoms until much later in life), and some patients show only cardiomyopathy and remain ambulant into their fifties or sixties. (43)

As in DMD, BMD patient could have some degree of mental impairment. In both Duchenne and Becker muscular dystrophies, a small fraction of female carriers, called manifesting carriers, show some degree of muscle

impairment, often asymmetric, with childhood or adulthood onset. (44, 45, 46)

Approximately 2/3 of DMD and BMD patients present large deletions or duplications, which occur in the 5' and central portion of the DMD gene. (47, 48)

However, the size and position of the deletion within the DMD gene does not correlate with the clinical phenotype. (49) Generally, if a deletion allows to maintain the expression of an internally truncated transcript witch leads to formation of a smaller, but functional dystrophin, the phenotype will be milder, like in BMD. Conversely if the deletion leads to a premature termination of translation, it will be often associated with exceptionally low levels or absence of dystrophin expression resulting in a DMD phenotype.

However, there are exceptions to this scheme and there are cases in which complete dystrophin deficiency may be associated with a relatively benign phenotype. (50)

The remaining 33% of DMD cases are caused by small deletions and point mutations that, in general, lead to premature stop codons (51, 52), these deletions and point mutations appear to be evenly distributed throughout the gene. (53, 54)

As mentioned before, there is no strong relationship between the mutation’s position and disease’s severity, but

in some cases, by looking at the localization of this mutations in the dystrophin domains, it is possible to identify the functional importance of the different domain.
For example, a missense mutation (Leu54Arg) at the N-terminal domain that leads to a DMD phenotype, highlights the importance of the actin-binding domain. It seems essential for dystrophin stability. (55)
Arahata et al. (1991), showed that generally the dystrophin C-terminal domain was preserved in BMD patients and was absent in DMD patients. (56)

Emery-Dreifuss muscular dystrophy

Emery-Dreifuss muscular dystrophy (EDMD) is X-linked or autosomal inherited disease.
The X-linked form of Emery-Dreifuss muscular dystrophy is caused by mutations of the *STA* gene at Xq28, which encodes the nuclear membrane protein emerin. (57)
Generally, in patients there is complete absence of emerin in muscle.
Autosomally inherited EDMD, usually with a dominant transmission, is caused by mutations in *LMNA* (gene locus 1q21), which encodes for lamins A and C (produced by alternative splicing), intermediate filament proteins associated with inner nuclear membrane. (58, 59)
This disorder is characterised by a triad of manifestations:

- An early contractures of the Achilles tendons, elbows, and posterior cervical muscles. The initial consequence is limitation of neck flexion, which gets worse limiting the flexion of the entire spine.
- A slowly progressive muscle wasting and weakness with a humeroperoneal distribution and later, involvement also of proximal limb-girdle musculature.
- A cardiomyopathy, often as conduction defects, ranging from sinus bradycardia, prolongation of PR interval, to complete heart block. Evidences of cardiac disease are usually present by age 30 years. The autosomal recessive form is often characterized by serious cardiac manifestations that could appear in the absence of any muscle weakness.

Initially it was thought that there could have been a relation between phenotypes and specific functional domains. (60) Further observations instead, showed that mutations in different portions of the gene lead to a great variety of clinical conditions, such as autosomal dominant or recessive EDMD, LGMD1B, dilated cardiomyopathy with conduction defects, Dunnigan-type partial lipodystrophy and Hutchinson-Gilford progeria syndrome. (61)

Congenital muscular dystrophies

Congenital muscular dystrophies (CMDs) are a heterogeneous group of autosomal recessively inherited disorders with early childhood onset. (62)

Due to the great heterogeneity there is no complete classification system; moreover, there is a large overlap of phenotypes, both between CMD subtypes and between CMDs, congenital myopathies, and limb-girdle muscular dystrophies. (63, 64)

Children present symptoms as hypotonia and muscles weakness already at birth or in the first few months of life. Several different forms exist, some of them with mental retardation. (65)

The main CMD subtypes, classified by the gene and the protein involved, are:

Laminin alpha-2 (merosin) deficiency (MDC1A),

Collagen VI-deficient CMD,

The dystroglycanopathies (caused by mutations in *POMT1, POMT2, FKTN, FKRP, LARGE, POMGNT1*, *ISPD* and the other glycosyltransferases)

SEPN1-related CMD,

LMNA-related CMD (L-CMD).

In a few patients less known CMD subtypes have been described.

The patients with dystroglycanopathies are characterized by different levels of cognitive impairment, from severe

intellectual deficit to mild cognitive delay, and by brain and eye abnormalities. (66)

MDC1A patients instead could have white matter abnormalities without major cognitive involvement.

Table 1. Classification of congenital muscular dystrophies. Adapted from Gene Table[54].

Disease phenotype (inheritance)	Gene symbol (chromosome) protein	All allelic disease phenotypes - disease symbols
Merosin deficient CMD – (AR)	LAMA2 (6q22–q23) laminin alpha 2 chain of merosin	Muscular dystrophy, congenital merosin-deficient - MDC1A Muscular dystrophy, congenital, due to partial LAMA2 deficiency
CMD with merosin deficiency – (AR)	? – (1q42)	Muscular dystrophy, congenital, 1B -MDC1B
CMD and abnormal glycosylation of dystroglycan – (AR)	FKRP (19q13.33) fukutin-related protein	Muscle-eye-brain disease -MEB Muscular dystrophy, congenital, 1C -MDC1C Muscular dystrophy, limb-girdle, type 2I -LGMD2I Walker-Warburg syndrome -WWS3
CMD and abnormal glycosylation of dystroglycan – (AR)	LARGE (22q12.3–q13.1) like-glycosyltransferase	Muscular dystrophy, congenital, with severe mental retardation -MDC1D
Fukuyama CMD – (AR)	FCMD (9q31–q33) fukutin	Muscular dystrophy, Fukuyama congenital -FCMD Muscular dystrophy, limb-girdle, type 2M -LGMD2M Walker-Warburg syndrome -WWS
Walker-Warburg syndrome – (AR)	FCMD (9q31–q33) fukutin	Muscular dystrophy, Fukuyama congenital -FCMD Muscular dystrophy, limb-girdle, type 2M -LGMD2M Walker-Warburg syndrome -WWS
Walker-Warburg syndrome – (AR)	POMT1 (9q34.1) protein-O-mannosyltransferase 1	Muscular dystrophy, limb-girdle, type 2K - LGMD2K Walker-Warburg syndrome -WWS
Walker-Warburg syndrome – (AR)	POMT2 (14q24.3) protein-O-mannosyltransferase 2	Muscle-eye-brain disease -MEB Walker-Warburg syndrome -WWS2
Walker-Warburg syndrome – (AR)	FKRP (19q13.33) fukutin-related protein	Muscle-eye-brain disease -MEB Muscular dystrophy, congenital, 1C -MDC1C Muscular dystrophy, limb-girdle, type 2I -LGMD2I Walker-Warburg syndrome -WWS3
Muscle-eye-brain disease – (AR)	POMGNT1 (1p34.1) O-linked mannose beta1,2-N-acetylglucosaminyltransferase	Muscle-eye-brain disease -MEB Walker-Warburg syndrome -WWS
Muscle-eye-brain disease – (AR)	FKRP (19q13.33) fukutin-related protein	Muscle-eye-brain disease -MEB Muscular dystrophy, congenital, 1C -MDC1C Muscular dystrophy, limb-girdle, type 2I -LGMD2I Walker-Warburg syndrome -WWS3
Muscle-eye-brain disease – (AR)	POMT2 (14q24.3) protein-O-mannosyltransferase 2	Muscle-eye-brain disease -MEB Walker-Warburg syndrome -WWS2
Rigid spine syndrome (RSS) – (AR)	SEPN1 (1p36.13) selenoprotein N1	Desmin-related myopathy with Mallory bodies -RSMD1 Minicore myopathy, severe classic form -RSMD1 Muscular dystrophy, rigid spine, 1 -MDRS1 Myopathy, congenital, with fiber-type disproportion -CFTD RSS
Ullrich syndrome – (AR)	COL6A1 (21q22.3) alpha 1 type VI collagen	Bethlem myopathy Ossification of the posterior longitudinal spinal ligaments -OPLL Ullrich congenital muscular dystrophy -UCMD
Ullrich syndrome – (AR)	COL6A2 (21q22.3) alpha 2 type VI collagen	Bethlem myopathy – Ullrich scleroatonic muscular dystrophy -UCMD
Ullrich syndrome – (AR)	COL6A3 (2q37) alpha 3 type VI collagen	Bethlem myopathy – Ullrich congenital muscular dystrophy -UCMD
Bethlem myopathy – (AD)	COL6A1 (21q22.3) alpha 1 type VI collagen	Bethlem myopathy Ossification of the posterior longitudinal spinal ligaments -OPLL – Ullrich congenital muscular dystrophy -UCMD
Bethlem myopathy – (AD)	COL6A3 (2q37) alpha 3 type VI collagen	Bethlem myopathy – Ullrich congenital muscular dystrophy -UCMD
Bethlem myopathy – (AD)	COL6A2 (21q22.3) alpha 2 type VI collagen	Bethlem myopathy Ullrich scleroatonic muscular dystrophy -UCMD -
CMD with integrin deficiency – (AR)	ITGA7 (12q13) integrin alpha 7 precursor	Myopathy, congenital -ITGA7

AD, autosomal dominant; AR, autosomal recessive; CMD, congenital muscular dystrophy.

Fig. 14 Classification of congenital muscular dystrophies
From Neuromusc Disord 2008;18:101-129.

Limb-girdle muscular dystrophies

Limb girdle muscular dystrophies (LGMDs) represent a heterogeneous group of muscular dystrophies characterized by progressive limb girdle weakness with autosomal dominant or recessive patterns of inheritance.

LGMDs are characterized by a great variability of clinical signs. The phenotype classically consists of proximal muscles weakness and by distal weakness that may occur later in the course or in severe cases.

Pathological features include muscle fiber necrosis and regeneration with proliferation of fibrotic and fatty tissue infiltration.

LGMD diagnosis could be difficult, due to the overlap with diseases such as congenital muscular dystrophies, myofibrillar myopathies, distal myopathies, metabolic myopathy, inflammatory myopathy, and neurogenic diseases.

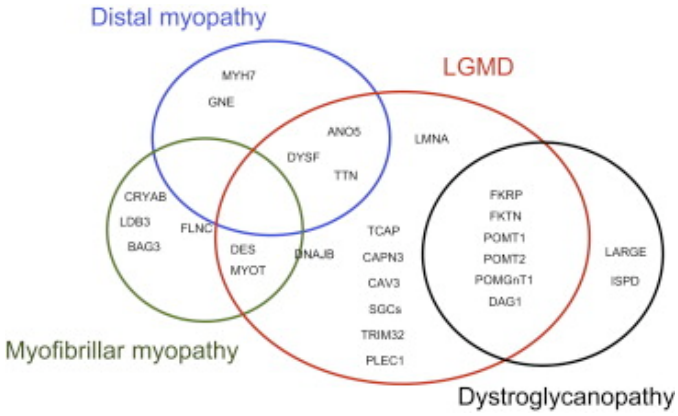

Fig.15 Overlap between LGMD and other myopathyes
from Update on the Genetics of Limb Girdle Muscular Dystrophy (Satomi Mitsuhashi)

Most LGMDs are autosomal recessive forms, while dominant types are rare and often less severe.

LGMD1 is the acronym indicating the autosomal-dominant forms, whereas LGMD2 indicates the autosomal-recessive forms.

More than 24 genes have been identified as causative of LGMDs and mutations in a single gene could cause numerous phenotypes and vice versa. (67)

The most common causative mutations found during the last two decades, are in the *CAPN3, DYSF, FKRP*, and the sarcoglycan (*SGCA, SGCB, SGCD*, and *SGCG*) genes.

Some of these forms are associated with significant cardiac involvement (i.e. types 1B, 1D, 2C, 2E, and 2F). (68)

Table I. LGMD classification.

Form	Locus	Gene	Proteinopathies	Key references
Autosomal dominant				
LGMD1A	5q31	*MYOTM*	Myotilinopathies	(9)
LGMD1B	1q11-q21	*LMNA*	Lamin A/C opathies	(10)
LGMD1C	3p25	*CAV3*	Caveolinopathies	(11)
LGMD1D	2q35	*DES*	Desminopathies	(12)
LGMD1E	7q36	*DNAJB6*	HSP40/DNAJ	(13,14)
LGMD1F	7q32.1-q32.2	-	-	(15)
LGMD1G	4p21	-	-	(16)
LGMD1H	3p23-p25	-	-	(17)
Autosomal recessive				
LGMD2A	15q15.1	*CAPN3*	Calpainopathy	(18)
LGMD2B	2p13	*DYSF*	Dysferlinopathies	(19)
LGMD2C[a]	13q12	*SGCG*	γ-sarcoglycanopathy	(20)
LGMD2D[a]	17q12-q21.33	*SGCA*	α-sarcoglycanopathy	(21)
LGMD2E[a]	4q12	*SGCB*	β-sarcoglycanopathy	(22)
LGMD2F[a]	5q33	*SGCD*	δ-sarcoglycanopathy	(23)
LGMD2G	17q12	*TCAP*	Telethoninopathy	(24)
LGMD2H	9q31-q34	*TRIM32*	E3-ubiquitin ligase	(25)
LGMD2I[b]	19q13	*FKRP*	Fukutin-related protein	(26)
LGMD2J	2q31	*TTN*	Titinopathies	(27)
LGMD2K[b]	9q34.1	*POMT1*	POMT1	(28)
LGMD2L	11p14.3	*ANO5*	Anoctaminopathies	(29)
LGMD2M[b]	9p3	*FKTN*	Fukutinopathies	(30)
LGMD2N[b]	14q10-q24	*POMT2*	POMT2	(31)
LGMD2O[b]	1p34-33	*POMGnT1*	POMGnT1	(32)
LGMD2P[b]	3p21	*DAG1*	Dystroglycan	(33,34)
LGMD2Q	8q24.3	*PLEC*	Plectinopathies	(35)

Nomenclature of LGMD1D/1E was according to OMIM. [a]Sarcoglycanopathies; [b]dystroglycanopathies. LGMD, limb-girdle muscular dystrophies.

Fig. 16 LGMD classification
from Limb-girdle muscular dystrophies: Where next after six decades from the first proposal (Review) (OMAR A. MAHMOOD)

Despite the specific muscles involved (limb girdles) the functions of the affected proteins are very variable.

There are structural proteins (i.e. dysferlin, caveolin 3 and anoctamin 5) with their role in muscle fibers preservation from repeated injury, proteins involved in fibers remodelling (i.e. calpain 3), proteins responsible for post-translational modifications (i.e. POMT1, POMT2, POMTGnT1) and proteins of unknown function.

With some exceptions, the majority of autosomal recessive LGMD forms have onset in adolescence and muscle weakness is progressive. An early childhood onset often indicates a sarcoglycanopathy or dystroglycanopathy.

Generally the majority of autosomal dominant LGMDs have onset after the second decade of life.

Fibrosis

Fibrosis is a pathological process that occurs during tissue healing and implies aberrant deposition of ECM components leading to loss of the tissue architecture and function.

It involves an imbalance of MMPs and their specific TIMPs, the release of fibrogenic cytokines, including transforming growth factor β1 (TGF-β1) (69), the alteration of proteoglycans such as decorin and biglycan (70) and the persistent production of growth factors, proteolytic enzymes and angiogenic factors. (71)

In acute inflammatory reactions, vascular changes, oedema and neutrophilic inflammation are rapidly resolved. Conversely, in chronic inflammation, inflammatory processes, tissue remodelling and repair occur simultaneously resulting in fibrosis.

The fibrotic process is often associated with chronic symptoms and occurs in a large variety of vital organs and tissues, including lung, liver, kidney and skeletal muscle. (72)

In severe muscular dystrophies, like DMD, the absence of dystrophin (or other DGC's components) leads to a reduction (or complete absence) of DGC itself in the

sarcolemma, causing the loss of its link with the cytoskeleton.

As consequence, muscle becomes unable to sustain mechanical stress and, with time, an increase in calcium permeability occurs. The consequent increased Ca++ concentration in the sarcoplasm activates proteases and dysregulates the general homeostasis of the muscle fibre leading to necrosis and degeneration. (73)

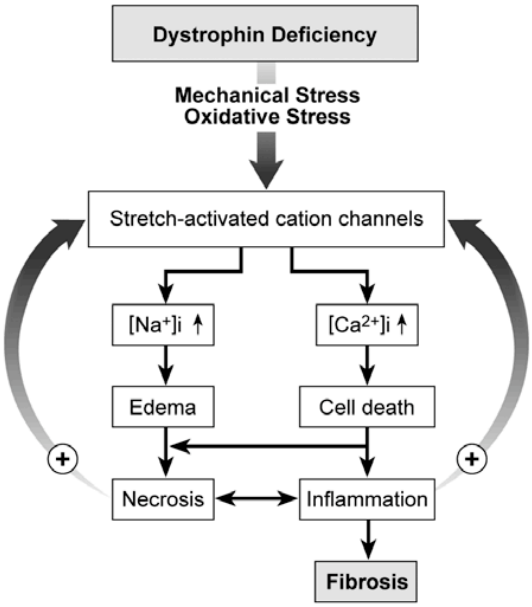

Fig.17 Effect of dystrophin deficiency
From The role of fibrosis in Duchenne muscular dystrophy (Werner Klingler)

Furthermore mononuclear cells and fibroblasts are recruited to phagocytise cellular debris and to deposit collagen and remodel tissue.

TGF-β1 is a key element in the fibrotic process. It is released from platelets and inflammatory cells at sites of injury, where it recruits and activates fibroblasts, inducing them to produce collagens and other ECM constituents and to stimulate connective tissue contraction.

The fibroblasts origin is still a matter of debate. It seems that they are differentiated from mesenchymal stem cells (74), or fibrocytes present in the blood circulation (75) or are originated from epithelia via epithelial-mesenchymal transition (EMT). (76)

In scarring-implied fibroblasts a myofibroblast phenotype is observed (fibroblast transactivation): they express α-smooth muscle actin (α-SMA), are characterized by enhanced contractility and by an increased of collagen type I and III secretion. (71)

In addition to protein production stimulation, TGF-β1 inhibits matrix degradation and controls adhesion proteins required for cell-matrix interactions. (77)

TGF-β1 expression has been found increased in fibrotic and inflammatory conditions in kidney, liver, and lung (78, 79, 80) and in DMD and LAMA2 muscles tissues. (81, 82)

In physiological conditions, after resolution of the injury and tissue repair, myofibroblasts are removed probably via apoptosis, and normal tissue function is restored.

Under pathological conditions however, chronic inflammatory stimulation and TGF-β1 aberrant expression involve a persistent activation of myofibroblasts that remain at the site of injury with excessive secretion of ECM proteins thus causing a severe impairment of the tissue function. (83)

Moreover, fibroblasts are likely to contribute to exacerbating the fibrotic process as they have intrinsic pro-fibrotic characteristics. To this regard, Zanotti and co-workers have shown that fibroblasts derived from muscles of DMD patients have a pro-fibrotic phenotype (as a consequence of their primary genetic defect) and resist to cell detachment apoptosis, are more adhesive and more prone to migrate than control fibroblasts. (84)

In normal muscle regeneration, inflammatory reactions induce the activation and proliferation of stem cells (satellite cells) that differentiate into myocytes and fuse to develop new myofibers with centralized nuclei, resulting in repair.

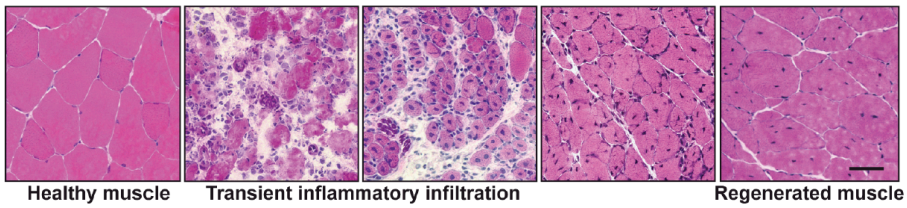

Fig. 18 Stages of muscle repair

In dystrophic muscles the abnormal repeated cycles of degeneration and regeneration cause a failure in the repair phase and the damaged fibers are not replaced by new fibers but by fat and connective tissue.

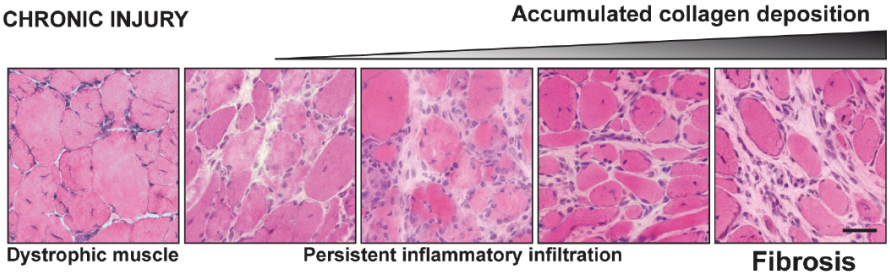

Fig. 19 Muscle repair under pathological conditions

Other important players of fibrotic process are neutrophils, macrophages and T cells that infiltrate the muscle before the establishment of fibrotic process.

In muscular dystrophies, signals released by degenerating myofibers recruit new monocytes that differentiate into different spectrum of mononuclear phagocytes to remove myofiber debris.

These pro-inflammatory cells, as mentioned above, secrete pro-inflammatory mediators such as TGF-β1, tumour necrosis factor (TNF), nitric oxide (NO) and IL-1.

In this process a fundamental role is also played by macrophages. They could be subdivided into M1 (classically activated macrophages) and M2.

M1 macrophages are involved in Th1 immune responses, are the first to invade injured muscles (following acute

injury) and are capable of damaging host tissue, lysing muscle cells with processes mediated by inducible nitric oxide synthase (iNOS). (85)

M2 macrophages instead, are involved in Th2 immune responses promoting tissue repair and arrive at site of injury later than M1. (86, 87)

They could be classified in M2a (activated by interleukin-4 (IL-4) and IL-13), M2b (activated by immune complexes or toll-like receptors) and M2c (activated by IL-10).

M1 could shift to M2 phenotype when iNOS levels decrease such as when IL-4 and IL-10 are released. (85)

Conversely TNF-α and IFN-γ, derived from both M1 macrophages and skeletal muscle cells, suppress the M1 transition to M2.

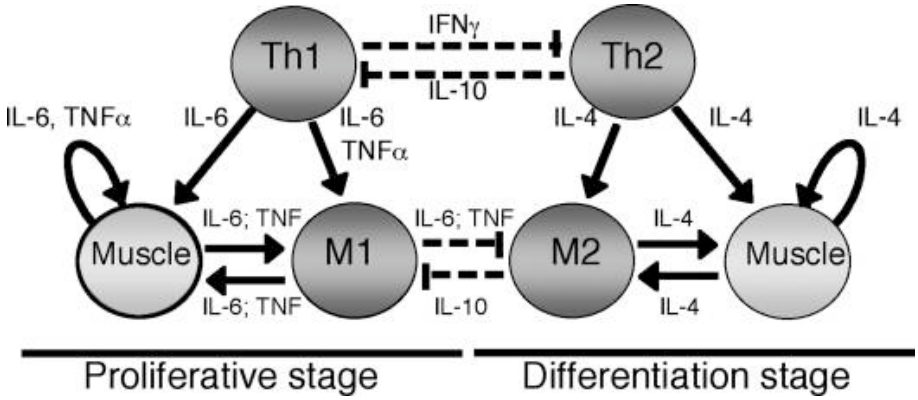

Fig. 20 Representation of transition between M1 and M2

Murine models for muscular dystrophies

In nature many animals exist having similar phenotypes to the one observed in human genetic diseases.
Moreover an increasing number of genetically engineered animal models for muscular dystrophy have been created.

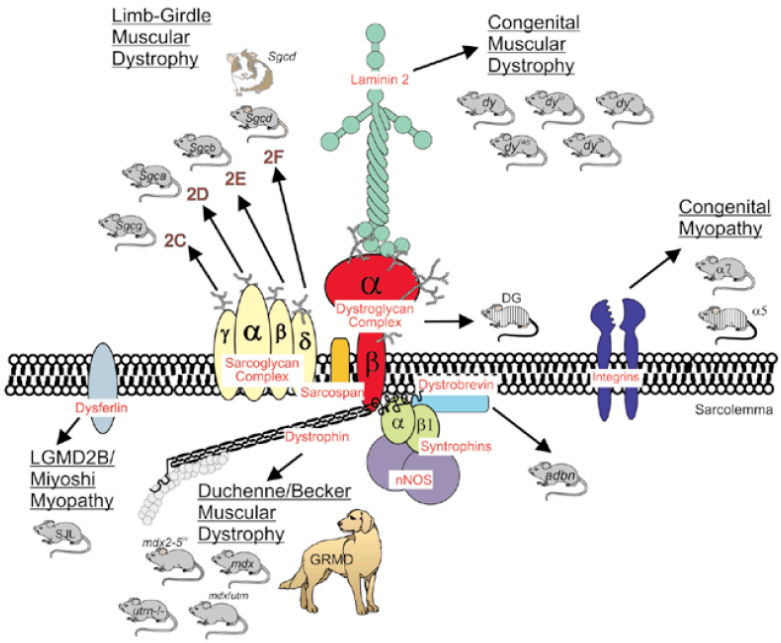

Fig. 21 Animal models of dystrophies

Dystrophin-deficient mice

The *mdx* mouse is the most used animal model for DMD. It is a spontaneous model discovered in the early 1980s in a colony of C57BL/10ScSn. It showed an elevated serum creatine kinase (CK) and histological evidences of myopathy. (88)

This model carries a nonsense point mutation (C-to-T transition) in exon 23 that prevents dystrophin expression. (89)

Mdx shows the same histopathological features found in DMD muscle, but has milder clinical symptoms, with mild weakness, modest fibrosis in limb muscles and a near-normal lifespan.

Between 3 to 6 weeks of age, skeletal muscles of this animal model undergo a strong phase of necrosis, followed by an extensive phase of regeneration with stem cell expansion and muscle hypertrophy.

Only the diaphragm muscle exhibits, from an early stage, the progressive muscle damage similar to that observed in human patients, with connective tissue proliferation and significant impairment of muscle function.

Severe dystrophic hallmarks, like muscle wasting, scoliosis and heart failure are only present in the late stages of life (up to after 15 months). (90)

In the last thirty years, several different genetic backgrounds have been used to generate *mdx* mice, showing a phenotypic exacerbation due to the different genetic strains.

The DBA/2-*mdx* mouse, for example, displaying greater fibrosis and less regeneration, could be a more representative model for human disease (91), while in

albino-*mdx* mice severe neurological dysfunction and higher circulating cytokines are present. (92)

In the late 80s, four chemical variant (cv) of *mdx* strains were created (93) on the C57BL/6 background using N-ethyl-N-nitrosourea (ENU). They carry different point mutation and are named as *mdx*2cv, *mdx*3cv, *mdx*4cv and *mdx*5cv.

Clinically they differ very little from *mdx*, but each line has unique features. For example, *mdx*3cv mice conserve a ~5% of full-length dystrophin protein expression (94) whereas *mdx*5cv mice have a more severe skeletal muscle phenotype. (95)

In addition, several new lines have been generated using various chemical or genetic engineering techniques on different genetic strains.

The mild clinical features of *mdx* could be due to compensatory mechanisms of utrophin (homologous protein over expressed on the sarcolemma of *mdx* muscles) or to species-specific properties of the muscle.

Eliminating compensatory mechanisms could generate mouse models that better resemble the dystrophic phenotype of DMD.

In utrophin/dystrophin and integrin/dystrophin double-knockout (dko) mice a very severe phenotype is observed but these animals are difficult to generate and handle, and

they often die prematurely. Zhou and coworkers suggest that utrophin heterozygous *mdx* mice are an intermediate model between the extreme dko mice and mildly affected *mdx* mice. (96)

Sarcoglycanopathy

As mentioned earlier, mutations in any of the (α -, β -, γ - and δ) -sarcoglycan genes cause distinct forms of muscular dystrophy: sarcoglycanopathies.

Mouse models of all sarcoglycanopathies have been obtained. (97)

All these models exhibit progressive muscular dystrophy of variable severity with different secondary reduction of the other members of the sarcoglycan–sarcospan and disruption of other components of the DGC. (98)

Sgca null mice lacking α-sarcoglycan, exclusively expressed in striated muscle, show as well a destabilization of α-dystroglycan in the sarcolemma, supporting the idea that sarcoglycan membrane expression is a prerequisite for proper targeting and stabilization of α-dystroglycan. This model does not show cardiomyopathy.

Sgcb null mice and *Sgcd* null mice, respectively deficient in β- and δ-sarcoglycan, both expressed in striated and smooth muscle, show focal areas of necrosis and fibrosis

in these compartments, and develop a severe progressive muscular dystrophy with cardiomyopathy. (97)

The loss of the entire sarcoglycan–sarcospan and dystroglycan complexes also affects the vascular smooth muscle leading to vascular irregularities that could aggravate skeletal pathology. (99)

Deficiency of β - and δ -sarcoglycan causes also the loss of the ε-sarcoglycan-containing complex in striated muscle. Like in skeletal muscle, absence of the sarcoglycan complex in smooth muscle produces membrane instability conferring to muscle cells increased susceptibility to ischemic damage.

Sgcg null mice, lacking γ-sarcoglycan, exhibit severe muscular dystrophy and cardiomyopathy. (100) This model presents β - and δ -sarcoglycan instability at the muscle membrane and reduction of α-sarcoglycan. On the other hand, it shows normal expression of dystroglycan and preservation of the link between the ECM and the cytoskeleton.

A signalling mechanism is likely to be responsible for γ-sarcoglycan-deficient muscular dystrophy; indeed the γ-sarcoglycan-deficient muscle shows normal resistance to mechanical strain (101)

Congenital muscular dystrophy (CMD) with deficiency in laminin α2 chain

A various number of spontaneous and experimental models of laminin α2 deficiency exist, including dy/dy, dy^{2J}/dy^{2J}, dy3K/dy3K, dyW/dyW, and dyPas/dyPas. The first two models were initially thought to be representative of DMD. They show, at about 3 weeks of age, progressive weakness and paralysis starting from hind limbs and suffer of a very severe form of muscular dystrophy.

In the dy/dy model death usually occurs before 6 months of age and mutant mice are usually sterile, while dy^{2J}/dy^{2J} have an almost normal life expectancy and may breed two or three times. In both models early increase in interstitial tissue and degenerative changes occur.

In the dy/dy mice laminin α2 is expressed in apparent normal size but with decreased amount (102) while in the dy^{2J}/dy^{2J} mutant a truncated form of the protein is expressed, despite the fact that this model exhibits a less severe dystrophy.

Dysferlinopathy

A spontaneous deletion in the dysferlin gene has been identified in SJL mice. This model exhibits a progressive muscular dystrophy affecting primarily proximal muscles,

thus making it a well representative model of LGMD2B and Miyoshi myopathy.

Other models

Dystroglycan deficiency in mice is embryonically lethal, but a chimeric mouse has been created which develops muscular dystrophy. Mouse models of integrin α7, and α-dystrobrevin deficiency also exist.

The spontaneous Large^{myd} mouse carries a mutation in the glycosyltransferase *LARGE* leading to altered glycosylation of α-DG and a severe phenotype with a progressive myopathy, abnormal posture, thoracic kyphosis, central nervous system defects, and reduced growth. (103)

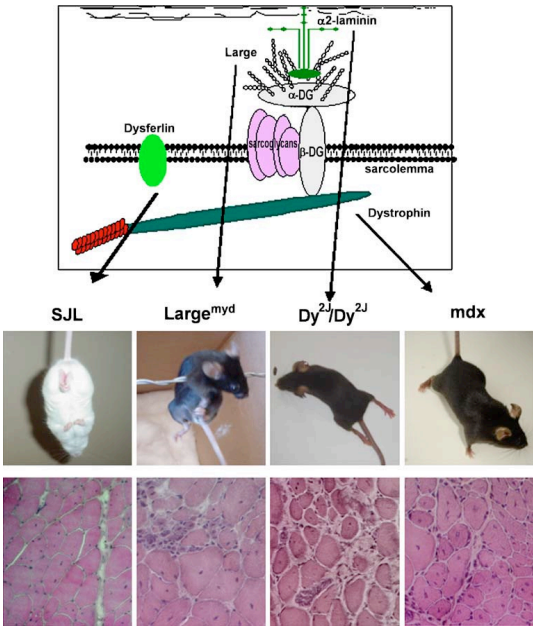

Fig. 22 Different histological features in dystrophy's animal models

MicroRNAs

MicroRNAs (miRNAs) are small non-coding RNAs which are post-transcriptional regulators of gene expression in plants and animals.

Up to now several hundred miRNAs have been characterized. It is known that each miRNA can act on several hundred mRNA targets and vice versa one single mRNA can be regulated by multiple microRNAs.

The first miRNA discovered was lin-4, identified through genetic studies in Caenorhabditis elegans. Lin-4 was thought to be a gene responsible for controlling the timing of larval development. This investigation revealed that lin-4 did not code for a protein but produced a pair of small RNAs. (104, 105)

Lin-4 is implicated in the negative control of the expression of the protein Lin-14. Wightman and cowokers demonstrated that the 3'-untranslated (3'UTR) region of lin-14 mRNA contained partially complementary sequence elements to lin-4, and that their interaction was necessary and sufficient for the post-transcriptional regulation.

Another important discovery was the observation that these small RNA molecules are highly conserved across species. (106)

Their implication in regulation of gene expression and in a large variety of biological processes including cell proliferation, differentiation, apoptosis, and development, improved the interest in these small molecules.

The main difference between miRNAs and the other classes of small RNAs is in their biogenesis. MiRNAs derive from transcripts that fold back on themselves to form distinctive hairpin structures.

Some miRNA genes form clusters and may be co-regulated with other members of the cluster. Most miRNA genes thou seem to be solitary, and are expressed under the control of their own promoters and regulatory sequences.

A minority of miRNAs lay their sequences in the intronic regions of their target genes. Being in the same orientation of the predicted mRNAs, they are process along with the intron, sharing regulatory elements and primary transcript with their pre-mRNA host genes. (107)

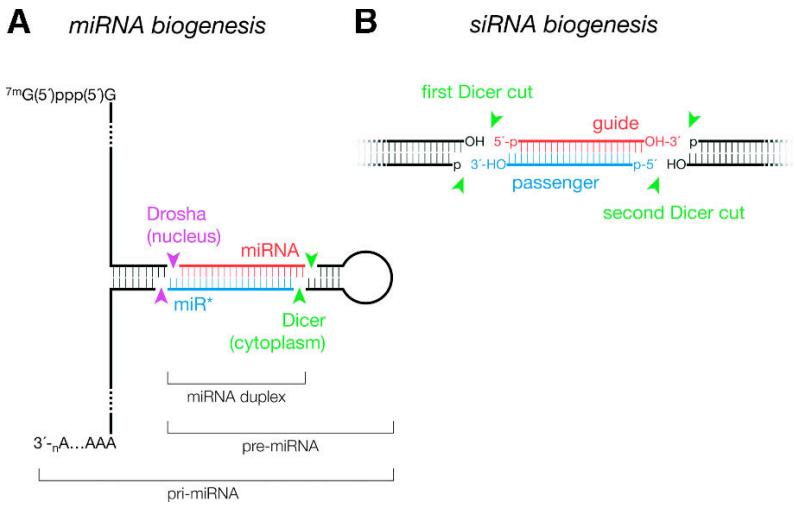

Fig. 23 miRNA biosynthesis from perspective: machines for RNAi

The biosynthesis of miRNAs is a multi-step process.

It is transcribed by RNA polymerase II resulting in a long (from several hundreds to several thousands nucleotides) capped and polyadenylated primary miRNA (pri-miRNA).

The pri-miRNA in the nucleus is then cleaved by ribonuclease (RNase) III Drosha-DGCR8 nuclear complex into a hairpin structure precursor miRNA (pre-miRNA) of about 60–100 nucleotides. It then binds exportin 5 to be exported into the cytoplasm and further cleaved by the RNase enzyme Dicer into double-stranded miRNA. (108, 109)

The two strands are then separated by helicases and the single strand miRNA (about 20-22 nucleotides) is subsequently incorporated into the RNA-induced silencing complex (RISC).

In plants, miRNAs and mRNA have almost perfect complementarity. The hybridization leads to an endonucleolytic cleavage of the mRNA by a mechanism similar to that occurring during RNA interference (RNAi).

In animals, however, miRNAs hybridizes imperfectly with mRNA 3'UTR region.

This imperfection (in the central portion of miRNA-mRNA duplexes) precludes RNAi-like cleavage but results in translational repression often leading to degradation of the mRNA. (110)

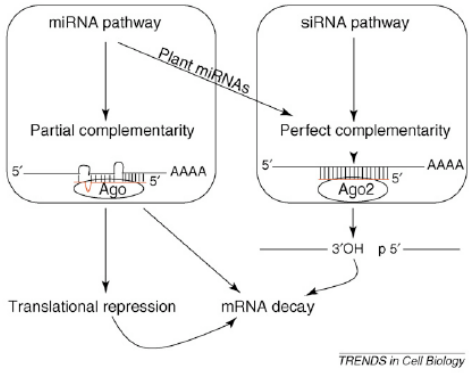

Fig. 24 miRNAs' mechanism of action

Classically miRNAs regulate gene expression by binding the 3'UTR of mRNA but recent evidences suggest that miRNAs can also bind different regions of DNA (promoter regions) or RNA (5′-UTR or coding regions).

Complementarity or pairing between 5' end of the miRNA (positions 2–7) and the mRNA targets, also known as the seed region match, is a crucial element for the regulation. (111) In addition sequences around miRNA-responsive

element contain specific features that could influence the effectiveness of silencing.

Until now very little is know about how miRNAs work.
Many studies sustain that miRNAs act by repressing the translating ribosomes (112) and that the interference intervenes after initiation (113) or before the accomplishment of the nascent polypeptide chain. (114)
It is hypothesised that miRNAs interfere during translation elongation by increasing termination efficiency. Other studies, in contrast, sustain that miRNAs degrade nascent polypeptide chain. (115) An agreement on the mechanism of action has yet to be found.
Further studies have demonstrated that miRNAs act on degradation of mRNA (116) by inducing deadenylation of target mRNAs followed by decapping (i.e. removal of the 5'-cap). (117)
Other miRNAs' mechanism of action have also been postulated, including mRNA sequestration.
More in depth studies are needed to clarify the mechanisms of action of miRNA.

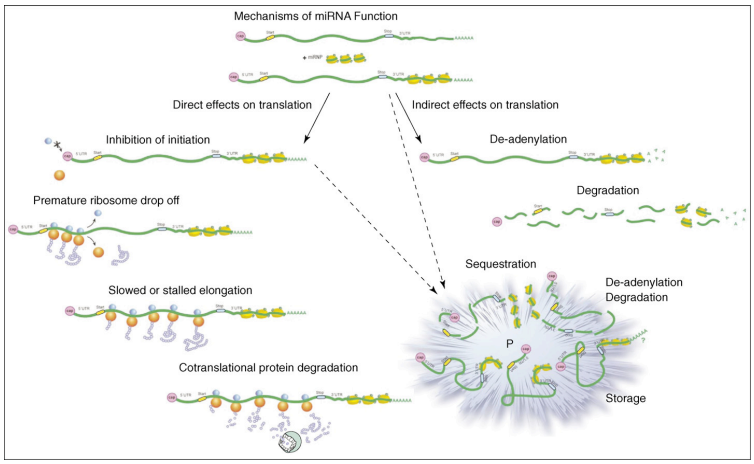

Fig. 25 Schematic representation of miRNAs' function

The role of miRNAs as negative regulators of gene expression has recently been flanked by the discovery that miRNAs could increase the translation of a target mRNA and consequently the protein level, interacting via protein complexes with the Au-rich elements of the mRNA. (118) Furthermore, Eiring and co-workers demonstrated that miRNAs could interfere with the function of regulatory proteins that block the target gene translation, indirectly inducing the protein increase. (119)

It is still unclear if these mechanisms of activation are just exceptions or normal events.

There is now evidence that miRNAs, in addition to regulate biological processes, are aberrantly expressed in multiple diseases as cancer, diabetes and heart failure.

Furthermore altered function of miRNAs might also be directly causative in human disease. (120)

This observation has made miRNAs attractive targets for therapeutic intervention.

To this regard, modulation of miRNA function could involve two strategies.

One is the induction of a gain-of-function using specific antagonists of miRNA which are oligonucleotides complementary to the endogenous miRNA, such anti-miRs, locked-nucleic acids (LNA) or antagomiRs. AntagomiRs, due to their chemical modification, which also protects them from nucleases degradation, have high affinity for the target miRNA, thus making the endogenous miRNA unable to be processed by RISC or, in alternative it is degraded.

AntagomiRs display increased bioavailability as well as greater stability and target affinity than all other used miRNA inhibitors and represent the most widely explored antagonists. (121)

The other strategy restores a loss-of-function with miRNA replacement using miRNA mimics. Generally mimic strategies require delivery vehicles (virus or non-virus delivery system) for delivery of double-stranded microRNA mimics.

In addition to the difficulty to deliver *in vivo* a double-stranded molecule, miRNA mimics could induce a non-specific interferon response. (122)

Treatment of Fibrosis

At the moment there is no effective cure for muscular dystrophies.

For DMD/BMD (as well for all other muscular dystrophies) many approaches are under evaluation such as gene replacement therapies, dystrophin-deficiency compensation and exon-skipping approach. However, at the moment, the adopted treatments, including corticosteroid administration, physical and speech therapy, orthopedic devices, surgery and medications, have the purpose to alleviate symptoms and prevent complications.

Table. Treatment Strategies for DMD/Becker MD

Strategy	Mechanism	Restores Dystrophin	Target Population	Status
Corticosteroids	Inhibition of muscle proteolysis	No	All patients with DMD	Off label, widespread use
Myostatin inhibition	Myostatin inhibition should augment muscle growth	No	All patients with DMD and other patients with muscle disease	Human clinical trials
Nitric oxide augmentation (Sildenafil, Tadalafil)	Phosphodiesterase inhibition reduces functional ischemia of muscle	No	All patients with DMD	Human clinical trials
Utrophin upregulation (SMT C1100)	Compensation of dystrophin deficiency by utrophin, a close homologue	No	All patients with DMD	Human clinical trials
Gene therapy (delivery of μ-dystrophin via AAV)	Viral vector-based delivery of dystrophin	Yes, truncated μ-dystrophin fits in AAV	All patients with DMD	Human clinical trials
Stem cell therapy	Cell-based delivery of dystrophin	Yes	All patients with DMD	Preclinical studies
ASO therapy (Eteplirsen, Drisapersen)	ASO-induced exon skipping restores reading frame of dystrophin	Yes, with certain exons missing	Currently approximately 13% of DMD population amenable to exon 51 skipping; other ASOs under development	Human clinical trials
Stop codon readthrough (Ataluren)	Biochemically induced readthrough of pathogenic stop codons	Yes	Approximately 13% of DMD population with nonsense mutations	Human clinical trials

Fig. 26 Treatment strategies for DMD/BMD

The research to find new treatments is carried out in independent laboratories with prevalent attention to four drug categories:

a) anti-inflammatory and immuno-modulators;

The inflammatory cascade represents an important target for drugs especially in early stages.

Corticosteroids (the main treatment in use) also exert an important anti-inflammatory and immunosuppressive effect.

The inhibition of TNFα activity, using for example neutralizing antibody infliximab (Remicade) (123) or a competitive inhibition of receptor-TNFα binding with etanercept (Enbrel) (124) is clinically effective to reduce symptoms of chronic inflammatory diseases. A worldwide discussion is open on the safety of these drugs due to their toxicity (enhanced risks of serious infections) and/or difficulty in finding proper doses in young patients.

Another anti-inflammatory strategy is the administration of classical non-steroidal anti-inflammatory drugs (NSAIDs), especially if combined with a nitric oxide (NO)-donating compound. (125)

Clinical trials in DMD boys with various anti-inflammatory compounds are under evaluation.

b) anti-oxidants;

High level or unbalanced production of reactive oxygen species (ROS) can damage tissues, including skeletal muscle.

N-acetyl-cysteine (NAC), a well-established anti-oxidant compound, contrasts abnormal calcium influx reducing membrane permeability. (126)

Other anti-oxidant compounds have been tested, like idebenone, (which has Coenzyme Q similar activity), green tea extracts (i.e. [-]-epigallocatechin gallate) and resveratrol. They show cardioprotective effects, improved voluntary wheel running performances and protective effects from necrosis in mice models of dystrophies. (127, 128, 129, 130)

c) anabolic compounds;

This class of compounds aims at increasing muscle mass and muscle strength.

Controversial results have been obtained, due to their capability to enlarge muscle fiber size, which could induce an increase in susceptibility to contraction-induced injury observed also with anabolic steroids (including testosterone and nandrolone). (131)

To this group also belongs the muscle specific β2-agonist Formeterol, which induces, together with anabolic action,

an enhancement of protein synthesis and decreased calpain activity without increasing susceptibility to contraction-induced injury. (132, 133, 134)
IGF-1 has been used with similar intent. A transgenic *mdx* mouse with specific over-expression of IGF-1 has shown a protective effect from necrosis. (135)
Another strategy involves interventions to contrast myostatin. The use of myostatin antibodies or follistatin (a natural antagonist of myostatin) has resulted in increase in muscle mass and size, with better muscle performance and reduction of muscle degeneration in *mdx* mice. (136, 137).

d) anti-fibrotic drugs;
Interfering with the fibrosis process could retard the loss of muscle function, postpone the onset of the need of wheelchair and other adverse consequences. Reducing pro-fibrotic cascade will induce muscle regeneration and increase muscle mass and strength.

TGF-β1, due to its central role in fibrotic process, is an important indisputable target for anti-fibrotic treatments.
Early blocking of TGF-β1 with a neutralizing antibody reduces drastically the level of tissue fibrosis, and treatment with antibody against all the three isoforms of

TGF-β markedly reduced hydroxyproline levels, that correlate to fibrosis and CK (plasma creatine kinase), improving respiratory function and grip strength in *mdx* mice. (138, 139)

Because of the critical role of TGF-β in immune system its chronic inhibition must be investigated to assess potential immunological consequence.

Another anti-fibrotic approach consists of using ACE inhibitors and the antagonists of type 1 receptor for angiotensin-II (AT1).

Losartan (AT1-antagonist) shows anti-fibrotic action reducing indirectly TGF-β1 activation in skeletal muscle. (140, 141)

Halofunginone shows promising results reducing collagen expression, improving respiratory, skeletal muscles and heart function. In addition Barzilai-Tutsch and co-workers demonstrated that halofuginone directly induce cell-cycle progression of satellite cells isolated from *mdx* and from dysf-/- mouse (model for dysferlinopathy) suggesting its effect on ameliorating the pathology, regardless of the mutation. (142)

It is postulated that Halofunginone works by inhibiting Smad 3 phosphorylation downstream of TGF-β1 with consequent reduction in fibroblasts differentiation,

reduction in the levels of ECM proteins and inhibition of fibrosis. (143)

Additional other molecules are under investigation as anti-fibrotic treatment, like Suramin, an anti-parasitic and antineoplastic drug approved by FDA.

Suramin is a TGF-β1 blocker, competitively binding its receptor thus leading to inhibition of muscle fibrosis and enhancement of muscle regeneration. (144)

Moreover, suramin induces inhibition of myostatin expression. (145)

Gamma interferon (γ-INF) is approved by the FDA for the treatment of hepatic fibrosis, and could be effective in muscle fibrosis as well. In fact it down regulates collagen expression and inhibits TGF-β1 signalling by up regulating smad7 expression in a muscle laceration model in mice. (146)

Decorin binds TGF-β1, interfering with its association to the receptor (147), and has anti-fibrotic effects in injured skeletal muscle improving muscle healing.

MMP treatment it is another approach aimed at reducing muscle fibrosis. MMPs regulate the degradation of collagens, therefore with a specific intervention on MMPs levels the collagens degradation could be enhanced.

Kaar and colleagues have shown that administration of recombinant human MMP-1 (metalloprotease which plays

a critical role in collagen I turnover) after muscle laceration reduces muscle fibrosis. (148)

In addiction, it has been demonstrated that osteoactivin-mediated increase in MMPs attenuates skeletal muscle fibrosis in osteoactivin-transgenic (OA-Tg) mice. (149)

It is evident that anti-fibrotic treatment in animal models induces the improvement of muscle function and ameliorates the phenotype, but in the majority of the reviewed studies, none of these treatments leads to complete muscle regeneration. A multifactorial approach is probably the optimal way to face this complex process.

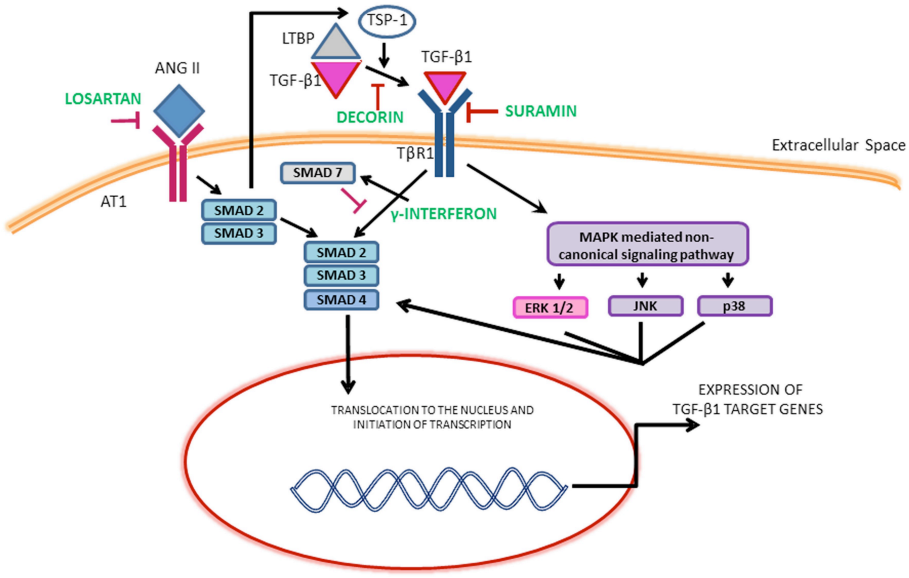

Fig. 27 Targets of anti-fibrotic drugs

Scope of the thesis

The focus of my PhD project has been to increase the understanding of pro-fibrotic mechanisms in dystrophic muscle by characterizing progression of muscle fibrosis and mechanisms leading to ECM protein deposition, in the *Sgcb-null* mouse model compared to the *mdx* model.

Moreover I have worked in assessing the anti-fibrotic effect of candidate molecules, selected on the basis of results of an in vitro study carried out in the laboratory.

Fibrosis is a pathological process, not completely understood, characterized by extensive deposition of collagens and other extracellular matrix (ECM) components that progressively replace functional tissues. Tissue fibrosis is a hallmark of severe muscular dystrophies, but is not exclusively of DMD and chronic myopathies, characterizing diseases of various tissues, including lung, liver, kidney, heart, skin and bladder.

The *mdx* mouse, lacking dystrophin, is the most used animal model for DMD, nevertheless the *mdx* mouse has milder clinical features than DMD patients, only diaphragm muscle exhibits progressive damage – similar to that observed in patients.

Mouse models of other muscular dystrophies have been obtained, and the *Sgcb-null* mouse, in particular, is knocked down for the β-sarcoglycan gene.

This model exhibits severe muscular dystrophy, cardiomyopathy, and vascular abnormalities.

In the first paper (chapter 2) we have characterized the progression of fibrosis in the *Sgcb-null* mouse, showing that this model develops severe and progressive fibrosis of limb muscles at early stage, and that fibrosis is greater than in the *mdx* model. Furthermore, early involvement of quadriceps is the main feature distinguishing the *Sgcb-null* model from *mdx*, rendering it more suitable for the investigation of the fibrotic process and the evaluation of anti-fibrotic drugs.

Many anti-fibrotic treatments have been proposed, but at the moment none of them is widely used for DMD patients.

Recent data indicate major involvement of microRNAs (miRNAs) in regulating pro- and anti-fibrotic genes. MiRNAs are small non-coding RNA molecules found in plants and animals, whose main function seems to be to downregulate gene expression by various mechanisms.

Modulation of their activity could be a very interesting anti-fibrotic approach.

In particular in an *in vitro* study we found an increase of miR-21 and a decrease of miR-29 in DMD muscles,

fibroblasts and myoblasts, with corresponding profibrotic alterations in target transcript and protein expression.

In the second paper (chapter 3) we have performed a pilot experiment on *mdx* mice, based on the results obtained *in vitro.*

We have treated a small group of mdx mice with antagomiR-21 and with scramble (negative control) for 4 weeks.

Our results suggested that antagomiR-21 treatment effectively reduces not only the levels of target transcripts but also the extent of fibrosis indicating that miR-21 inhibition is promising as treatment for contrasting muscle fibrosis.

REFERENCES:

1. Andrew Engel, Betty Q. Banker - Myology: Basic and Clinical, Volume 2 - Ed.McGraw-Hill - 1986

2. Hwang PM, Sykes BD - Targeting the sarcomere to correct muscle function - Nat Rev Drug Discov - 2015

3. Richard L. Lieber - Skeletal Muscle Structure, Function, and Plasticity - Ed. Lippincott Williams & Wilkins - 2002

4. Koenig M and Kunkel LM - Detailed analysis of the repeat domain of dystrophin reveals four potential hinge segments that may confer flexibility - J Biol Chem - 1990

5. Suzuki A, Yoshida M, Ozawa E - Mammalian alpha1- and beta1-syntrophin bind to the alternative splice-prone region of the dystrophin COOH terminus - J Cell Biol – 1995

6. Ervasti JM, Ohlendieck K, Kahl SD, Gaver MG, Campbell KP – Deficiency of a glycoprotein component of the dystrophin complex in dystrophic muscle - Nature - 1990

7. Ervasti JM, Campbell KP - Membrane organization of the dystrophin-glycoprotein complex - Cell - 1991

8. Ibraghimov-Beskrovnaya O, Ervasti JM, Leveille CJ, Slaughter CA, Sernett SW, Campbell KP - Primary structure of dystrophin-associated glycoproteins linking dystrophin to the extracellular matrix - Nature – 1992

9. Sparks S, Quijano-Roy S, Harper A, et al. - Congenital Muscular Dystrophy Overview - Ed. GeneReviews - 2001 [Updated 2012]

10. Michele DE and Campbell KP - Dystrophin-glycoprotein complex: post-translational processing and dystroglycan function - J Biol Chem - 2003

11. Jung D, Yang B, Meyer J, Chamberlain JS, Campbell KP - Identification and characterization of the dystrophin anchoring site on beta-dystroglycan - J Biol Chem - 1995

12. Michele DE, Barresi R, Kanagawa M, Saito F, Cohn RD, Satz JS, Dollar J, Nishino I, Kelley RI, Somer H, Straub V, Mathews KD, Moore SA, Campbell KP - Post-translational disruption of dystroglycan-ligand interactions in congenital muscular dystrophies - Nature – 2002

13. Allikian MJ, McNally EM - Processing and assembly of the dystrophin glycoprotein complex - Traffic - 2007

14. Bönnemann CG, Passos-Bueno MR, McNally EM, Vainzof M, de Sá Moreira E, Marie SK, Pavanello RC, Noguchi S, Ozawa E, Zatz M, Kunkel LM - Genomic screening for beta-sarcoglycan gene mutations: missense mutations may cause severe limb-girdle muscular dystrophy type 2E (LGMD 2E) - Hum Mol Genet - 1996

15. Peters MF, O'Brien KF, Sadoulet-Puccio HM, Kunkel LM, Adams ME, Froehner SC - Beta-dystrobrevin, a new member of the dystrophin family. Identification, cloning, and protein associations - J Biol Chem – 1997

16. Kuhn K - The collagen family-variations in the molecular and supermolecular structure - Rheumatology - 1986

17. Kivirikko KI, Myllyla R - Post-Translational Processing of Procollagens. Ann N Y Acad Sci - 1985

18. Vuorio E and de Crombrugghe B - The family of collagen genes - Annu Rev Biochem - 1990

19. Takala TE, Virtanen P - Biochemical composition of muscle extracellular matrix: the effect of loading - Scand J Med Sci Sports - 2000

20. Duance VC, Restall DJ, Beard H, Bourne FJ, Bailey AJ - The location of three collagen types in skeletal muscle - FEBS Lett - 1977

21. Bailey AJ, Shellswell GB, Duance VC - Identification and change of collagen types in differentiating myoblasts and developing chick muscle - Nature - 1979

22. Foidart M, Foidart JM, Engel WK - Collagen Localization in Normal and Fibrotic Human Skeletal Muscle –Arch Neurol - 1981

23. Light N, Champion AE - Characterization of muscle epimysium, perimysium and endomysium collagens - Biochem J - 1984

24. Garcia-Bunuel L, Garcia-Bunuel VM - Connective tissue and the pentose phosphate pathway in denervated muscle - Nature - 1967

25. Kovanen V, Suominen H, Heikkinen E - Connective tissue of ‘‘fast’’ and ‘‘slow’’ skeletal muscle in rats, effects of endurance training - Acta Physiol Scand - 1980

26. Kovanen V, Suominen H, Heikkinen E - Collagen in slow twitch and fast twitch muscle fibres in different types of rat skeletal muscle - Eur J Appl Physiol - 1984

27. Engvall E, Wewer UM - Domains of laminin - J Cell Biochem. - 1996

28. Leivo I, Engvall E - Merosin, a protein specific for basement membranes of Schwann cells, striated muscle, and trophoblast, is expressed late in nerve and muscle development - Proc Natl Acad Sci USA - 1988

29. Krusius T, Ruoslahti E - Primary structure of an extracellular matrix proteoglycan core protein deduced from cloned cDNA -

Proc Natl Acad Sci USA - 1986

30. Vogel KG, Paulsson M, Heinegård D - Specific inhibition of type I and type II collagen fibrillogenesis by the small proteoglycan of tendon - Biochem J - 1984

31. Kobe B, Deisenhofer J - The leucine-rich repeat: a versatile binding motif - Trends Biochem Sci - 1994

32. Velleman SG - The Role of the Extracellular Matrix in Skeletal Muscle Development - Poultry Science - 1999

33. Velleman SG, Shin J, Li X, Song Y - Review: The skeletal muscle extracellular matrix: Possible roles in the regulation of muscle development and growth - Can J Anim Sci - 2011

34. Emery AEH - Population frequencies of inherited neuromuscular diseases-a world survey - Neuromusc Dis - 1991

35. Emery AEH - Duchenne muscular dystrophy-Meryon's disease - Neuromuscul Disord - 1993

36. Meryon E - On fatty degeneration of the voluntary muscles: report of the Royal Medical and Chirurgical Society - Lancet - 1851

37. Duchenne GBA - Case 68: Paraplégie cérébrale, congénitale, hypertrophique - L'Électrisation localisée et de son application a la pathologie et a la thérapeutique, 2nd ed. Paris: J-B Baillière et Fils

38. Duchenne GBA - Recherches sur la paralysie musculaire pseudohypertrophique ou paralysie myo-sclérosique - Archives Générales Médecine - 1868

39. Koenig M, Hoffman EP, Bertelson CJ, Monaco AP, Feener C, Kunkel LM - Complete cloning of the Duchenne muscular dystrophy (DMD) cDNA and preliminary genomic organization

of the DMD gene in normal and affected individuals - Cell - 1987

40. Emery AEH, Muntoni F - Duchenne muscular dystrophy - Hum Gen - 2004

41. Becker PE, Kiener F - Eine neue x-chromosomale Muskeldystrophie - Archiv für Psychiatrie und Nervenkrankheiten - 1955

42. Becker PE - Two new families of benign sex-linked recessive muscular dystrophy - Rev Can Biol - 1962

43. Yazaki M, Yoshida K, Nakamura A, Koyama J, Nanba T, Ohori N, Ikeda S. - Clinical characteristics of aged Becker muscular dystrophy patients with onset after 30 years - Eur Neurol - 1999

44. Viggiano E, Picillo E, Cirillo A, Politano L - Comparison of X-chromosome inactivation in Duchenne muscle/myocardium-manifesting carriers, non-manifesting carriers and related daughters - Clin Genet - 2013

45. Bushby KM, Goodship JA, Nicholson LV, Johnson MA, Haggerty ID, Gardner-Medwin D - Variability in clinical, genetic and protein abnormalities in manifesting carriers of Duchenne and Becker muscular dystrophy - Neuromuscul Disord - 1993

46. Mirabella M, Servidei S, Manfredi G, Ricci E, Frustaci A, Bertini E, Rana M, Tonali P - Cardiomyopathy may be the only clinical manifestation in female carriers of Duchenne muscular dystrophy - Neurology - 1993

47. Koenig M, Beggs AH, Moyer M, Scherpf S, Heindrich K, Bettecken T, Meng G, Müller CR, Lindlöf M, Kaariainen H, de la Chapelle A, Kiuru A, Savontaus ML, Gilgenkrantz H, Récan D, Chelly J, Kaplan JC, Covone AE, Archidiacono N, Romeo G, Liechti-Gallati S, Schneider V, Braga S, Moser H, Darras BT, Murphy P, Francke U, Chen JD, Morgan G, Denton M, Greenberg CR, Wrogemann K, Blonden LAJ, van Paassen

HMB, van Ommen GJB, and Kunkel LM - The molecular basis for Duchenne versus Becker muscular dystrophy: correlation of severity with type of deletion - Am J Hum Gen - 1989

48. Monaco AP, Bertelson CJ, Middlesworth W, Colletti CA, Aldridge J, Fischbeck KH, Bartlett R, Pericak-Vance MA, Roses AD, Kunkel LM - Detection of deletions spanning the Duchenne muscular dystrophy locus using a tightly linked DNA segment - Nature - 1985

49. Monaco AP, Bertelson CJ, Liechti-Gallati S, Moser H, Kunkel LM - An explanation for the phenotypic differences between patients bearing partial deletions of the DMD locus - Genomics - 1988

50. Hattori N, Kaido M, Nishigaki T, Inui K, Fujimura H, Nishimura T, Naka T, Hazama T - Undetectable dystrophin can still result in a relatively benign phenotype of dystrophinopathy - Neuromuscul Disord - 1999

51. Lenk U, Hanke R, Thiele H, Speer A - Point mutations at the carboxy terminus of the human dystrophin gene: implications for an association with mental retardation in DMD patients - Hum Mol Genet - 1993

52. Roberts RG, Gardner RJ, Bobrow M - Searching for the 1 in 2,400,000: a review of dystrophin gene point mutations - Hum Mutat - 1994

53. Gardner RJ, Bobrow M, Roberts RG - The identification of point mutations in Duchenne muscular dystrophy patients by using reverse-transcription PCR and the protein truncation test - Am J Hum Genet - 1995

54. Prior TW, Bartolo C, Pearl DK, Papp AC, Snyder PJ, Sedra MS, Burghes AH, Mendell JR - Spectrum of small mutations in the dystrophin coding region - Am J Hum Genet - 1995

55. Prior TW, Papp AC, Snyder PJ, Burghes AH, Bartolo C, Sedra

MS, Western LM, Mendell JR - A missense mutation in the dystrophin gene in a Duchenne muscular dystrophy patient - Nat Genet - 1993

56. Arahata K, Beggs AH, Honda H, Ito S, Ishiura S, Tsukahara T, Ishiguro T, Eguchi C, Orimo S, Arikawa E, et al. - Preservation of the C-terminus of dystrophin molecule in the skeletal muscle from Becker muscular dystrophy - J Neurol Sci - 1991

57. Bione S, Maestrini E, Rivella S, Mancini M, Regis S, Romeo G, Toniolo D - Identification of a novel X-linked gene responsible for Emery-Dreifuss muscular dystrophy - Nat Genet - 1994

58. Bonne G, Di Barletta MR, Varnous S, Bécane HM, Hammouda EH, Merlini L, Muntoni F, Greenberg CR, Gary F, Urtizberea JA, Duboc D, Fardeau M, Toniolo D, Schwartz K - Mutations in the gene encoding lamin A/C cause autosomal dominant Emery-Dreifuss muscular dystrophy - Nat Genet - 1999

59. Raffaele Di Barletta M, Ricci E, Galluzzi G, Tonali P, Mora M, Morandi L, Romorini A, Voit T, Orstavik KH, Merlini L, Trevisan C, Biancalana V, Housmanowa-Petrusewicz I, Bione S, Ricotti R, Schwartz K, Bonne G, Toniolo D - Different mutations in the LMNA gene cause autosomal dominant and autosomal recessive Emery-Dreifuss muscular dystrophy - Am J Hum Genet - 2000

60. Fatkin D, MacRae C, Sasaki T, Wolff MR, Porcu M, Frenneaux M, Atherton J, Vidaillet HJ Jr, Spudich S, De Girolami U, Seidman JG, Seidman C, Muntoni F, Müehle G, Johnson W, McDonough B - Missense mutations in the rod domain of the lamin A/C gene as causes of dilated cardiomyopathy and conduction-system disease - N Engl J Med - 1999

61. Morris GE - The role of the nuclear envelope in Emery-Dreifuss muscular dystrophy - Trends Mol Med. 2001

62. Bönnemann CG - Congenital muscular dystrophy - ed. Encyclopedia of Neuroscience. Vol 3. Oxford, UK: Oxford

Academic Press; 2009

63. Kirschner J, Bönnemann CG - The congenital and limb-girdle muscular dystrophies: sharpening the focus, blurring the boundaries - Arch Neurol - 2004

64. Bönnemann CG, Wang CH, Quijano-Roy S, Deconinck N, Bertini E, Ferreiro A, Muntoni F, Sewry C, Béroud C, Mathews KD, Moore SA, Bellini J, Rutkowski A, North KN, et al. - Diagnostic approach to the congenital muscular dystrophies - Neuromuscul Disord - 2014

65. Muntoni F, Voit T - The congenital muscular dystrophies in 2004: a century of exciting progress - Neuromuscul Disord - 2004

66. Messina S, Tortorella G, Concolino D, Spanò M, D'Amico A, Bruno C, Santorelli FM, Mercuri E, Bertini E - Congenital muscular dystrophy with defective alpha-dystroglycan, cerebellar hypoplasia, and epilepsy - Neurology - 2009

67. Mahmood OA, Jiang XM - Limb-girdle muscular dystrophies: where next after six decades from the first proposal (Review) - Mol Med Rep - 2014

68. Hermans MC, Pinto YM, Merkies IS, de Die-Smulders CE, Crijns HJ, Faber CG - Hereditary muscular dystrophies and the heart - Neuromuscul Disord - 2010

69. Mauviel A - Transforming growth factor-beta: a key mediator of fibrosis - Methods Mol Med - 2005

70. Westergren-Thorsson G, Hernnäs J, Särnstrand B, Oldberg A, Heinegård D, Malmström A - Altered expression of small proteoglycans, collagen, and transforming growth factor-beta 1 in developing bleomycin-induced pulmonary fibrosis in rats - J Clin Invest - 1993

71. Wynn TA - Common and unique mechanisms regulate fibrosis

in various fibroproliferative diseases - J Clin Invest - 2007

72. Wynn TA - Cellular and molecular mechanisms of fibrosis - J Pathol - 2008

73. Zhou L, Lu H - Targeting fibrosis in Duchenne muscular dystrophy - J Neuropathol Exp Neurol - 2010

74. Li C, Kong Y, Wang H, Wang S, Yu H, Liu X, Yang L, Jiang X, Li L, Li L - Homing of bone marrow mesenchymal stem cells mediated by sphingosine 1-phosphate contributes to liver fibrosis - J Hepatol - 2009

75. Zavadil J, Bottinger EP - TGF-beta and epithelial-to-mesenchymal transitions - Oncogene - 2005

76. Guarino M, Tosoni A, Nebuloni M - Direct contribution of epithelium to organ fibrosis: epithelial-mesenchymal transition - Hum Pathol - 2009

77. Montesano R, Orci L - Transforming growth factor beta stimulates collagen-matrix contraction by fibroblasts: implications for wound healing - Proc Natl Acad Sci USA - 1988

78. Border WA and Ruoslahti E - Transforming growth factor-beta in disease: the dark side of tissue repair - J Clin Invest - 1992

79. Iredale JP - Models of liver fibrosis: exploring the dynamic nature of inflammation and repair in a solid organ - J Clin Invest - 2007

80. Sime PJ, Xing Z, Graham FL, Csaky KG, Gauldie J - Adenovector-mediated gene transfer of active transforming growth factor-beta1 induces prolonged severe fibrosis in rat lun - J Clin Invest - 1997

81. Bernasconi P, Torchiana E, Confalonieri P, Brugnoni R, Barresi R, Mora M, Cornelio F, Morandi L, Mantegazza R - Expression of transforming growth factor-beta 1 in dystrophic patient

muscles correlates with fibrosis - pathogenetic role of a fibrogenic cytokine - J Clin Invest - 1995

82. Zanotti S, Negri T, Cappelletti C, Bernasconi P, Canioni E, Di Blasi C, Pegoraro E, Angelini C, Ciscato P, Prelle A, Mantegazza R, Morandi L, Mora M - Decorin and biglycan expression is differentially altered in several muscular dystrophies - Brain - 2005

83. Desmoulière A, Chaponnier C, Gabbiani G - Tissue repair, contraction, and the myofibroblast - Wound Repair Regen - 2005

84. Zanotti S, Gibertini S, Bragato C, Mantegazza R, Morandi L, Mora M - Fibroblasts from the muscles of Duchenne muscular dystrophy patients are resistant to cell detachment apoptosis - Exp Cell Res - 2011

85. Villalta SA, Nguyen HX, Deng B, Gotoh T, Tidball JG - Shifts in macrophage phenotypes and macrophage competition for arginine metabolism affect the severity of muscle pathology in muscular dystrophy - Hum Mol Genet - 2009

86. Gordon S - Alternative activation of macrophages - Nat Rev Immunol - 2003

87. Tidball TG, Villalta A - Regulatory interactions between muscle and the immune system during muscle regeneration -Am J Physiol Regul Integr Comp Physiol - 2010

88. Bulfield G, Siller WG, Wight PA, Moore KJ - X chromosome-linked muscular dystrophy (*mdx*) in the mouse - Proc Natl Acad Sci USA - 1984

89. Sicinski P, Geng Y, Ryder-Cook AS, Barnard EA, Darlison MG, Barnard PJ - The molecular basis of muscular dystrophy in the *mdx* mouse: a point mutation - Science - 1989

90. Lefaucheur JP, Pastoret C, Sebille A - Phenotype of

dystrophinopathy in old *mdx* mice - Anat Rec -1995

91. Fukada S, Morikawa D, Yamamoto Y, Yoshida T, Sumie N, Yamaguchi M, Ito T, Miyagoe-Suzuki Y, Takeda S, Tsujikawa K, Yamamoto H - Genetic background affects properties of satellite cells and *mdx* phenotypes - Am J Pathol - 2010

92. Stenina MA, Krivov LI, Voevodin DA, Yarygin VN - Phenotypic differences between *mdx* black mice and *mdx* albino mice. Comparison of cytokine levels in the blood - Bull Exp Biol Med - 2013

93. Chapman VM, Miller DR, Armstrong D, Caskey CT - Recovery of induced mutations for X chromosome-linked muscular dystrophy in mice - Proc Natl Acad Sci USA - 1989

94. Li D, Yue Y, Duan D - Preservation of muscle force in *Mdx*3cv mice correlates with low-level expression of a near full-length dystrophin protein - Am J Pathol - 2008

95. Beastrom N, Lu H, Macke A, Canan BD, Johnson EK, Penton CM, Kaspar BK, Rodino-Klapac LR, Zhou L, Janssen PM, Montanaro F - *mdx*(^{5}cv) mice manifest more severe muscle dysfunction and diaphragm force deficits than do *mdx* Mice - Am J Pathol - 2011

96. Zhou L, Rafael-Fortney JA, Huang P, Zhao XS, Cheng G, Zhou X, Kaminski HJ, Liu L, Ransohoff RM - Haploinsufficiency of utrophin gene worsens skeletal muscle inflammation and fibrosis in *mdx* mice - J Neurol Sci - 2008

97. Durbeej M, Campbell KP - Muscular dystrophies involving the dystrophin-glycoprotein complex: an overview of current mouse models - Curr Opin Genet Dev – 2002

98. Barresi R, Confalonieri V, Lanfossi M, Di Blasi C, Torchiana E, Mantegazza R, Jarre L, Nardocci N, Boffi P, Tezzon F et al. - Concomitant deficiency of β- and γ-sarcoglycans in 20 α-sarcoglycan (adhalin)-deficient patients: immunohistochemical

analysis and clinical aspects - Acta Neuropathol – 1997

99. Cohn RD, Durbeej M, Moore SA, Coral-Vazquez R, Prouty S, Campbell KP - Prevention of cardiomyopathy in mouse models lacking the smooth muscle sarcoglycan-sarcospan complex - J Clin Invest – 2001

100. Hack AA, Ly CT, Jiang F, Clendenin CJ, Sigrist KS, Wollmann RL, McNally EM - γ-sarcoglycan deficiency leads to muscle membrane defects and apoptosis independent of dystrophin - J Cell Biol – 1998

101. Hack AA, Cordier L, Shoturma DI, Lam MY, Sweeney HL, McNally EM - Muscle degeneration without mechanical injury in sarcoglycan deficiency - Proc Natl Acad Sci USA - 1999

102. Sunada Y, Bernier SM, Kozak CA, Yamada Y, Campbell KP - Deficiency of merosin in dystrophic dy mice and genetic linkage of laminin M chain gene to dy locus - J Biol Chem - 1994

103. Lane PW, Beamer TC, Myers DD - Myodystrophy, a new myopathy on chromosome 8 of the mouse - J Hered - 1976

104. Lee RC, Feinbaum RL, Ambros V - The C. elegans heterochronic gene lin-4 encodes small RNAs with antisense complementarity to lin-14 - Cell - 1993

105. Wightman B, Ha I, Ruvkun G - Posttranscriptional regulation of the heterochronic gene lin-14 by lin-4 mediates temporal pattern formation in C. elegans - Cell - 1993

106. Pasquinelli AE, Reinhart BJ, Slack F, Martindale MQ, Kuroda MI, Maller B, Hayward DC, Ball EE, Degnan B, Müller P, Spring J, Srinivasan A, Fishman M, Finnerty J, Corbo J, Levine M, Leahy P, Davidson E, Ruvkun G - Conservation of the sequence and temporal expression of let-7 heterochronic regulatory RNA - Nature - 2000

107. Bartel DP - MicroRNAs: genomics, biogenesis, mechanism, and

function - Cell - 2004

108. Lee Y, Jeon K, Lee JT, Kim S, KimVN - MicroRNA maturation: stepwise processing and subcellular localization - EMBO - 2002

109. Lee Y, Ahn C, Han J, Choi H, Kim J, Yim J, Lee J, Provost P, Rådmark O, Kim S, Kim VN - The nuclear RNase III Drosha initiates microRNA processing - Nature - 2003

110. Ambros V - The functions of animal microRNAs - Nature - 2004

111. Brennecke J, Stark A, Russell RB, Cohen SM - Principles of microRNA-target recognition - PLoS Biol - 2005

112. Maroney PA, Yu Y, Fisher J, Nilsen TW - Evidence that microRNAs are associated with translating messenger RNAs in human cells - Nat Struct Mol Biol - 2006

113. Olsen PH, Ambros V - The lin-4 regulatory RNA controls developmental timing in Caenorhabditis elegans by blocking LIN-14 protein synthesis after the initiation of translation - Dev Biol - 1999

114. Petersen CP, Bordeleau ME, Pelletier J, Sharp PA - Short RNAs repress translation after initiation in mammalian cells - Mol Cell - 2006

115. Nottrott S, Simard MJ, Richter JD - Human let-7a miRNA blocks protein production on actively translating polyribosomes - Nat Struct Mol Biol - 2006

116. Bagga S, Bracht J, Hunter S, Massirer K, Holtz J, Eachus R, Pasquinelli AE - Regulation by let-7 and lin-4 miRNAs results in target mRNA degradation - Cell - 2005

117. Giraldez AJ, Mishima Y, Rihel J, Grocock RJ, Van Dongen S, Inoue K, Enright AJ, Schier AF - Zebrafish MiR-430 promotes deadenylation and clearance of maternal mRNAs - Science - 2006

118. Vasudevan S, Tong Y, Steitz JA - Switching from repression to activation: microRNAs can up-regulate translation - Science - 2007

119. Eiring AM, Harb JG, Neviani P, Garton C, Oaks JJ, Spizzo R, Liu S, Schwind S, Santhanam R, Hickey CJ, Becker H, Chandler JC, Andino R, Cortes J, Hokland P, Huettner CS, Bhatia R, Roy DC, Liebhaber SA, Caligiuri MA, Marcucci G, Garzon R, Croce CM, Calin GA, Perrotti D - miR-328 functions as an RNA decoy to modulate hnRNP E2 regulation of mRNA translation in leukemic blasts - Cell - 2010

120. Abelson JF, Kwan KY, O'Roak BJ, Baek DY, Stillman AA, Morgan TM, Mathews CA, Pauls DL, Rasin MR, Gunel M, Davis NR, Ercan-Sencicek AG, Guez DH, Spertus JA, Leckman JF, Dure LS 4th, Kurlan R, Singer HS, Gilbert DL, Farhi A, Louvi A, Lifton RP, Sestan N, State MW - Sequence variants in SLITRK1 are associated with Tourette's syndrome - Science - 2005

121. Gandellini P, Profumo V, Folini M, Zaffaroni N - MicroRNAs as new therapeutic targets and tools in cancer - Expert Opin Ther Targets - 2011

122. Peacock H, Fucini RV, Jayalath P, Ibarra-Soza JM, Haringsma HJ, Flanagan WM, Willingham A, Beal PA - Nucleobase and ribose modifications control immunostimulation by a microRNA-122-mimetic RNA - J Am Chem Soc - 2011

123. Grounds MD, Torrisi J - Anti-TNFalpha (Remicade) therapy protects dystrophic skeletal muscle from necrosis - FASEB J - 2004

124. Hodgetts S, Radley H, Davies M - Reduced necrosis of dystrophic muscle by depletion of host neutrophils, or blocking TNFalpha function with Etanercept in *mdx* mice - Neuromuscul Disord - 2006

125. Sciorati C, Buono R, Azzoni E, Casati S, Ciuffreda P, D'Angelo

G, Cattaneo D, Brunelli S, Clementi E - Co-administration of ibuprofen and nitric oxide is an effective experimental therapy for muscular dystrophy, with immediate applicability to humans - Br J Pharmacol - 2010

126. Whitehead NP, Pham C, Gervasio OL - N-Acetylcysteine ameliorates skeletal muscle pathophysiology in *mdx* mice - J Physiol - 2008

127. Buyse GM, Van der Mieren G, Erb M, D'hooge J, Herijgers P, Verbeken E, Jara A, Van Den Bergh A, Mertens L, Courdier-Fruh I, Barzaghi P, Meier T -Long-term blinded placebo-controlled study of SNT-MC17/idebenone in the dystrophin deficient *mdx* mouse: cardiac protection and improved exercise Performance - Eur Heart J - 2009

128. Buetler TM, Renard M, Offord EA, Schneider H, Ruegg UT - Green tea extract decreases muscle necrosis in *mdx* mice and protects against reactive oxygen species - Am J Clin Nutr - 2002

129. Dorchies OM, Wagner S, Vuadens O, Waldhauser K, Buetler TM, Kucera P, Ruegg UT - Green tea extract and its major polyphenol (-)-epigallocatechin gallate improve muscle function in a mouse model for Duchenne muscular dystrophy - Am J Physiol Cell Physiol - 2006

130. Hori YS, Kuno A, Hosoda R, Tanno M, Miura T, Shimamoto K, Horio Y - Resveratrol ameliorates muscular pathology in the dystrophic *mdx* mouse, a model for Duchenne muscular dystrophy - J Pharmacol Exp Ther - 2011

131. Krahn MJ, Anderson JE - Anabolic steroid treatment increases myofiber damage in *mdx* mouse muscular dystrophy - J Neurol Sci - 1994

132. Harcourt LJ, Schertzer JD, Ryall JG, Lynch GS - Low dose formoterol administration improves muscle function in dystrophic *mdx* mice without increasing fatigue - Neuromuscul

Disord - 2007

133. Gehrig SM, Koopman R, Naim T, Tjoakarfa C, Lynch GS - Making fast-twitch dystrophic muscles bigger protects them from contraction injury and attenuates the dystrophic pathology - Am J Pathol - 2010

134. Koopman R, Gehrig SM, Léger B, Trieu J, Walrand S, Murphy KT, Lynch GS - Cellular mechanisms underlying temporal changes in skeletal muscle protein synthesis and breakdown during chronic {beta}-adrenoceptor stimulation in mice - J Physiol - 2010

135. Barton ER, Morris L, Musaro A, Rosenthal N, Sweeney HL - Muscle-specific expression of insulin-like growth factor I counters muscle decline in *mdx* mice - J Cell Biol - 2002

136. Bogdanovich S, Krag TO, Barton ER, Morris LD, Whittemore LA, Ahima RS, Khurana TS - Functional improvement of dystrophic muscle by myostatin blockade Nature - 2002

137. Nakatani M, Takehara Y, Sugino H, Matsumoto M, Hashimoto O, Hasegawa Y, Murakami T, Uezumi A, Takeda S, Noji S, Sunada Y, Tsuchida K - Transgenic expression of a myostatin inhibitor derived from follistatin increases skeletal muscle mass and ameliorates dystrophic pathology in *mdx* mice - FASEB J - 2008

138. Andreetta F, Bernasconi P, Baggi F, Ferro P, Oliva L, Arnoldi E, Cornelio F, Mantegazza R, Confalonieri P - Immunomodulation of TGF-beta 1 in *mdx* mouse inhibits connective tissue proliferation in diaphragm but increases inflammatory response: implications for antifibrotic therapy - J Neuroimmunol - 2006

139. Nelson CA, Hunter RB, Quigley LA, Girgenrath S, Weber WD, McCullough JA, Dinardo CJ, Keefe KA, Ceci L, Clayton NP, McVie-Wylie A, Cheng SH, Leonard JP, Wentworth BM - Inhibiting TGF-β activity improves respiratory function in *mdx* mice - Am J Pathol - 2011

140. Cohn RD, van Erp C, Habashi JP, Soleimani AA, Klein EC, Lisi MT, Gamradt M, ap Rhys CM, Holm TM, Loeys BL, Ramirez F, Judge DP, Ward CW, Dietz HC - Angiotensin II type 1 receptor blockade attenuates TGF-beta-induced failure of muscle regeneration in multiple myopathic states - Nat Med - 2007

141. Chamberlain JS - ACE inhibitor bulks up muscle - Nat Med - 2007

142. Barzilai-Tutsch H, Bodanovsky A, Maimon H, Pines M, Halevy O - Halofuginone promotes satellite cell activation and survival in muscular dystrophies - Biochim Biophys Acta - 2015

143. Pines M, Spector I - Halofuginone - the multifaceted molecule - Molecules - 2015

144. Chan YS, Li Y, Foster W, Horaguchi T, Somogyi G, Fu FH, Huard J - Antifibrotic effects of suramin in injured skeletal muscle after laceration - J Appl Physiol - 2003

145. Chan YS, Li Y, Foster W, Fu FH, Huard J - The use of suramin, an antifibrotic agent, to improve muscle recovery after strain injury - Am J Sports Med - 2005

146. Foster W, Li Y, Usas A, Somogyi G, Huard J - Gamma interferon as an antifibrosis agent in skeletal muscle - J Orthop Res - 2003

147. Li Y, Foster W, Deasy BM, Chan Y, Prisk V, Tang Y, Cummins J, Huard J - Transforming growth factor-beta1 induces the differentiation of myogenic cells into fibrotic cells in injured skeletal muscle: a key event in muscle fibrogenesis - Am J Pathol - 2004

148. Kaar JL, Li Y, Blair HC, Asche G, Koepsel RR, Huard J, Russell AJ - Matrix metalloproteinase-1 treatment of muscle fibrosis - Acta Biomater - 2008

149. Tonogai I, Takahashi M, Yukata K, Sato R, Nikawa T, Yasui N, Sairyo K - Osteoactivin attenuates skeletal muscle fibrosis after distraction osteogenesis by promoting extracellular matrix degradation/remodeling - J Pediatr Orthop B - 2015

Chapter 2:

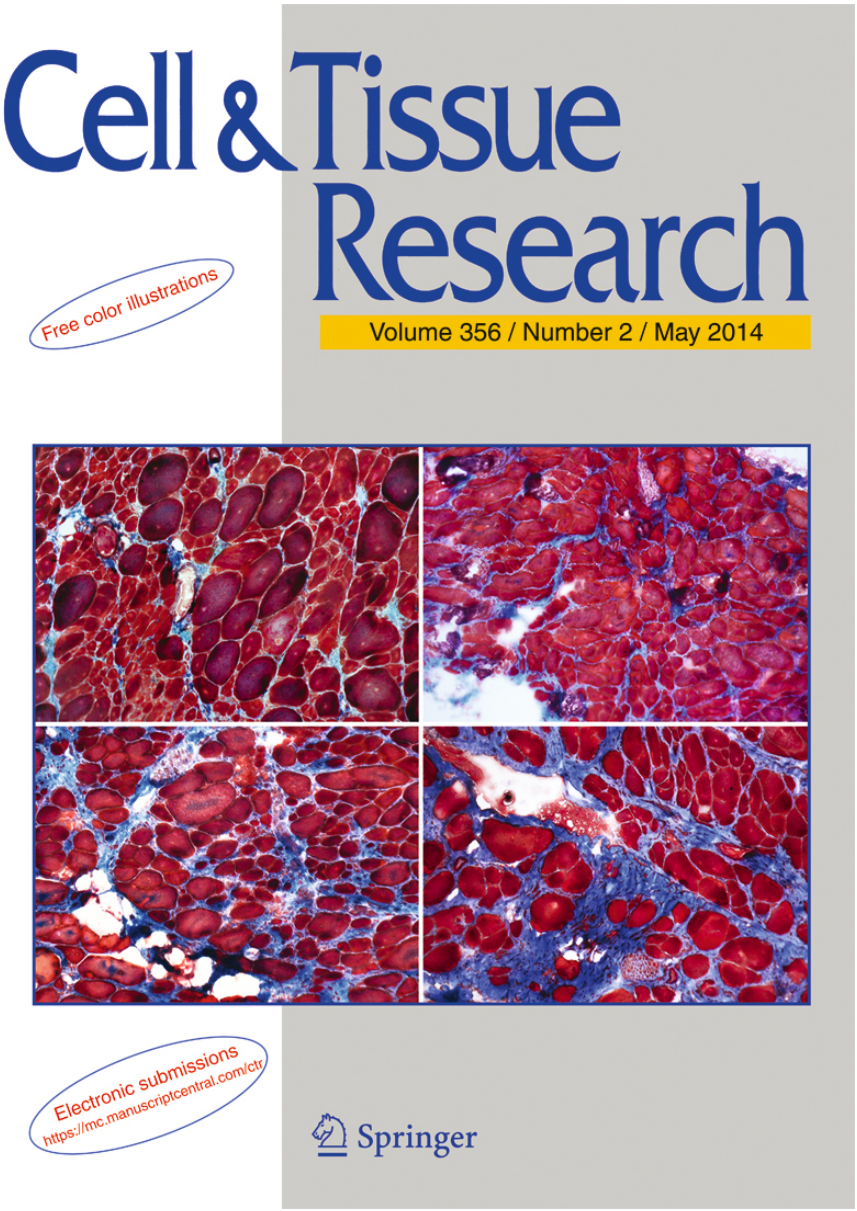
Cell & Tissue Research
Free color illustrations
Volume 356 / Number 2 / May 2014
Electronic submissions
https://mc.manuscriptcentral.com/ctr
Springer

Fibrosis and inflammation are greater in muscles of beta-sarcoglycan-null mouse than mdx mouse

Sara Gibertini, Simona Zanotti, Paolo Savadori, Maurizio Curcio, Simona Saredi, Franco Salerno, Francesca Andreetta, Pia Bernasconi, Renato Mantegazza, Marina Mora.

Cell Tissue Res. 2014 May;356(2):427-43.

doi: 10.1007/s00441-014-1854-4. Epub 2014 Apr 11

ABSTRACT

The *Sgcb-null* mouse, with knocked-down β-sarcoglycan, develops severe muscular dystrophy as in type 2E human limb girdle muscular dystrophy. The *mdx* mouse, lacking dystrophin, is the most-used model for Duchenne muscular dystrophy (DMD). Unlike DMD, the *mdx* mouse has mild clinical features and shows little fibrosis in limb muscles.

To characterize ECM protein deposition and the progression of muscle fibrosis, we evaluated protein and transcript levels of collagens I, III and VI, decorin, and TGF-β1, in quadriceps and diaphragm, at 2, 4, 8, 12, 26 and 52 weeks in *Sgcb-null* mice, and protein levels at 12, 26 and 52 weeks in *mdx* mice. In *Sgcb-null* mice, severe morphological disruption was present from 4 weeks in both quadriceps and diaphragm, and included conspicuous deposition of extracellular matrix components. Histopathological features of *Sgcb-null* mouse muscles were similar to those of age-matched *mdx* muscles at all ages examined, but in the *Sgcb-null* mouse the extent of connective tissue deposition was generally greater than *mdx*. Furthermore, in the *Sgcb-null* mouse the amount all of three collagen isoforms increased steadily, while in the *mdx* they remained stable. We also found that at 12 weeks macrophages were significantly more numerous in mildly

inflamed areas of *Sgcb-null* quadriceps compared to *mdx* quadriceps (but not in highly inflamed regions), while, in the diaphragm, macrophages did not differ significantly between the two models, in either region. Osteopontin mRNA was also significantly greater at 12 weeks in laser dissected highly inflamed areas of the *Sgcb-null* quadriceps compared to the *mdx* quadriceps. TGF-β1 was present in areas of degeneration-regeneration, but levels were highly variable and in general did not differ significantly between the two models and controls. The roles of the various subtypes of macrophages in muscle repair and fibrosis in the two models require further study. The *Sgcb-null* mouse, which develops early fibrosis in limb muscles, appears more promising than the *mdx* mouse for probing pathogenetic mechanisms of muscle fibrosis and for developing anti-fibrotic treatments.

Highlights

- The *Sgcb-null* mouse develops severe muscular dystrophy, the *mdx* mouse does not.
- Fibrosis developed earlier in *Sgcb-null* quadriceps and diaphragm than *mdx*.

- Macrophages were commoner in mildly inflamed parts of *Sgcb-null* quadriceps than *mdx*.
- The *Sgcb-null* model appears more useful than *mdx* for studying fibrotic mechanisms.
- The *Sgcb-null* model also appears more useful for developing anti-fibrotic treatments.

Key words: muscle fibrosis, extracellular matrix, muscle inflammation, β-sarcoglycan, *mdx*, collagens, decorin, TGF-β, macrophages.

Abbreviations

ECM: extracellular matrix; MMPs: matrix metalloproteases; TIMPs: tissue inhibitors of metalloproteases; TGF-β1: transforming growth factor-β1; DGC: dystrophin-glycoprotein complex; H&E: Hematoxylin & Eosin; MyHC: myosin heavy chain; FITC: Fluorescein isothiocyanate

INTRODUCTION

Muscle fibrosis, a hallmark of severe muscular dystrophies, is characterized by extensive deposition of collagens and other extracellular matrix (ECM) components that progressively replace muscle fibres. The extensive structural disorganization and remodelling that characterize the fibrotic process involve altered expression of enzymes such as metalloproteases (MMPs) and their inhibitors (TIMPs), release of fibrogenic cytokines, including transforming growth factor-β1 (TGF-β1), and altered expression of inflammation-related molecules, including osteopontin (Lund et al., 2009), and of proteoglycans.

The *mdx* mouse, lacking dystrophin, is the most used animal model for Duchenne muscular dystrophy (DMD). Unlike DMD, the *mdx* mouse has mild clinical features, with significant muscle regeneration and little endomysial fibrosis in limb muscles. However diaphragm muscle exhibits progressive damage – similar to that observed in patients – from an early stage, with connective tissue proliferation and significant increase in the expression of TGF-β1 (Andreetta at al., 2006; Gosselin et al., 2004), and proteoglycans, notably decorin and biglycan (Càceres et al., 2000).

In skeletal and cardiac muscle, dystrophin is associated with a large complex of sarcolemmal and cytoskeletal proteins (Henry and Campbell, 1996; Ozawa et al., 1998 and Straub and Campbell, 1997), forming the dystrophin-glycoprotein complex (DGC), that provides a structural link between laminin 2 in the extracellular matrix and the actin-based intracellular cytoskeleton (Ervasti and Campbell, 1993). Mutations in the genes encoding several components of the DGC have been associated with muscular dystrophies (Ozawa et al., 1998; Straub and Campbell, 1997). In particular, mutations in sarcoglycan genes cause autosomal recessive limb-girdle muscular dystrophies (types 2C-2F, LGMD2C-F), (Bönnemann et al., 1995; Lim et al., 1995; McNally et al., 1996 and Nigro et al., 1996) that have similar clinical and histopathological features to DMD, although severity is variable.

Mouse models of all sarcoglycanopathies have been obtained (Durbeej and Campbell, 2002). The *Sgcb-null* mouse is one such model, in which the β-sarcoglycan gene has been knocked down (Durbeej et al., 2000). This model exhibits disruption of the sarcoglycan and dystroglycan complexes in skeletal, cardiac, and smooth muscle, resulting in severe muscular dystrophy, cardiomyopathy, and vascular abnormalities; pathological features of skeletal muscle are fibre necrosis, fibre

calcification, endomysial fibrosis, and fatty infiltration (present by 2 months of age).

Collagens are major components of the ECM. Collagen fibrils are synthesized and secreted by fibroblasts, but how these processes are orchestrated and controlled, particularly during regeneration and tissue repair, is poorly understood. Collagens secreted by cells self-assemble in the ECM where molecules such as decorin can bind to collagen fibrils and modulate their diameter (Reed and Iozzo, 2002). Dysregulation of fibrillogenesis may affect the normal activity of MMPs and contribute to the progressive shift, in fibrosis, from normal low density basement membrane-like matrix to interstitial type matrix containing fibril-forming collagens (Friedman, 2000).

In order to elucidate mechanisms leading to ECM protein deposition, and characterize the progression of muscle fibrosis, we have now evaluated histopathological and molecular features in *Sgcb-null* mice at different ages, and compared them (at selected ages) with age-matched *mdx* mice. In particular, in *Sgcb*-null mouse quadriceps and diaphragm (selected after preliminary screening of several muscles in adult animals), we assessed extent of fibrosis, numbers of necrotic, regenerating and centronucleated fibres, and performed sequential evaluation of collagen

and decorin deposition and TGF-β1 expression. We assessed collagen I, III, and VI, decorin, and TGF-β1 transcript and protein levels, at 2, 8, 12, 26, and 52 weeks, and also assessed collagens, decorin and TGF-β1 proteins at 4 weeks. We then compared extent of fibrosis, expression of collagens and decorin, and expression of TGF-β1, at 12, 26 and 52 weeks, and macrophage numbers and osteopontin transcript levels at 12 weeks, between *Sgcb-null* and *mdx* mice.

MATERIALS AND METHODS

Animals

The *Sgcb-null* mice were kindly donated by Dr. KP Campbell of Iowa University, College of Medicine. Animal studies were approved by the Ethics Committee of the 'Carlo Besta' Neurological Institute, in accordance with the guidelines of the Italian Ministry of Health. The use and care of animals followed Italian law DL 116/1992 and EU directive 2010/63/EU The animals were housed in our facility under 12h light/12h dark conditions with free access to food and water. C57BL6J wild-type littermates were used as controls.

Eighteen *Sgcb-null*, 18 age-matched wild-type mice between 2 and 52 weeks, and 10 *mdx* mice of 12, 26 and 52 weeks were used. The animals were sacrificed by cervical dislocation under anaesthesia; muscles were rapidly removed, frozen in isopentane pre-cooled in liquid nitrogen, and maintained in liquid nitrogen pending use. Genotypes were determined by PCR on DNA from tail biopsies.

Morphology

Hematoxylin and eosin (H&E), Gomori modified trichrome, Masson's trichrome, acid phosphatase, and immunohistochemical stainings were performed on consecutive 6-8 μm thick cryostat muscle sections.

Sections were incubated for 120 min in the following primary antibodies: anti-collagen I, III or VI (polyclonals purchased from: Chemicon - Millipore, Billerica, MA, USA, Thermo Fisher Scientific, Waltham, MA, USA, and Santa Cruz Biotechnology, Santa Cruz, CA, USA, diluted respectively 1:40, 1:500 and 1:100); anti-TGF-β1 (polyclonal from Abcam Plc. Cambridge, UK; 1:250); anti-decorin (kindly donated by Dr. Larry Fisher of Craniofacial and Skeletal Diseases Branch, NIDCR, NIH, DHHS,

Bethesda, MD, USA; 1:100); anti CD45 (polyclonal anti-rat from eBioscience, Inc. Headquarters San Diego, CA, USA**;** 1:100); anti-component 3 of complement (C3) (polyclonal from Dako, Copenhagen, Denmark; 1:200); anti-albumin (polyclonal from Nordic Immunological Laboratories, Langendijk, Eindhoven, The Netherlands; 1:10000); and anti-foetal myosin heavy chain (MyHC) (monoclonal from DSHB, University of Iowa, USA; 1:5). Primary antibody incubation was followed by incubation for 60 min with one of the following secondary antibodies: Alexa 488- or Alexa 546-goat anti-rabbit IgG (Molecular Probes Inc, Eugene, OR, USA; 1:2000); FITC-goat anti-rat IgG (Santa Cruz Biotechnology; 1:500); Biotin-SP-AffiniPure goat anti-rabbit IgG; and Biotin-SP-AffiniPure goat anti-mouse IgG (Jackson ImmunoResearch Laboratories, Inc., Westgrove PA, USA; 1:250). When secondary biotinylated antibodies were used, incubation in Rhodamine Red-X-conjugated avidin (Invitrogen Life Technologies, Carlsbad, CA, USA; 1:250) followed for further 30 min.

To block non-specific binding, sections were preincubated for 30 min with 10% goat serum (Jackson ImmunoResearch) in PBS. As control, sections were either incubated with rabbit non-immune serum, or with isotype-specific non-immune IgG (Dako), or the primary antibody

was omitted. Sections were examined under a Zeiss Axioplan2 fluorescence microscope.

Quantitation of muscle fibrosis

The extent of total connective tissue in quadriceps and diaphragm was determined on Masson's trichrome-stained sections at 20x magnification using the NIH ImageJ software version 1.44 (http://rsb.info.nih.gov/nih-image/), as described (Zanotti et al., 2005). Briefly, 4 randomly selected fields were photographed from each section and digitalized. Using the software, a threshold was applied to the photographs to obtain black and white images with areas positive for collagens in black and negative areas in white. Manual corrections were sometimes applied to eliminate non-muscle/non-fibrosis areas or to add areas not recognized by the software. The area positive for collagens was calculated as a percentage of the entire image, and the mean percentage for each group of animals calculated. Extents of collagens I, III and VI, and decorin were assessed on consecutive immunostained sections, in a similar manner (Zanotti et al., 2005), except that the digitized images were first inverted.

Degenerating/necrotic fibres were identified on H&E- or Gomori trichrome-stained sections as those with cytoplasmic swelling (early necrosis) or as fibres invaded by macrophages (late necrosis); and by immunohistochemistry as fibres positive for C3 or albumin (Zanotti et al., 2011) (early necrosis) or for CD45, marker of mononucleated cells (late necrosis). Regenerating fibres were identified as those of smaller diameter and bluish colour on H&E-stained sections, and by immunohistochemistry as fibres positive to foetal myosin heavy chain immunostaining. Centronucleated fibres were counted on H&E-stained sections. Fibres were counted on 4 randomly selected fields from each section, after photographing at 10x and digitizing.

Macrophages were counted by an operator blind to mouse genotype on photographs of acid phosphatase-stained sections, randomly taken by another operator also blind to genotype, and were expressed as number of cells per field. Four fields per muscle were photographed; 2 fields were from a highly inflamed region and 2 from a mildly inflamed region. The number of acid-phosphatase-positive cells was calculated by dividing the total area positive for acid phosphatase (calculated with ImageJ software as above) in each field, by the area of a single cell (calculated as mean area of 200 individually detected cells).

Tissue microdissection analysis

Laser microdissection was performed on 20 µm thick consecutive H&E-stained cryosections taken from the quadriceps of 12 week old *Sgcb-null* and *mdx* mice, using a Nikon mmiCell Cut laser microdissection system. At least 50 regions of interest were cut from highly inflamed and 50 from mildly inflamed regions in each quadriceps muscle (3 from *Sgcb-null* and 3 from *mdx* mice). Total RNA was isolated from the cut sections by using RNeasy Micro Plus Kit (Qiagen, Hilden, Germany) according to the manufacturer's instructions. RNA was reverse-transcribed with Transcriptor First Strand cDNA Synthesis Kit (Roche Diagnostic, Penzberg, Germany) according to the manufacturer's instructions. The reaction product was stored at −20°C pending use. A preamplification step with TaqMan PreAmp Master Mix Kit (Applied Biosystems, CA, USA) was performed according to the manufacturer's instructions, to increase the quantity of specific cDNA targets for gene expression analysis.

cDNA synthesis

Total RNA was isolated from muscle tissue by using TRI Reagent (Molecular Research Center, Inc., Cincinnati, OH,

USA) according to the manufacturer's instructions and checked spectrophotometrically for quantity and purity.

Aliquots of RNA (1 µg) were reverse-transcribed with Transcriptor First Strand cDNA Synthesis Kit (Roche Diagnostic) according to the manufacturer's instructions. The reaction product was stored at −20°C pending use.

cDNA integrity was assessed by PCR amplification of mouse actin (NM_009606.2) with specific primers (forward 5′-AGCCATGTACGTAGCCATCC-3′ and reverse 5′-CTCTCAGCTGTGGTGGTGAA-3′). PCR conditions were: 94°C for 2 min, followed by 35 cycles with 95°C for 30s, 55°C for 1 min and 72°C for 45s, 7 min at 72°C.

Real time PCR

Target gene expression was analysed by quantitative real time PCR. TaqMan Universal PCR MasterMix and Assays-on-Demand Gene Expression probes (COL1a1: Mm00801666_g1; COL3a1: Mm01254476_m1; COL6a1: Mm00487160_m1; TGFβ1: Mm03024053_m1; DCN: Mm00514535_m1; Spp1: Mm00436767_m1; mouse ACTB: 4352341E all from Applied Biosystems, CA, USA) were used for the PCR step. Reactions were performed in 96-well plates with 25 µl volumes. All samples were

analysed in duplicate. Cycling parameters were: 2 min at 50°C, 10min at 95°C followed by 40 cycles of PCR reaction (15 s at 95°C and 1 min at 60°C).

Products were detected with the ABI Prism 7000 sequence detection system (Applied Biosystems). The expression of each target gene in control and *Sgcb-null* mutant muscles was normalized to the expression of β-actin and calculated from the formula 2-ΔΔCt, where ΔΔCT=CtTarget-Ctβ-actin as described in the manufacturer's instructions (user bulletin #2, Applied Biosystems).

Western blot

Western blot of TGF-β1 was performed in muscle homogenates as described (Zanotti et al., 2011). Briefly, frozen sections from *Sgcb-null*, *mdx* and control mouse muscles were solubilized in 25 µl lysis buffer. The protein extracts were boiled, separated by 10% SDS-PAGE and transferred to nitrocellulose membranes (Schleicher and Schuell Inc., Keene NH, USA). Membranes were probed with TGF-β1 mouse monoclonal antibody (Novocastra, Newcastle Upon Tyne, UK) diluted 1:300. Biotin-conjugated secondary antibody was then applied (Jackson ImmunoResearch; 1:2000), followed by alkaline

phosphatase-conjugated streptavidin (Jackson ImmunoResearch 1:4000), and by detection with 1-Step NBT/BCIP reagent (Thermo Scientific, Rockford, IL, USA) as described in the manufacturer's instructions.

TGF-β1 Western blot bands were quantitated densitometrically using ImageJ, and normalized to β-tubulin.

Statistical analysis

Data were expressed as means and standard deviations (±SD) and standard error (±SE). The two-tailed Student's *t*-test was used to assess the differences between control and *Sgcb-null* mice, and ANOVA to assess the differences between control, *Sgcb-null* and *mdx* mice. P values <0.05 were considered significant.

RESULTS

Major disruption of *Sgcb-null* muscle starts at 4 weeks

At 2 weeks, the morphology of both quadriceps and diaphragm of *Sgcb-null* mice was well-preserved, with homogeneous fibre diameters; rare centronucleated and

necrotic degenerating fibres; and no connective tissue proliferation (Figs. 1, 2).

At 4 weeks, in *Sgcb-null* diaphragm a few small foci of degeneration and regeneration were present; connective tissue was only slightly increased, and centronucleated fibres were uncommon (Figs. 1, 2). In quadriceps, centronucleated fibres were more numerous; degeneration-regeneration was present, but varied from animal to animal; connective tissue was slightly increased and varied from area to area; and mononucleated cells were prominent at degeneration-regeneration foci.

At 8 weeks, major tissue disruption was present in diaphragm and quadriceps, with large areas of degeneration-regeneration; highly variable fibre diameter; often calcified necrotic fibres; numerous mononucleated cells invading and surrounding most fibres within the areas of degeneration-regeneration; and most fibres centronucleated. Connective tissue was variably increased in quadriceps; while in diaphragm the increase was widespread and more extensive (Figs. 1-3).

At 12 weeks, histopathological features were closely similar to those at 8 weeks, but connective tissue was more extensive (Fig. 2).

At 26 weeks, diaphragm and quadriceps were characterized by: central nuclei in most fibres, numerous necrotic calcified fibres, and numerous regenerating fibres often in groups. Necrotic fibres were often invaded by mononucleated cells. Connective tissue proliferation was extensive, but more marked in diaphragm (Figs. 1, 2).

At 52 weeks, diaphragm and quadriceps were severely affected. Most fibres were centronucleated and fibre diameter was highly variable. In quadriceps, numerous necrotic and regenerating fibres were still present, while in diaphragm, necrotic and regenerating fibres were rare. Connective tissue proliferation was more extensive than at 26 weeks, especially in diaphragm (Figs. 1-3).

Sgcb-null heart muscle alteration is evident after 26 weeks

The heart was histologically normal up to 26 weeks. At 52 weeks small rare foci of necrosis were present as was increased connective tissue, mainly at the myocardial periphery. Marked connective tissue proliferation was evident at 2 years in two additional animals that had died of natural causes (Fig. 4).

Protein levels of collagen I, III, and VI, and decorin are significantly increased in *Sgcb-null* quadriceps and diaphragm from an early age

Collagen I was present in perimysium and some areas of endomysium of *Sgcb-null* muscles, but was almost undetectable in controls. Positivity was evident as an extensive network of rounded patterns (Figs. 5, 6). In quadriceps, collagen I was significantly more extensive in *Sgcb-null* mice than controls from 2 weeks; while in diaphragm the difference was significant from 8 weeks and increased with age (Fig. 8).

Collagen III was present in *Sgcb-null* muscle as patches of positivity in perimysium and as dots around and inside some degenerating fibres (Figs. 5, 6); it was almost undetectable in controls. In quadriceps, collagen III was significantly more extensive in *Sgcb-null* than control at 2 and 4 weeks, decreased to control levels at 8 weeks, and increased again from 12 weeks on. In diaphragm, collagen III was significantly more extensive than control from 4 weeks, and the difference increased with age (Fig. 8).

Collagen VI was present in perimysium and endomysium of both *Sgcb-null* and control muscles (Figs. 5, 6). While in control mice, collagen VI extent remained constant with age, in *Sgcb-null* mice it was significantly greater than

control from 2 weeks on in quadriceps, and from 4 weeks on in diaphragm (Fig. 8).

Decorin was prominently localized in perimysium and endomysium; it was also present in association with fibre surfaces, and, notably, was absent from necrotic areas (Figs. 5, 6). Quantitation showed that, while in control mice the extent of decorin remained constant with age, in *Sgcb-null* quadriceps it was significantly greater than control at 2 weeks, comparable to control at 4 weeks, and significantly greater than control from 8 weeks on. In diaphragm, decorin levels were significantly above control at all ages (Fig. 8).

Collagen transcript trends are similar to those of the corresponding proteins; decorin transcripts increase, decline and increase again in late stage disease

mRNA levels of collagen I, III and VI, and of decorin varied greatly within and among groups. Collagen I transcript levels in *Sgcb-null* quadriceps were markedly and significantly greater than in wild type at 12 weeks, and significantly greater at 8, 26 and 52 weeks. In diaphragm, transcript was significantly lower at 2 weeks, and significantly higher than control from 8 weeks (Fig. 9).

Collagen III transcript was significantly lower at 2 weeks, and significantly higher from 12 weeks on, in *Sgcb-null* quadriceps compared to control. In diaphragm it was markedly and significantly greater at 2 weeks, significantly greater at 8 weeks, decreased to control levels at 12 weeks and was again increased at 26 and 52 weeks (Fig. 9).

Collagen VI transcript levels were significantly higher in *Sgcb-null* than control quadriceps at 26 and 52 weeks and significantly lower at 8 weeks. In diaphragm, collagen VI transcript was significantly above control only at 2 and 26 weeks.

Although decorin transcript in *Sgcb-null* quadriceps was higher than control at 2 weeks, the difference was not significant; at 8 and 12 weeks decorin mRNA was significantly lower, and at 26 weeks significantly higher than control, then returned to control levels at 52 weeks. In diaphragm decorin was markedly and significantly higher at 2 weeks, significantly lower at 8, 12 and 26 weeks, and again significantly higher at 52 weeks.

Levels of TGF-β1 protein and transcript are highly variable

TGF-β1 was observed mainly in areas of degeneration-regeneration and at foci of inflammation (Fig. 7A). Quantitation of Western blot bands (see representative blots in Fig. 7B) showed that protein levels were significantly greater then control only at 12 weeks in diaphragm; while in quadriceps, differences were not significant in relation to great variation between samples (Fig. 8).

TGF-β1 mRNA was significantly higher than control in quadriceps at 26 and 52 weeks. In diaphragm it was significantly higher than control at 12 weeks, and significantly lower than control at 26 weeks (Fig. 9).

Histopathological features of *Sgcb-null* and *mdx* muscle are similar, but fibrosis develops earlier (12 weeks) in *Sgcb-null* quadriceps

Histopathological features in *Sgcb-null* and age-matched *mdx* mice were similar at all examined ages (12, 26 and 52 weeks) except that connective tissue proliferation was generally greater in *Sgcb-null* mice. This was particularly evident in quadriceps, where endomysial connective tissue was prominent and collagen extent was significantly greater in *Sgcb-null* mice at all ages (except collagen I at

26 weeks in diaphragm) than *mdx* (Fig. 10). Furthermore, while in the *Sgcb-null* mouse the quantity of all three collagens increased steadily with age, in *mdx* they remained stable.

Extent of decorin expression was significantly higher in *Sgcb-null* than *mdx* in quadriceps only at 52 weeks, and significantly lower in diaphragm only at 26 weeks (Fig. 10).

In *mdx* muscles TGF-β1 was present in areas of degeneration-regeneration, as in *Sgcb-null* muscles (Fig. 7). Quantitation of immunoblot bands showed great variability and in general no significant differences between the two models and also compared to controls, except that *Sgcb-null* mouse diaphragm had significantly higher TGF-β1 protein than *mdx* and control at 12 weeks (Fig. 8).

Macrophage counts at 12 weeks were significantly higher in mildly-inflamed areas of quadriceps in the *Sgcb-null* mouse than similar areas of *mdx* quadriceps (but not in highly inflamed regions). In diaphragm, macrophage counts did not differ significantly between the two models, in either region (Fig. 11).

Tissue microdissection analysis shows higher osteopontin, but not TGF-β1 transcript levels in highly inflamed regions of *Sgcb-null* quadriceps

Osteopontin transcript levels in highly inflamed microdissected areas in the quadriceps muscle at 12 weeks were significantly higher in the *Sgcb-null* mouse than in the *mdx*, while levels in mildly inflamed microdissected areas were undetectable in both animal models (Fig. 11E). TGF-β1 mRNA was not significantly different between *Sgcb-null* and *mdx* mice in highly inflamed microdissected areas and was undetectable in mildly inflamed areas in both animal models (Fig. 11F).

DISCUSSION

In the present study we have shown that the *Sgcb-null* mouse develops severe and progressive fibrosis of limb muscles at an early stage, and that fibrosis is greater than in the *mdx* model. While in the *mdx* mouse, quantities of the three collagens studied remained stable with age, in the *Sgcb-null* mouse they increased steadily throughout life. Although the histopathological features of *mdx* mouse muscle have been extensively characterized, little information on the progressive deposition of collagens in

diaphragm is available (Carberry et al., 2012) and data on collagen isoform deposition in limb muscles appears to be lacking.

In addition to fibrosis, other signs of muscle deterioration appeared early (4 weeks) in both the diaphragm and quadriceps of the *Sgcb-null* mouse, with appearance of degenerating and regenerating fibres (present at all ages, but diminishing with increasing age) and an abrupt increase in centronucleated fibres between 2 and 8 weeks, reflecting the summation of multiple degeneration-regeneration processes occurring during this period.

We evaluated collagens I and VI as they are major components of connective tissue in DMD and MDC1A (Verrecchia and Mauviel, 2007 and Zanotti et al., 2011); we evaluated collagen III as it is critical for collagen I fibrillogenesis (Liu et al., 1997); and we evaluated decorin as it regulates collagen fibril formation and organisation by interacting with collagens I and VI via different binding sites (Nareyeck et al., 2004 and Reed and Iozzo, 2002). Furthermore, collagen I, III, V and VI transcripts have been found increased by microarray in DMD (Haslett et al., 2002 and Porter et al., 2002).

We found that collagen I and VI levels increased with age in the *Sgcb*-null mouse; not surprisingly collagen I

increased more than collagen VI, as the former is the more abundant isoform in the ECM, both in physiological and pathological conditions (Verrecchia and Mauviel, 2007). We also found that collagen III was greatly increased at 2 weeks in quadriceps and at 4 weeks in diaphragm, followed by a moderate decrease, and later increase. Similar findings were reported by Hurme et al. (1991) following trauma-induced muscle rupture: fibronectin (protein and transcript) started being expressed, closely followed by type III collagen; fibronectin and collagen III levels then decreased, followed by production of type I collagen that remained elevated for several weeks.

Expression of the collagen I, III and VI transcripts in *Sgcb-null* mice had trends similar to those of the proteins, including a decrease in collagen III mRNA at 12 weeks followed by later increase.

We found that decorin protein levels were also significantly increased in both *Sgcb-null* quadriceps and diaphragm, compared to control, a finding consistent with decorin's known role in collagen fibrillogenesis (Zhang et al., 2006). Decorin also orchestrates multiple signalling pathways and is a crucial regulator of the inflammatory response. In fact decorin protein is a natural inhibitor of TGF-β1, as it binds the cytokine with high affinity preventing its interaction with

pro-fibrotic receptors (Baghy et al., 2012). Recent data show that decorin is protective against fibrosis (Li et al., 2007).

Notwithstanding increased levels of decorin in *Sgcb-null* muscle generally, it was absent from sites of active necrosis. This could be due to a local increase in TGF-β1 (see Fig. 7) and to tissue reorganization and inflammatory reaction. However, to accomplish its regulatory functions in inflammation, decorin must be soluble so its absence at necrotic/inflammation sites could be due to local sequestration by ligands, rendering it inaccessible to antibody, or perhaps to loss during slide preparation as result of high solubility (Moreth et al., 2012).

On the other hand decorin transcripts were variably expressed in quadriceps and diaphragm, with low levels generally present during major muscle remodelling (8-26 weeks). This finding is consistent with the reduced levels of decorin mRNA we found previously in DMD and MDC1A compared to control patients (Zanotti et al., 2005) and is likely to be related to increase in TGF-β1. TGF-β downregulates decorin mRNA transcription in muscle-derived fibroblasts and chondrocytes *in vitro* (Demoor-Fossard et al., 2001 and Zanotti et al., 2010).

We found that TGF-β1 transcript was variably increased in the *Sgcb-null* mouse, being significantly higher than control in quadriceps at 26 and 52 weeks, and, in diaphragm, significantly higher than control at 12 weeks, and significantly lower at 26 weeks. These findings are similar to those of Andreetta et al. (2006) who found an increase in TGF-β1 transcript in diaphragm at 24 weeks, followed by a decrease. Similarly, in both quadriceps and diaphragm, Zhou et al. (2006) found an early (8 weeks) and significant increase in TGF-β1 transcript localized to inflammatory infiltrates and regenerating fibres, with lower levels of the cytokine in diaphragm in late stage disease, and significantly elevated levels at 8 weeks and 8 months in quadriceps.

By contrast, we found that TGF-β1 protein levels were not, in general, significantly greater than control. However, our Western blot findings varied markedly within groups probably due to the high solubility of the active cytokine resulting in variable loss during tissue preparation (Grainger, 2000).

As noted, the most striking finding of the present study is that fibrosis develops early in *Sgcb-null* limb muscles, with levels of collagen I and VI proteins significantly increased. This contrasts with the lack of fibrosis in the *mdx*

quadriceps which may be due to efficient removal, by macrophages, of factors promoting ECM deposition (e.g. growth factors, fibrogenic cytokines, signalling peptides), or greater regenerative capacity of *mdx* muscle. A recent paper by Li et al. (2009) presented data indicating that sub-physiological sarcoglycan expression in *mdx* may be sufficient to protect muscle from contraction-induced injury. In skeletal, cardiac, and smooth muscle of the *Sgcb-null* mouse, the sarcoglycan and dystroglycan complexes are disrupted (Durbeej et al., 2000) and therefore such protection is lacking. Furthermore β-sarcoglycan plays a critical role as core protein in assembling the sarcoglycan complex (Chan Y. et al. 1998). Therefore lack of β-sarcoglycan in the *Sgcb-null* mouse may result in greater fibre degeneration and greater recruitment of macrophages, which, depending on their subtype (Mann et al., 2011) may either remove fibrotic stimuli or induce greater fibrosis.

Our finding of significantly higher levels of macrophages in regions of mild inflammation in *Sgcb-null* quadriceps compared to similar regions of *mdx* quadriceps, is consistent with the hypothesis that these may be type M2a macrophages. M2a macrophages are abundant in advanced stages of tissue repair and have been found in the fibrotic muscle of *mdx* mice (Villalta et al., 2009). While

M2a macrophages seem to promote tissue repair, their homeostatic and tissue repair functions can be subverted by chronic insult when they can promote muscle injury (Wynn et al. 2013). Further studies are required to identify macrophage subtypes in muscle fibrosis. This will require FACS studies on fresh tissue as most marker antibodies do not work on tissue sections in mice.

Osteopontin mRNA was also increased in highly inflamed areas of *Sgcb-null* quadriceps compared to similar regions of *mdx* quadriceps, while the TGF-β1 transcript was not. Osteopontin is a pleiotropic extracellular protein involved in physiological roles such as regulation of immune functions (Lund et al., 2007), vascular remodelling, wound repair and developmental processes (Denhardt et al., 2001), and in pathological conditions such as tissue injury, infection, autoimmune disease and tumour growth (Anborgh et al., 2010). In dystrophic mouse muscle osteopontin promotes fibrosis by modulating immune cell subsets and intramuscular TGF-β (Vetrone et al., 2009). It is likely that the higher levels of osteopontin we observed in the *Sgcb-null* mouse contribute to the greater fibrosis of this animal model through early inflammation-associated mechanisms, while TGF-β intervenes at later stages.

Finally, the differing extents of fibrosis in the limb muscles of the two mouse models could also be due to the abnormally leaky vascular walls present in *Sgcb-null* mice (Durbeej et al., 2000) but not in *mdx*. Leaky walls may worsen fibrosis by allowing increased numbers of circulating macrophages to reach the muscle.

Interestingly we found that cardiac fibrosis manifests late in the *Sgcb-null* mouse, as it does in *mdx*, (Van Erp et al., 2010) and thus does not appear to differ greatly between the two models.

To conclude, characterization of the histopathology in the *Sgcb-null* mouse has revealed marked deterioration in muscle tissue from 4 weeks and early fibrosis not only in the diaphragm but also the quadriceps. Early involvement of quadriceps is the main feature distinguishing the *Sgcb-null* model from *mdx*, rendering it more suitable for investigating the fibrotic process and testing anti-fibrotic drugs. Finally our data suggest that earlier marked limb fibrosis in the *Sgcb-null* mouse may be due at least in part to the greater numbers of macrophages present in areas of mild inflammation in the *Sgcb-null* quadriceps compared to similar regions in *mdx* quadriceps (no difference in the diaphragms) and to the greater osteopontin levels that may contribute to greater inflammation-associated fibrosis.

However, the roles of macrophages and their various subtypes in muscle repair and fibrosis in the two models require further study.

Acknowledgements

This work was supported by the Italian Ministry of Health. The authors thank Don Ward for help with the English.

We thank K.P. Campbell of Iowa University for kindly providing *Sgcb-null* mice.

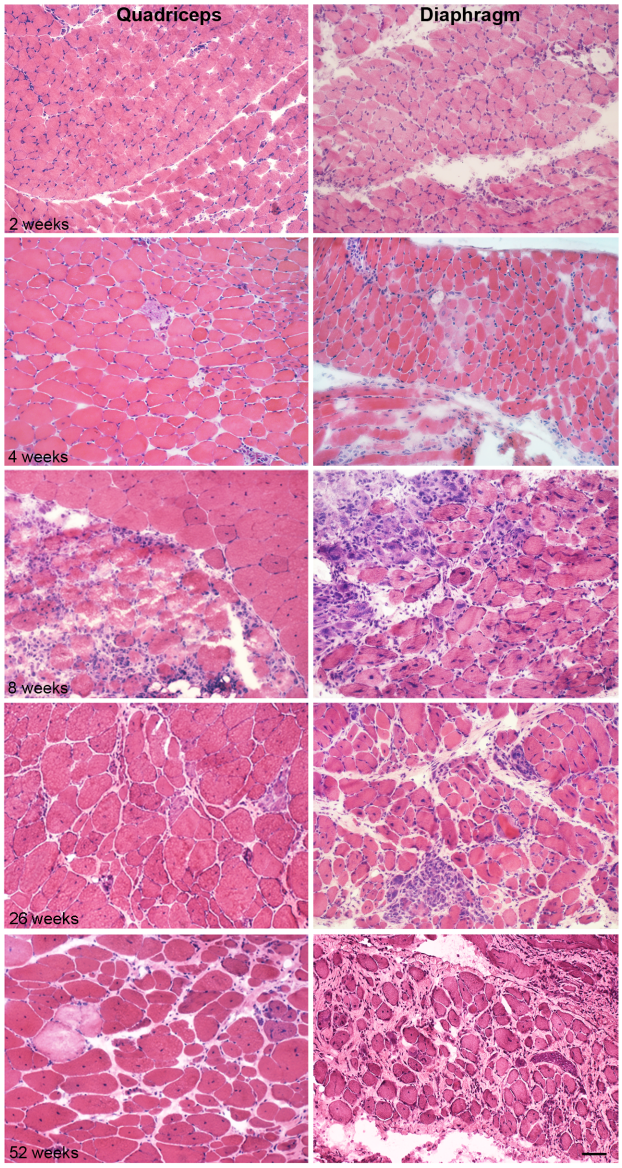

Fig. 1. General morphology of *Sgcb-null* mouse muscles at selected ages. H&E sections show normal morphology of quadriceps and diaphragm at 2 weeks; initial disruption of muscle tissue due to degeneration-regeneration in both muscles at 4 weeks; major disruption of muscle tissue in both muscles at 8 weeks; endomysial connective tissue proliferation in quadriceps and diaphragm, with numerous regenerating fibres in the latter, at 26 weeks; and pronounced fibrosis plus sparse necrotic fibres in quadriceps, and marked fibrosis in diaphragm, at 52 weeks. All images at same magnification: bar = 50 µm

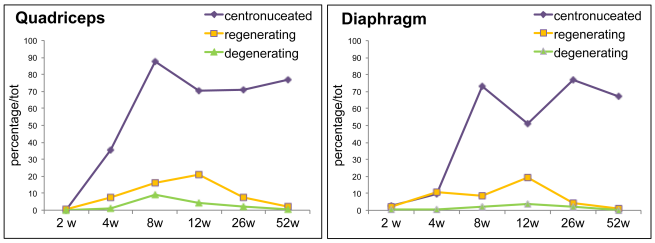

Fig. 2. Percentages (expressed as mean percentage ± standard error of the total of all analysed fields) of centronucleated, regenerating, and degenerating muscle fibres in *Sgcb-null* muscles at various ages. In both quadriceps and diaphragm, low levels of degenerating and regenerating fibres persist until late stages, while centronucleated fibres increase abruptly from 4 to 8 weeks and remain high subsequently.

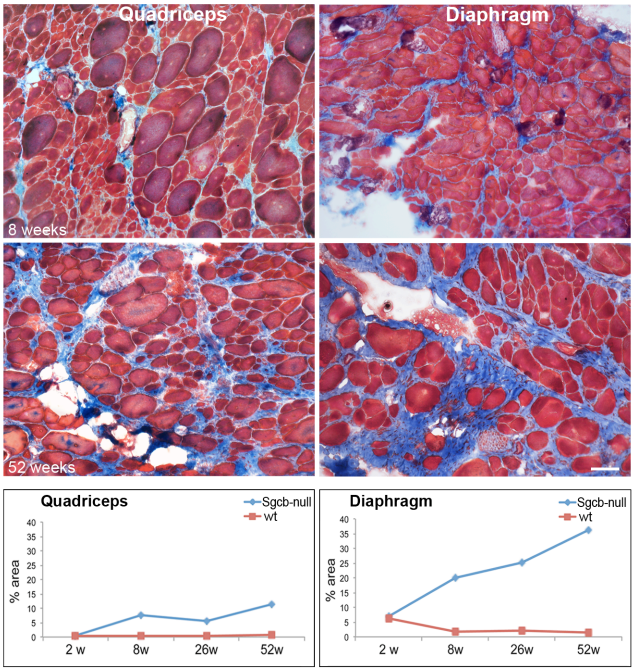

Fig. 3. Total collagen deposition in Sgcb-null muscles.

Upper panel: Representative images of Masson's trichrome-stained sections, showing mild collagen increase at 8 weeks, and marked collagen increase at 52 weeks in quadriceps; and marked collagen increase in diaphragm at 8 and 52 weeks. Bar = 50 µm.

Lower panel: Quantitation of total collagen, expressed as mean percentage ± standard error of the total of all analysed fields, on Masson's trichrome-stained sections.

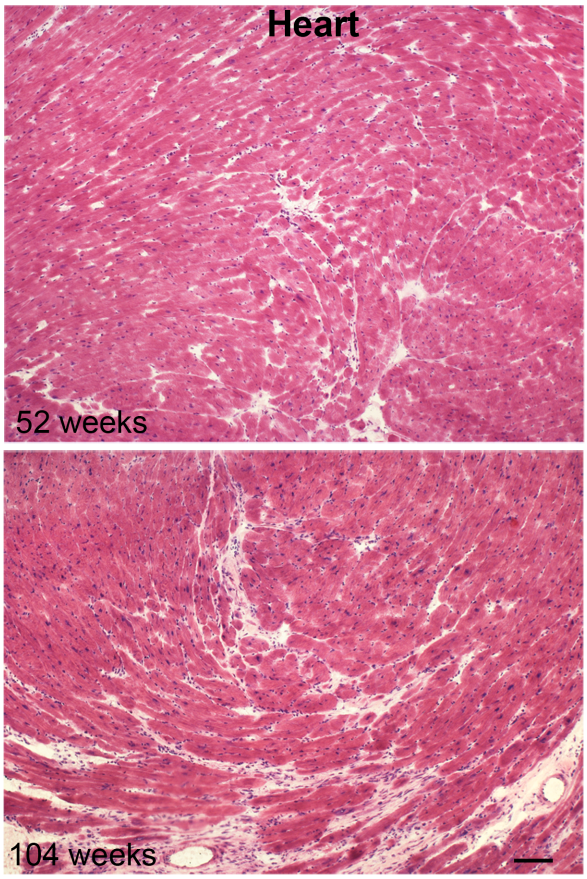

Fig. 4. Morphology of heart in *Sgcb-null* mouse. H&E-stained sections show presence of fibrosis at late disease stages. Bar = 50 μm.

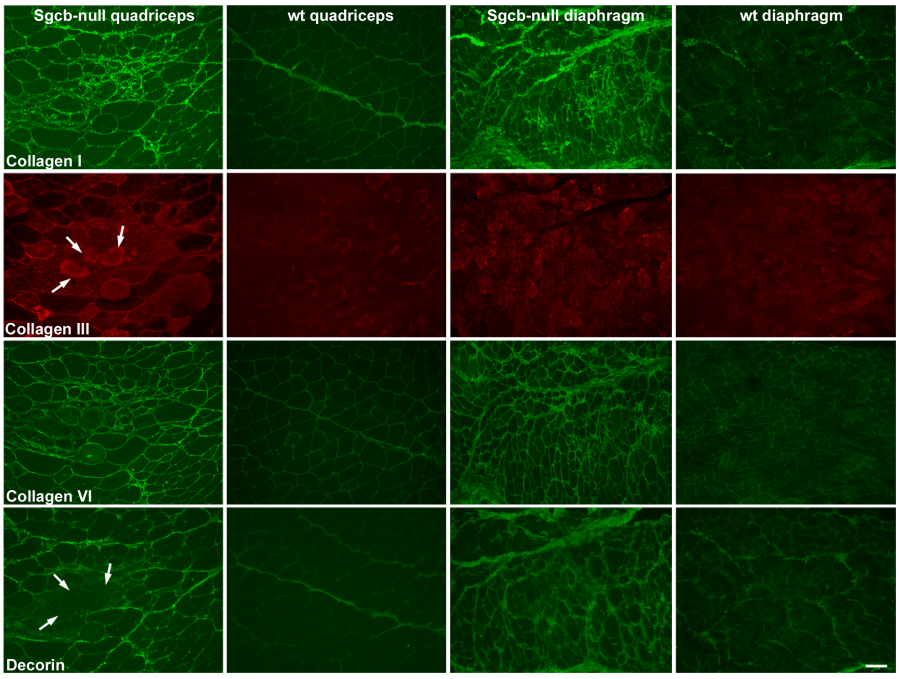

Fig. 5. Consecutive *Sgcb-null* muscle sections from quadriceps and diaphragm at 8 weeks showing immunostaining for collagen I, III, VI, and decorin. The arrows point to necrotic fibres. Bar = 50 µm.

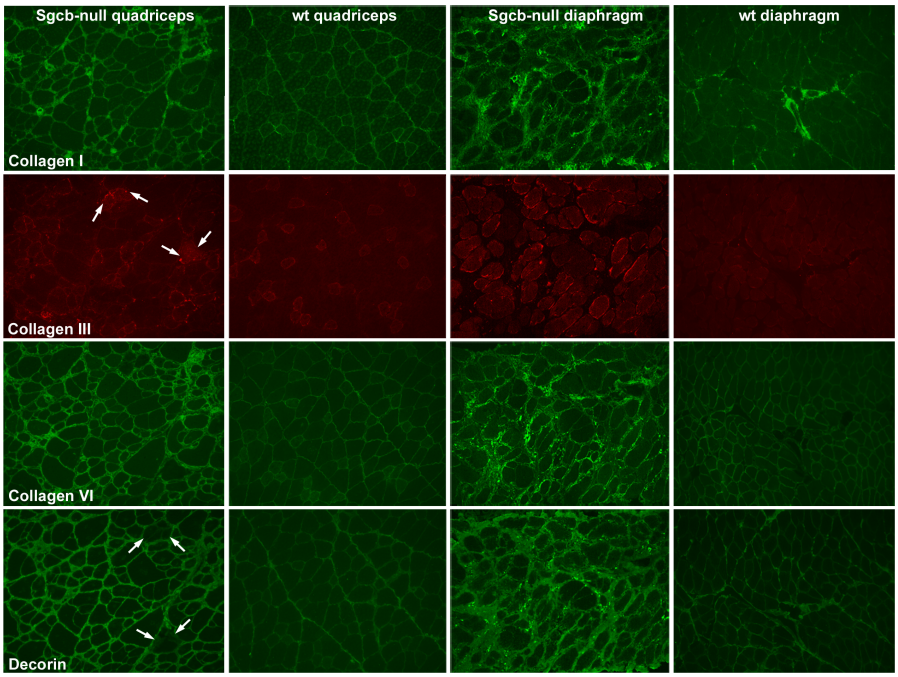

Fig. 6. Consecutive *Sgcb-null* muscle sections from quadriceps and diaphragm at 52 weeks showing immunostaining for collagen I, III, VI, and decorin. The arrows point to necrotic fibres. Bar = 50 µm.

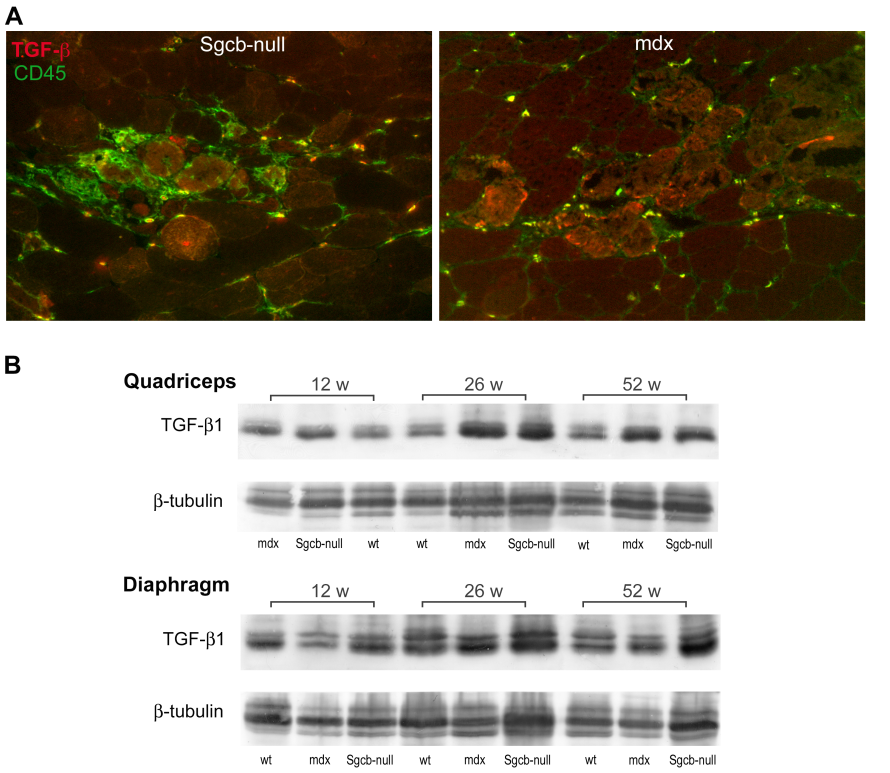

Fig. 7. Expression of TGF-β1 protein in *Sgcb-null* muscle. (A) TGF-β1 immunostaining showing localization of the cytokine (red) mainly in areas of degeneration-regeneration and at foci of inflammation positive for CD45 (green). Bar = 50 μm. (B) Representative Western blots from quadriceps and diaphragm at various ages showing double bands of variable intensity corresponding to TGF-β1.

Fig. 8. Quantitation of collagens I, III, and VI, decorin, and TGF-β1 proteins in *Sgcb-null* mouse at different ages. The extent of collagen I and VI, and decorin (evaluated on immunostained sections) increased with age, while collagen III was more variable. TGF-β1 protein expression (evaluated by Western blot) did not differ from control quadriceps and diaphragm except in the latter at 12 weeks.

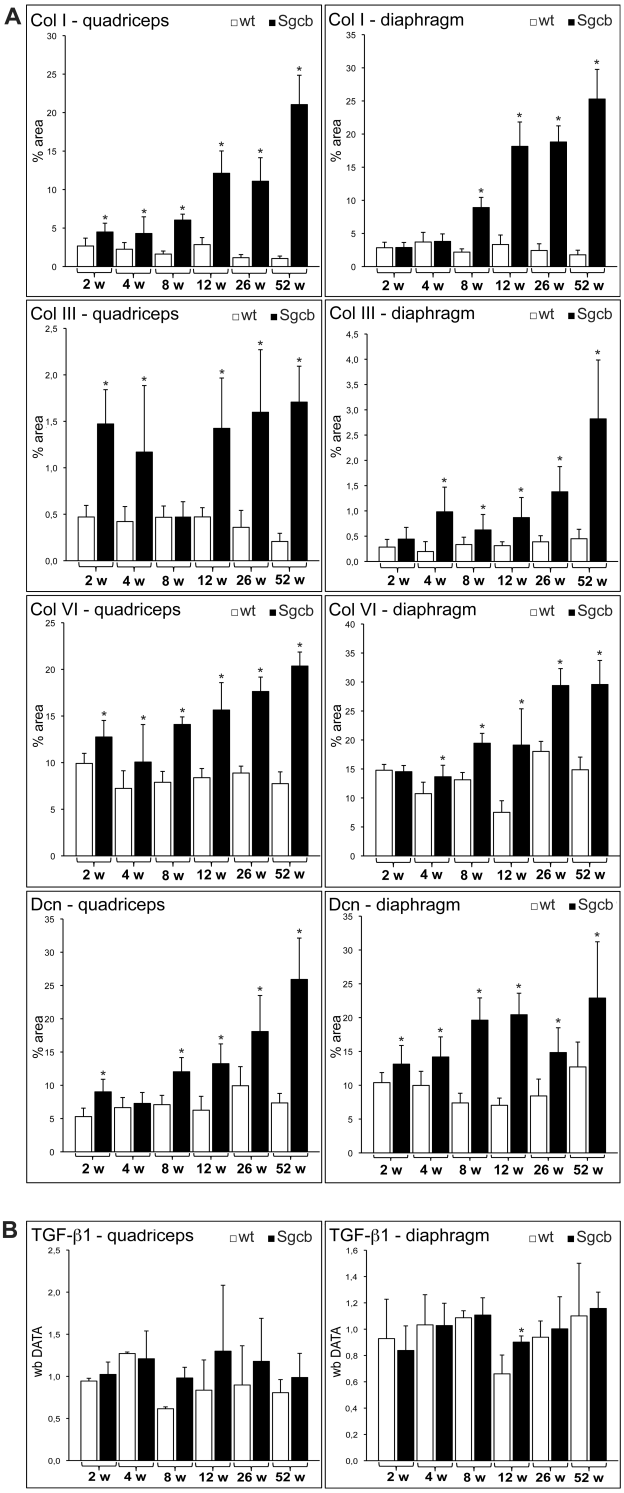
A
Col I - quadriceps
wt
Sgcb
% area
2 w
4 w
8 w
12 w
26 w
52 w
Col I - diaphragm
Col III - quadriceps
Col III - diaphragm
Col VI - quadriceps
Col VI - diaphragm
Dcn - quadriceps
Dcn - diaphragm
B
TGF-β1 - quadriceps
wb DATA
TGF-β1 - diaphragm

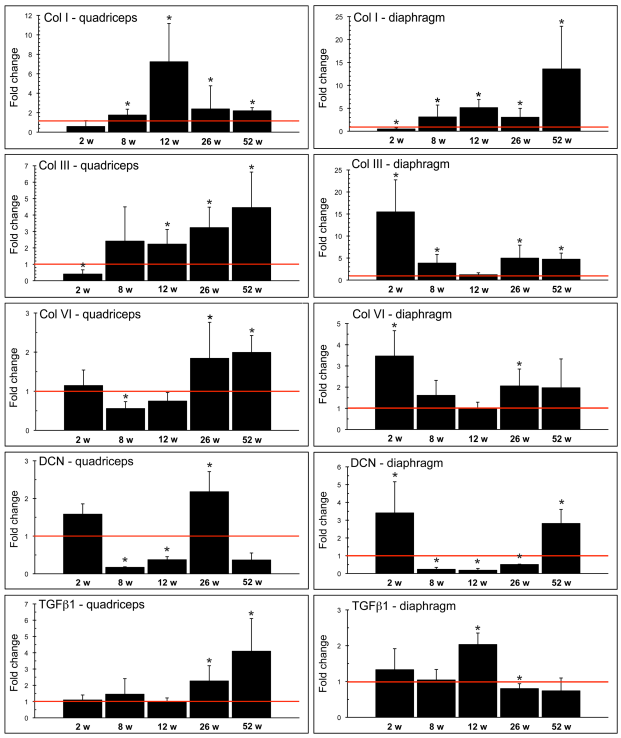

Fig. 9. Quantitation of collagen I, III, and VI, and of decorin and TGF-β1 transcripts in *Sgcb-null* mouse at different ages. Collagen I, III and VI transcript expression trends were similar to those of the respective proteins, including decrease in collagen III mRNA at 12 weeks followed by later increase, in both quadriceps and diaphragm. After an initial increase, decorin mRNA declined at 8 and 12 weeks and increased later in both muscles. TGF-β1 mRNA levels differed from controls only at 26 and 52 weeks in quadriceps, and at 12 and 26 weeks in diaphragm.

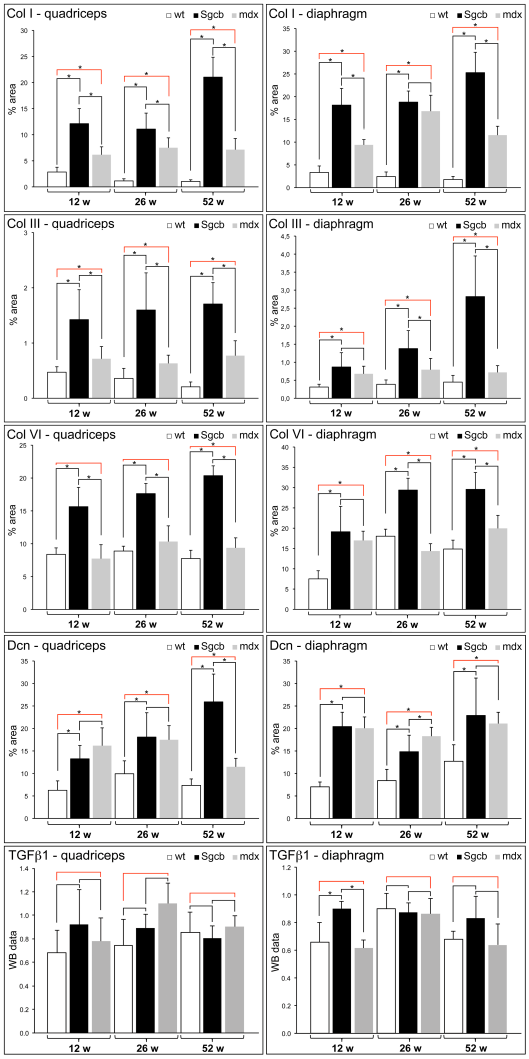

Fig. 10. Comparison of collagens I, III, and VI, decorin, and TGF-β1 protein expression in *Sgcb-null*, *mdx* and control mice. In the *Sgcb-null* mouse the quantity of all three collagens increased steadily with age, while in the *mdx* they remained stable. Extent of decorin expression was significantly higher in the *Sgcb-null* mouse, compared to *mdx,* in quadriceps only at 52 weeks, and significantly lower in diaphragm only at 26 weeks. TGF-β1 quantitation of immunoblot bands showed great variability and in general no significant differences between the two animal models and controls.

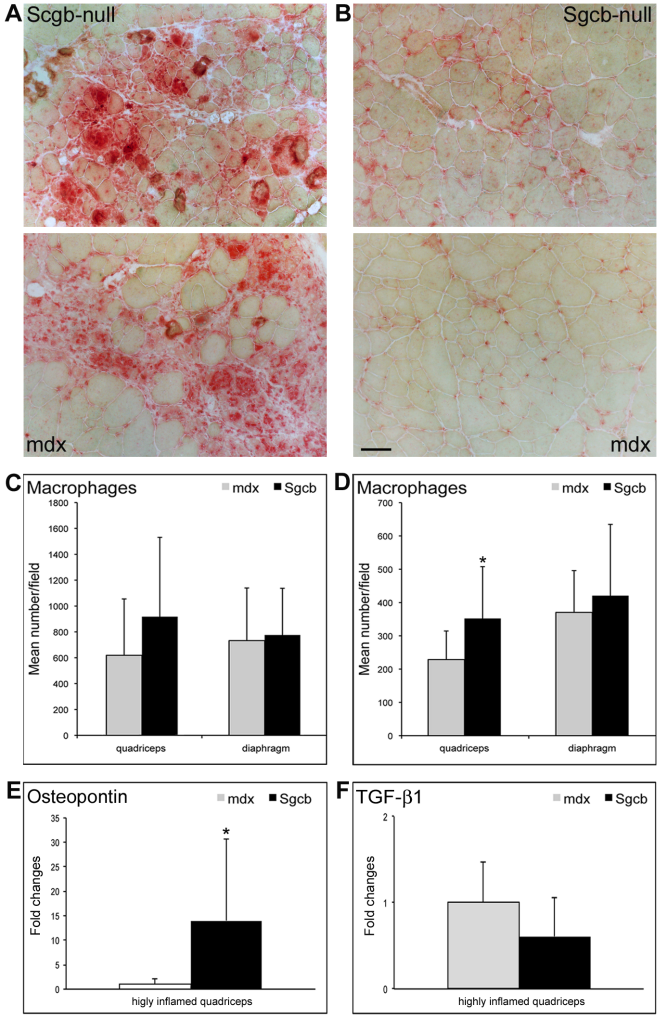

Fig.11. Detection and quantitation of macrophages in *Sgcb-null* and *mdx* mice at 12 weeks. (A, B) Acid phosphatase-stained sections from *Sgcb-null* and *mdx* quadriceps showing (A) highly inflamed regions and (B) mildly inflamed regions. Bar 50 μm. (C, D) Quantitation of acid phosphatase-positive macrophages in (C) highly inflamed regions and (D) mildly inflamed regions in quadriceps and diaphragm of *Sgcb-null* and *mdx* mice. (E) Osteopontin and (F) TGF-β1 transcript levels from highly inflamed microdissected regions in the quadriceps muscle of *Sgcb-null* and *mdx* mice at 12 weeks.

REFERENCES

Anborgh, P.H., Mutrie, J.C., Tuck, A.B., Chambers, A.F., 2010. Role of the metastasis-promoting protein osteopontin in the tumour microenvironment. J. Cell Mol. Med. 14, 2037-2044.

Andreetta, F., Bernasconi, P., Baggi, F., Ferro, P., Oliva, L., Arnoldi, E., Cornelio, F., Mantegazza, R., Confalonieri, P., 2006. Immunomodulation of TGF-beta 1 in *mdx* mouse inhibits connective tissue proliferation in diaphragm but increases inflammatory response: implications for antifibrotic therapy. J. Neuroimmunol. 175, 77-86.

Baghy, K., Iozzo, R.V., Kovalszky, I., 2012. Decorin-TGFβ axis in hepatic fibrosis and cirrhosis. J. Histochem. Cytochem. 60, 262-268.

Bönnemann, C.G., Modi, R., Noguchi, S., Mizuno, Y., Yoshida, M., Gussoni, E., McNally, E.M., Duggan, D.J., Angelini, C., Hoffman, E.P., 1995. Beta-sarcoglycan (A3b) mutations cause autosomal recessive muscular dystrophy with loss of the sarcoglycan complex. Nat. Genet. 11, 266-273.

Cáceres, S., Cuellar, C., Casar, J.C., Garrido, J., Schaefer, L., Kresse, H., Brandan, E., 2000. Synthesis of proteoglycans is augmented in dystrophic *mdx* mouse skeletal muscle. Eur. J. Cell Biol. 79, 173-181.

Carberry, S., Zweyer, M., Swandulla, D., Ohlendieck, K., 2012. Proteomics reveals drastic increase of extracellular matrix proteins collagen and dermatopontin in the aged *mdx* diaphragm model of Duchenne muscular dystrophy. Int. J. Mol. Med. 30, 229-234.

Chan, Y.M., Bönnemann, C.G., Lidov, H.G., Kunkel, L.M., 1998. Molecular organization of sarcoglycan complex in mouse myotubes in culture. J. Cell Biol. 1998 143, 2033-2044.

Demoor-Fossard, M., Galéra, P., Santra, M., Iozzo, R.V., Pujol, J.P., Rédini, F., 2001. A composite element binding the vitamin D receptor and the retinoic X receptor alpha mediates the

transforming growth factor-beta inhibition of decorin gene expression in articular chondrocytes. J. Biol. Chem. 276, 36983-36992.

Denhardt, D.T., Noda, M., O'Regan, A.W., Pavlin, D., Berman, J.S., 2001. Osteopontin as a means to cope with environmental insults: regulation of inflammation, tissue remodeling, and cell survival. J. Clin. Invest. 107, 1055-1061.

Durbeej, M., Campbell, K.P., 2002. Muscular dystrophies involving the dystrophin-glycoprotein complex: an overview of current mouse models. Curr. Opin. Genet. Dev. 12, 349-361.

Durbeej, M., Cohn, R.D., Hrstka, R.F., Moore, S.A., Allamand, V., Davidson, B.L., Williamson, R.A., Campbell, K.P., 2000. Disruption of the beta-sarcoglycan gene reveals pathogenetic complexity of limb-girdle muscular dystrophy type 2E. Mol. Cell. 5, 141-151.

Ervasti, J.M., Campbell, K.P., 1993. A role for the dystrophin-glycoprotein complex as a transmembrane linker between laminin and actin. J. Cell Biol. 122, 809-823.

Friedman, S.L., 2000. Molecular regulation of hepatic fibrosis, an integrated cellular response to tissue injury. J. Biol. Chem.. 275, 2247-2250.

Gosselin, L.E., Williams, J.E., Deering, M., Brazeau, D., Koury, S., Martinez, D.A., 2004. Localization and early time course of TGF-beta 1 mRNA expression in dystrophic muscle. Muscle Nerve. 30, 645-653.

Grainger, D.J., Mosedale, D.E., Metcalfe, J.C. 2000. TGF-beta in blood: a complex problem. Cytokine Growth Factor Rev. 11, 133-145.

Haslett, J.N., Sanoudou, D., Kho, A.T., Bennett, R.R., Greenberg, S.A., Kohane, I.S., Beggs, A.H., Kunkel, L.M., 2002. Gene expression comparison of biopsies from Duchenne muscular dystrophy (DMD) and normal skeletal muscle. Proc. Natl. Acad. Sci. U.S.A. 99, 15000-15005.

Henry, M.D., Campbell, K.P., 1996. Dystroglycan: an extracellular matrix receptor linked to the cytoskeleton. Curr. Opin. Cell Biol. 8,

625-631.

Hurme, T., Kalimo, H., Sandberg, M., Lehto, M., Vuorio, E., 1991. Localization of type I and III collagen and fibronectin production in injured gastrocnemius muscle. Lab. Invest. 64, 76-84.

Li, D., Long, C., Yue, Y., Duan, D., 2009. Sub-physiological sarcoglycan expression contributes to compensatory muscle protection in *mdx* mice. Hum. Mol. Genet. 18, 1209-1220.

Li, Y., Li, J., Zhu, J., Sun, B., Branca, M., Tang, Y., Foster, W., Xiao, X., Huard, J., 2007. Decorin gene transfer promotes muscle cell differentiation and muscle regeneration. Mol. Ther. 15, 1616-1622.

Lim, L.E., Duclos, F., Broux, O., Bourg, N., Sunada, Y., Allamand, V., Meyer, J., Richard, I., Moomaw, C., Slaughter, C., Tomé, F.M.S., Fardeau, M., Jackson, C.E., Beckmann, J.S., Campbell, K.P., 1995. Beta-sarcoglycan: characterization and role in limb-girdle muscular dystrophy linked to 4q12. Nat. Genet. 11, 257-265.

Liu, X., Wu, H., Byrne, M., Krane, S., Jaenisch, R., 1997. Type III collagen is crucial for collagen I fibrillogenesis and for normal cardiovascular development. Proc. Natl. Acad. Sci. U.S.A. 94, 1852-1856.

Lund, S.A., Giachelli, C.M., Scatena, M., 2009. The role of osteopontin in inflammatory processes. J. Cell Commun. Signal. 3, 311-322.

Mann, C.J., Perdiguero, E., Kharraz, Y., Aguilar, S., Pessina, P., Serrano, A.L., Muñoz-Cánoves, P., 2011. Aberrant repair and fibrosis development in skeletal muscle. Skelet. Muscle. 1, 21

McNally, E.M., Duggan, D., Gorospe, J.R., Bönnemann, C.G., Fanin, M., Pegoraro, E., Lidov, H.G., Noguchi, S., Ozawa, E., Finkel, R.S., Cruse, R.P., Angelini, C., Kunkel, L.M., Hoffman, E.P., 1996. Mutations that disrupt the carboxyl-terminus of gamma-sarcoglycan cause muscular dystrophy. Hum. Mol. Genet. 5, 1841-1847.

Moreth, K., Iozzo, R.V., Schaefer, L., 2012. Small leucine-rich proteoglycans orchestrate receptor crosstalk during inflammation. Cell Cycle. 11, 2084-2091.

Nareyeck, G., Seidler, D.G., Troyer, D., Rauterberg, J., Kresse, H., Schönherr, E., 2004. Differential interactions of decorin and decorin mutants with type I and type VI collagens. Eur. J. Biochem. 271, 3389-3398.

Nigro, V., de Sá Moreira, E., Piluso, G., Vainzof, M., Belsito, A., Politano, L., Puca, A.A., Passos-Bueno, M.R., Zatz, M., 1996. Autosomal recessive limb-girdle muscular dystrophy, LGMD2F, is caused by a mutation in the delta-sarcoglycan gene. Nat. Genet. 14, 195-198.

Ozawa, E., Noguchi, S., Mizuno, Y., Hagiwara, Y., Yoshida, M., 1998. From dystrophinopathy to sarcoglycanopathy: evolution of a concept of muscular dystrophy. Muscle Nerve 21, 421-438.

Porter, J.D., Khanna, S., Kaminski, H.J., Rao, J.S., Merriam, A.P., Richmonds, C.R., Leahy, P., Li, J., Guo, W., Andrade, F.H., 2002. A chronic inflammatory response dominates the skeletal muscle molecular signature in dystrophin-deficient *mdx* mice. Hum. Mol. Genet. 11, 263-272.

Reed, C.C., Iozzo, R.V., 2002. The role of decorin in collagen fibrillogenesis and skin homeostasis. Glycoconj J. 19, 249-255.

Straub, V., Campbell, K.P., 1997. Muscular dystrophies and the dystrophin-glycoprotein complex. Curr. Opin. Neurol. 10, 168-175.

Van Erp, C., Loch, D., Laws, N., Trebbin, A., Hoey, A.J., 2010. Timeline of cardiac dystrophy in 3-18-month-old *mdx* mice. Muscle Nerve. 42, 504-513.

Verrecchia, F., Mauviel, A., 2007. Transforming growth factor-beta and fibrosis. World J. Gastroenterol. 13, 3056-3062.

Vetrone, S.A., Montecino-Rodriguez, E., Kudryashova, E., Kramerova, I., Hoffman, E.P., Liu, S.D., Miceli, M.C., Spencer, M.J., 2009. Osteopontin promotes fibrosis in dystrophic mouse muscle by modulating immune cell subsets and intramuscular TGF-beta. J. Clin. Invest. 119, 1583-1594.

Villalta, S.A., Nguyen, H.X., Deng, B., Gotoh, T., Tidball, J.G., 2009. Shifts in macrophage phenotypes and macrophage competition for arginine metabolism affect the severity of muscle pathology in

muscular dystrophy. Hum. Mol. Genet. 18, 482-496.

Wynn, T.A., Chawla, A., Pollard, J.W., 2013. Macrophage biology in development, homeostasis and disease. Nature. 496, 445–455.

Zanotti, S., Gibertini, S., Di Blasi, C., Cappelletti, C., Bernasconi, P., Mantegazza, R., Morandi, L., Mora, M., 2011. Osteopontin is highly expressed in severely dystrophic muscle and seems to play a role in muscle regeneration and fibrosis. Histopathology 59, 1215-1228.

Zanotti, S., Gibertini, S., Mora, M., 2010. Altered production of extra-cellular matrix components by muscle-derived Duchenne muscular dystrophy fibroblasts before and after TGF-beta1 treatment. Cell Tissue Res. 339, 397-410

Zanotti, S., Negri, T., Cappelletti, C., Bernasconi, P., Canioni, E., Di Blasi, C., Pegoraro, E., Angelini, C., Ciscato, P., Prelle, A., Mantegazza, R., Morandi, L., Mora, M., 2005. Decorin and biglycan expression is differentially altered in several muscular dystrophies. Brain 128, 2546-2555.

Zhang, G., Ezura, Y., Chervoneva, I., Robinson, P.S., Beason, D.P., Carine, E.T., Soslowsky, L.J., Iozzo, R.V., Birk, D.E., 2006. Decorin regulates assembly of collagen fibrils and acquisition of biomechanical properties during tendon development. J. Cell Biochem. 98, 1436-1449.

Zhou, L., Porter, J.D., Cheng, G., Gong, B., Hatala, D.A., Merriam, A.P., Zhou, X., Rafael, J.A., Kaminski, H.J., 2006. Temporal and spatial mRNA expression patterns of TGF-beta1, 2, 3 and TbetaRI, II, III in skeletal muscles of *mdx* mice. Neuromuscul. Disord. 16, 32-38.

Chapter 3:

Opposing roles of miR-21 and miR-29 in the progression of fibrosis in Duchenne muscular dystrophy

Simona Zanotti, Sara Gibertini, Maurizio Curcio, Paolo Savadori, Barbara Pasanisi, Lucia Morandi, Ferdinando Cornelio, Renato Mantegazza, Marina Mora.

Biochim Biophys Acta. 2015 Jul;1852(7):1451-64. doi: 10.1016/j.bbadis.2015.04.013. Epub 2015 Apr 17.

Abstract

Excessive extracellular matrix deposition progressively replacing muscle fibres is the endpoint of most severe muscle diseases. Recent data indicate major involvement of microRNAs in regulating pro- and anti-fibrotic genes.

To investigate the roles of miR-21 and miR-29 in muscle fibrosis in Duchenne muscle dystrophy, we evaluated their expression in muscle biopsies from 14 patients, and in muscle-derived fibroblasts and myoblasts.

In Duchenne muscle biopsies, miR-21 expression was significantly increased, and correlated directly with COL1A1 and COL6A1 transcript levels. MiR-21 expression was also significantly increased in Duchenne fibroblasts, more so after TGF-β1 treatment.

In Duchenne fibroblasts the expression of miR-21 target transcripts PTEN (phosphatase and tensin homolog deleted on chromosome 10) and SPRY-1 (Sprouty homolog 1) was significantly reduced; while collagen I and VI transcript levels and soluble collagen production were significantly increased. MiR-29a and miR-29c were significantly reduced in Duchenne muscle and myoblasts, and miR-29 target transcripts, COL3A1, FBN1 and YY1, significantly increased. MiR-21 silencing in *mdx* mice

reduced fibrosis in the diaphragm muscle and in both Duchenne fibroblasts and *mdx* mice restored PTEN and SPRY-1 expression, and significantly reduced collagen I and VI expression; while miR-29 mimicking in Duchenne myoblasts significantly decreased miR-29 target transcripts.

These findings indicate that miR-21 and miR-29 play opposing roles in Duchenne muscle fibrosis and suggest that pharmacological modulation of their expression has therapeutic potential for reducing fibrosis in this condition.

Keywords: miR-21, fibroblasts, miR-29, myoblasts, fibrosis, Duchenne muscular dystrophy, *mdx* mouse

Abbreviations:

α-SMA = α-smooth muscle actin
COL1A1 = collagen type I alpha 1
COL3A1 = collagen type III alpha 1
COL6A1 = collagen type VI alpha 1
DMD = Duchenne muscle dystrophy
ECM= extracellular matrix
ERK = extracellular signal-regulated kinase
FBN1 = fibrillin 1
HMGA2 = high-mobility group AT-hook 2

miRNAs = microRNAs
PAI-1 = plasminogen activator inhibitor-1
PTEN = phosphatase and tensin homologue deleted on chromosome 10
SPRY-1 = Sprouty homolog-1
TGF-β1 = transforming growth factor-β1
TWF1 = twinfilin-1
YY1 = Yin Yang 1

1. Introduction

In severe muscular dystrophies such as congenital muscular dystrophies and Duchenne muscular dystrophy (DMD), the primary defect leads to continuous myofibre injury and degeneration. In DMD, chronic muscle tissue damage and inflammatory infiltrates persist, resident satellite cells are unable to keep pace with the requirement for new fibres, and fibrogenic cells are continuously activated, eventually leading to massive connective tissue deposition (fibrosis) [41]. In addition to impeding fibre regeneration, fibrosis may obstruct the targeting of specific therapies (drugs or cells) to muscle, and worsen disease progression by obstructing nutrient delivery.

Fibrosis is not a peculiarity of DMD and chronic myopathies, but characterizes diseases of various tissues, including lung [40], liver [20], kidney [39], heart [22], skin [42], and bladder [11].

Fibroblasts play a major role in fibrosis. Normally they are involved in the repair response to injury by secreting proteins of the extracellular matrix (ECM) and growth factors, and by differentiating into contractile and secretory myofibroblasts, characterized by α-smooth muscle actin (α-SMA) expression and active ECM synthesis [29]. The cytokine TGF-β1 is also a major player in fibrosis and in particular induces differentiation of fibroblasts to myofibroblasts [10]. In fibrotic conditions in general, myofibroblasts remain at injury sites where they secrete ECM proteins in excess to thereby severely impair tissue function.

Our previous study showed that primary fibroblasts derived from DMD muscles have a pro-fibrotic phenotype probably due to intrinsic memory of their native environment, which is altered by the primary genetic defect [54, 55]. We have also shown that transcript expression and protein modulation of several ECM components are altered in DMD myotubes [58]. These findings indicate that both myogenic cells and resident fibroblasts contribute to

fibrosis in DMD skeletal muscle, and to elucidate the molecular mechanisms of the fibrotic process it is essential to better understand the roles played by fibroblast and myoblast cell lineages.

MicroRNAs (miRNAs) are small non-coding RNA molecules found in plants and animals, whose main function seems to be to downregulate gene expression by various mechanisms, including, translation repression, and mRNA cleavage and deadenylation.

Recent evidence indicates that miRNAs also play fundamental roles in other biological and also pathological processes. In particular, aberrant expression of miRNAs has been related to the development of fibrosis in various tissues through regulation of anti- and pro-fibrotic genes [5].

MiR-21 was originally considered an oncomiR, as it is over-expressed in most cancer types [27], but recent data show that it is one of the most highly upregulated miRNAs during tissue injury, and that its persistent overexpression disrupts tissue repair and contributes to tissue fibrosis in heart [6], kidney[12], liver [32] and lung [23].

MiR-21 is also upregulated during the wound contraction and collagen deposition phases of skin wound healing [48],

and promotes keratinocyte migration by inhibiting TIMP-3 [52]. MiR-21 is rapidly induced by TGF-β1 treatment, suggesting that it may be involved in the pro-fibrotic effects of TGF-β1 [5].

Finally, in mice with experimentally-induced or age-associated (*mdx*) muscle fibrosis, miR-21 biogenesis is regulated by the extracellular PAI-1/plasmin system [3].

Recent studies have also shown that the miR-29 family of miRNAs is involved in heart, liver, lung, and skin fibrosis [9, 16, 37, 44]. MiR-29 downregulates the expression of ECM components collagens, fibrillins and elastin, while its downregulation in the dystrophic muscles of *mdx* mice not only results in impaired regeneration, but also directly contributes to muscle fibrosis [47].

MiR-29 also inhibits TGF-β1 induced-transdifferentiation of myoblasts into myofibroblasts [59].

These findings suggest that miR-29 miRNAs have an anti-fibrotic role.

In view of the emerging roles of miR-21 and miR-29 in fibrotic disorders, we evaluated their expression in DMD and control muscle biopsies.

We also analysed miR-21 expression in DMD and control

muscle-derived fibroblast cultures (since preliminary studies, not presented, indicated that miR-21 is predominantly expressed in this cell lineage) and miR-29 expression in myoblast cultures (since our preliminary data indicate that miR-29 is predominantly expressed in these cells). We assessed the expression of these miRNAs in cultures treated and not treated with TGF-β1.

To further probe the roles of miR-21 and miR-29 in muscle fibrosis, we investigated expression levels of miR-21 and miR-29 targets before and after cell transfection with miR-21 inhibitor in DMD fibroblasts, and miR-29 mimics in DMD myoblasts, respectively.

We also examined the PAI-1/plasmin system in fibroblasts since we have previously shown that muscle-derived fibroblasts from DMD patients are fibrogenic [54, 55] and the system is involved in ECM remodelling and regulation of miR-21 biogenesis [3].

Finally, to assess the therapeutic potential of miR-21 inhibition, we treated *mdx* mice with antagomiR-21.

2. Materials and Methods

2.1. Muscle biopsies and cell cultures

Quadriceps muscle biopsies were obtained after informed parental consent from 14 DMD patients (age 1–8 years; no one has ever been under steroid treatment), 5 patients with congenital muscular dystrophy 1A (MDC1A) as positive controls (age 1 month–3 years) and 11 age-matched controls (age 1–7 years) with suspected neuromuscular disease, but normal muscle on biopsy. Investigations on human tissue were approved by our institutional review board and were in accordance with the Italian law.

DMD and MDC1A were diagnosed by dystrophin/laminin alpha2 chain testing and gene analysis.

Fibroblasts and myoblasts were obtained from three DMD patients (aged 2–6 years) and three age-matched controls (age 3–4 years), by immunomagnetic selection from primary muscle biopsy-derived cell cultures, as described elsewhere [58]. Fibroblasts were cultured in Dulbecco's modified Eagle's medium (DMEM; Lonza Group Ltd, Basel, Switzerland), supplemented with 10% heat-inactivated foetal bovine serum (FBS; Gibco Life Technologies,

Carlsbad, CA, USA), 1% penicillin–streptomycin (Lonza), and 2 mM L-glutamine (Lonza).

Myoblasts were cultured in DMEM supplemented with 20% FBS, 1% penicillin–streptomycin, 2 mM L-glutamine, 10 µg/ml insulin (Sigma Aldrich, St. Louis, MO, USA), 2.5 ng/ml basic fibroblast growth factor (bFGF; Gibco), and 10 ng/ml epidermal growth factor (EGF; Gibco). Experiments were performed on early passages (3–10 passages) of normal and dystrophic fibroblasts and myoblasts.

Control and DMD fibroblasts and myoblasts were treated with 10 ng/ml h-recombinant TGF-β1 (Peprotech EC, London, UK) for 48 h, as described previously [55].

2.2. Purification and quantification of miRNA

The miRNA fraction was isolated using a miRNA isolation kit (mirVana, Ambion, Austin, TX, USA) according to the manufacturer's instructions. MiRNA was reverse-transcribed with the TaqMan miRNA Reverse Transcription kit (Life Technologies) according to the manufacturer's instructions.

MiR-21 (hsa-miR-21-3p), miR-29a (hsa-miR-29a-3p) and miR-29c (hsa-miR-29c-3p) expression levels were

quantified using the TaqMan assay for miRNA and the TaqMan Universal Master Mix (both from Applied Biosystems, Carlsbad, CA, USA). MiR-U6B was used as endogenous control for miR-21, miR-29a and miR-29c.

The expression of each miRNA in control and DMD fibroblasts, myoblasts and muscle was normalized to the expression of miR-U6B and determined as the ratio of the target miRNA to the miR-U6B calculated by $2^{-\Delta\Delta Ct}$, where $\Delta\Delta Ct = Ct_{Target} - Ct_{U6B}$. Quantitative PCR data were expressed as “fold changes” relative to control levels expressed as 1.

Each analysis was performed in duplicate and repeated at least three times with RNA from three different control and three different DMD cell lines.

2.3. Real time PCR

Total RNAwas isolated from fibroblasts, myoblasts and muscle tissues using TRI Reagent (Ambion) according to the manufacturer's instructions, and checked spectrophotometrically for quantity and purity using a Nanodrop 2000C spectrophotometer (Thermo Scientific, Waltham, MA, USA). RNA aliquots (1 µg) were reverse-transcribed in the presence of 5× first strand buffer (Life

Technologies), 1mMeach deoxynucleoside triphosphate, 8 pM random hexamers, 10 μM dithiothreitol, 1 IU/μl RNAse inhibitor (Roche Molecular Biochemicals, Basel, Switzerland), and 10 IU/μl M-MLV reverse transcriptase (Life Technologies) with incubation at 37 °C for 1 h and at 95 °C for 5 min. The reaction product was stored at−20 °C pending use. cDNA integrity was assessed by PCR amplification of human glyceraldehyde-3-phosphate dehydrogenase (NM_002046.5) with specific primers (forward 5′-GAAGGTGAAGGTCGGAGTC-3′ and reverse 5′-GAAGATGGTGATGGGATTTC-3′). PCR conditions were: 94 °C for 1 min, 54 °C for 1 min, and 72 °C for 1 min, for 35 cycles. Mouse cDNA integrity was assessed by PCR amplification of mouse actin (NM_009606.3) with specific primers (forward 5′-AGCCATGTACGTAGCCATCC-3′ and reverse 5′-CTCTCAGCTGTGGTGGTGAA-3′).

Human COL1A1 (Hs01076772_gH), COL3A1 (Hs00943809_m1), COL6A1 (Hs01095579_g1), PTEN (Hs02621230_s1), SPRY-1 (Hs01083036_s1), FBN1 (Hs00171191_m1), YY1 (Hs00231533_m1), PAI-1 (Hs01126604_m1, SERPINE), HMGA2 (Hs00971725_m1), and TWF1 (Hs00702289_s1) transcripts; and mouse PTEN (Mm00477208_m1), SPRY-1 (Mm01285700_m1) and ACTB (4352341E) transcripts, were quantified by quantitative real time PCR using

TaqMan Universal PCR Master Mix and Assays-on-Demand Gene Expression probes (Applied Biosystems). Reactions were performed in 96-well plates with 25 µl volumes. Cycling conditions were: 2 min at 50 °C, 95 °C for 10 min, and followed by 40 cycles of PCR (15 s at 95 °C and 1 min at 60 °C). Products were detected with the ABI Prism7000 sequence detection system (Applied Biosystems).

The expression of each transcript in control and DMD fibroblasts, myoblasts and muscle was normalized to the expression of β-actin and determined as the ratio of the target transcript to the β-actin transcript calculated by $2^{-\Delta\Delta Ct}$, where $\Delta\Delta Ct = Ct_{Target} - Ct_{ß\text{-}actin}$. Quantitative PCR data were expressed as “fold changes” relative to control levels expressed as 1. Each real-time RT-PCR analysis was performed in duplicate and repeated at least three times with RNA from three different control and three different DMD cell lines.

2.4. Transfection of miR-21 inhibitor and miR-29 mimic

5 × 105 cells (fibroblasts or myoblasts) were seeded into six-well plates and grown to 60% confluence. Human hsa-

miR-21 (MIMAT0004494) inhibitor, hsa-miR-29a (MIMAT0000086) and hsa-miR-29c (MIMAT0000681) mimics (Life Technologies) and controls (scrambled miRNAs) were allowed to form transfection complexes with Lipofectamine RNAiMax transfection reagent (Life Technologies) in Opti-MEM I Reduced Serum Medium (Life Technologies) at a final concentration of 30 nM for 15 min at room temperature.

After 24 h, the culture medium was changed; after 48 h samples were either collected for extraction of mRNA and miRNAs, or cells were analysed for immunocytochemistry and culture media collected for further analyses. Transfection conditions were defined by preliminary tests using FAM dye-labelled miRNA random sequence (Applied Biosystems). The let-7c/HMGA2 (High Mobility Group AT-hook 2) (Applied Biosystems) system was used as positive

control in fibroblast miRNA inhibition experiments, while miR-1/TWF1 (Applied Biosystems) system was used as positive control in myoblast miRNA mimic experiments. After miRNA inhibitor let-7c transfection, a significant increase in mRNA levels of HMGA2 was detected in fibroblasts; while after miRNA mimic miR-1 transfection, a significant decrease in TWF1 mRNA levels was detected in myoblasts, as expected (data not shown).

2.5. Quantification of soluble/extracellular collagen in cell cultures

Total soluble (non cross-linked) collagen was measured in supernatants from control and DMD fibroblasts and myoblasts, by a quantitative dye-binding method using the Sircol collagen assay (Biocolor, Belfast, N. Ireland), according to the manufacturer's instructions. Protein concentration in collected supernatants was determined using the DC Protein Assay Reagent (Bio-Rad Laboratories, Hercules, CA, USA) and used for normalization of soluble collagen.

2.6. PAI-1 secretion and plasmin activity

PAI-1 secretion in cell cultureswas evaluated by ELISA (Life Technologies) following the manufacturer's instructions, before and after TGF-β1 treatment, and after miR-21 inhibition.

Plasmin activity was measured indirectly in control and DMD fibroblasts using the plasmin-specific chromogenic substrate D-Val-Leu-Lys p-nitroanilide dihydrochloride (Sigma Aldrich). Culture supernatants (35 µl) were incubated at 37 °C in a 96-well plate with 25 µl 0.1 M Tris–HCl (pH 7.6) containing 2 mM EDTA and with 10 µl 1.5

mM chromogenic substrate. P-nitroanilide release over 120 min was monitored by measuring absorbance at 405 nm with a microplate reader (Victor Wallac 1420, Perkin Elmer, San Diego, CA, USA). Plasmin activity was normalized to cell number (determined by MTT assay, as described in [56]) in each well.

2.7. Immunocytochemistry

After fixation in 4% paraformaldehyde for 30 min and permeabilization with 0.1% Triton-X 100 for 10 min, cells were incubated in PBS containing 1% BSA for 30 min at room temperature, and overnight at 4 °C with one of the following antibodies: mouse monoclonal anti-PTEN (Sigma, 1:30 dilution), rabbit polyclonal anti-collagen I (Chemicon, Millipore, Billerica, MA, USA; 1:150 dilution), mouse monoclonal anti-collagen VI (Chemicon; 1:150 dilution) and rabbit polyclonal anti-PAI-1 (Santa Cruz Biotechnology, Santa Cruz, CA, USA; 1:100 dilution). The cells were then incubated in Alexa 488-conjugated goat anti-rabbit IgG (for collagen I) or in Alexa 488-conjugated goat anti-mouse IgG (for PTEN and collagen VI) (both diluted 1:2000, Life Technologies) for 2 h, followed by DAPI (Sigma) 1:30,000 for 10 min. Cells were examined under a Zeiss Axioplan fluorescence microscope (Carl

Zeiss AG, Oberkochen, Germany) and pictures were taken with the same exposure settings. Muscle cryosections were incubated for 90 min in anti-collagen I or anti-collagen VI primary antibody, followed by incubation in Alexa 488-conjugated goat anti-mouse or anti-rabbit IgG, 1:2000, for 2 h.

Connective tissue extent was measured on collagen VI- and collagen I immunostained sections at ×20 magnification using the NIH Image software version 1.62 (http://rsb.info.nih.gov/nih-image/), as previously described [57].

2.8. Western blot

Fibroblasts transfected with miR-21 inhibitor were washed with PBS and lysed in extraction buffer (10 mM Tris–HCl pH 7.4, 150 mM NaCl, 1 mM EDTA, 1 mM EGTA, 0.5% Nonidet-P, 1% Triton X-100) containing a protease inhibitor cocktail (Pierce Biotechnology, Rockford, IL, USA)

for 30 min on ice. The lysate was centrifuged (18,000 g, 15 min, 4 °C), the supernatant collected, and its protein concentration determined with DC Protein Assay Reagent (Bio-Rad). Aliquots containing 30 μg protein were solubilized in 2× Laemmli buffer (0.5 M Tris–HCl, pH 6.8,

20% glycerol, 2% SDS, 5% 2-mercaptoethanol, 1% bromophenol blue), boiled, separated by 4–10% SDS polyacrylamide gel electrophoresis (SDSPAGE), and transferred to nitrocellulose membranes (Schleicher and Schuell, Keene, NH, USA). Membranes were probed with anti-PTEN (mouse monoclonal, 1:500; Sigma), anti-Spry-1 (rabbit polyclonal, 1:250; Santa Cruz) anti-AKT (rabbit polyclonal, 1:300; Cell Signaling Technology, Boston, MA, USA), and anti-pAKT (mouse monoclonal, 1:300; Cell Signaling Technology).

Extracellularly secreted collagen I was detected in culture medium.

Supernatant proteins were separated on 4–10% SDS-PAGE. In the absence of a reference standard (not available for extracellularly secreted proteins) all lanes were loaded with equal amounts (40 μg) of total protein.

After separation biotin-conjugated secondary antibody was applied (1:2500; Jackson ImmunoResearch), followed by peroxidase-conjugated streptavidin (1:3000; Jackson ImmunoResearch), and detection with the ECL chemiluminescence reagent (Amersham Biosciences).

2.9. Animals and experiments on mdx mice

C57BL/10ScSn-Dmd*mdx*/J mice were from Jackson Laboratory (Bar Harbor, Maine, USA). Animal studies were approved by our review board, in accordance with the Italian Health Ministry guidelines. Animal care and use was in accordance with the Italian law and the EU directive 2010/63/EU. The animals were housed in our facility under 12 h light/12 h dark conditions with free access to food and water.

To knockdown miR-21 expression in three-month-old *mdx* mice (5 per group), antagomiR-21 (5′-CCATCGACTGCTGTT-3′) or scrambled (5′-ACGTCTATACGCCCA-3′) locked nucleic acid oligonucleotides (Exiqon A/S, Vedbaek, Denmark) were injected intraperitoneally (10 mg/kg in PBS) using a 26-gauge needle. Three injections were given (day 1, 48 h after first injection, and 15 days after first injection).

Four weeks after first injection, the animals were sacrificed by cervical dislocation under anaesthesia; the diaphragm muscles were rapidly removed, frozen in isopentane pre-cooled in liquid nitrogen, and maintained in liquid nitrogen pending use. Haematoxylin and eosin (H&E), Gomori modified trichrome, acid phosphatase, and immunohistochemical stainings were performed on consecutive 6–8 μm-thick cryosections.

Numbers of acid-phosphatase-positive cells from highly inflamed and mildly inflamed regions were counted on micrographs of acid phosphatase-stained sections, as described in Gibertini et al. [13].

Muscle fibrosis was quantified on diaphragm preparations immunostained to reveal collagens I and VI together. To block non-specific binding, sections were pre-incubated (30min)with 10% goat serum (Jackson ImmunoResearch) in PBS, followed by incubation (2 h) with both anti-collagen

I (Chemicon, 1:40) and anti-collagen VI (Santa Cruz, 1:100) polyclonals. Incubation (60 min) with Alexa 488-goat anti-rabbit IgG (1:2000, Life Technologies) followed. As control, sections were incubated either with rabbit non-immune serum, or isotype-specific non immune IgG (Dako), or the primary antibodies were omitted. The area of collagen immunostaining, as indicator of fibrosis, was determined at ×20 magnification as described [13]. Briefly, 4 randomly selected fields were photographed from each section and digitalized. Using the software, the photographs were inverted and a threshold was applied to obtain black and white images with areas positive for collagens in black and negative areas in white. Manual corrections were sometimes applied to eliminate non-muscle/non-fibrosis areas or to add areas not recognized

by the software. The area positive for collagens was calculated as a percentage of the entire image, and the mean percentage for each group of animals calculated.

2.10. Quantitation of soluble collagens in mdx diaphragm

Acid-soluble collagen concentration was determined in mouse diaphragms by the Sircol Collagen Assay (Biocolor), according to the manufacturer's instructions. Briefly, tissue samples were incubated over-night at 4 °C in 0.5Macetic acid. 20 µl of samples' acid-soluble collagens and reference standard were added to 200 µl of the colorimetric reagent and gently mixed for 30 min, followed by centrifugation at 10,000 g for 10 min. To remove unbound dye a wash with ice-cold Acid-Salt Buffer wash was performed. The SR dye was released from the pellet with Alkali Reagent and colorimetric readings were taken in duplicate at 550 nm. The amount of soluble collagens was expressed as µg of collagens per mg of tissue.

2.11. Statistical methods

Results were expressed as means and standard

deviations (±). Differences between DMD and control were assessed by the two-tailed Student's t-test or one-way ANOVA with post-hoc Dunnett's test, where appropriate. Differences in gene expression between cells treated and not treated with TGF-β1 were assessed using a mathematical model based on PCR efficiency described by Pfaffl [36]. P values ≤ 0.05 were considered significant. ELISA data were processed using a four parameter logistic model (Readerfit programme; http://www.readerfit.com/). Each experiment, performed in duplicate or triplicate, used separate cultures obtained from three DMD patients and three controls.

Associations of miRNA (miR-21, miR-29a, miR-29c) expression levels with levels of collagen I and VI transcripts and proteins (considered markers of fibrosis, [61]), and patient age (considered an indicator of disease progression [18]), were assessed by Pearson's linear regression analysis.

3. Results

3.1. MiR-21 was increased and miR-29 decreased in DMD muscle; miR-21 was upregulated in DMD fibroblasts, and miR-21, miR-29a and miR-

29c levels were downregulated in DMD myoblasts

In DMD muscles, levels of miR-21 (6.95 ±6.40, $p<0.001$) were significantly higher, and levels of miR-29a (0.29 ± 0.12, $p<0.001$) and miR-29c (0.32 ± 0.15, $p<0.001$) significantly lower than in control muscles (Fig. 1G). Similarly, in MDC1A muscles, levels of miR-21 were significantly higher (3.06 ± 0.54, $p<0.001$), and levels of miR-29a (0.10 ± 0.05, p b 0.001) and miR-29c (0.015 ± 0.007, $p<0.001$) were significantly lower than in controls (not shown).

MiR-21 expression ($R = 0.74$, $p<0.05$) (Fig. 1A) and COL1A1 mRNA levels ($R=0.62$; $p<0.05$) correlated directly with patient age (Pearson's linear regression, Fig. 1B). MiR-21 levels also correlated with COL1A1 ($R = 0.91$, $p<0.001$) and COL6A1 mRNA levels ($R = 0.69$, $p<0.05$) (Figs. 1C, D), but not with the related proteins collagen I ($R = 0.09$, $p=0.77$) or collagen VI ($R=-0.12$, $p=0.51$) (not shown), both evaluated as indicative of connective tissue extent.

MiR-29a correlated directly with both COL1A1 ($R = 0.81$, $p<0.05$) and COL6A1 ($R=0.81$, $p<0.05$) transcript levels (Figs. 1E, F). No correlation was found between miR-29a and connective tissue extent evaluated by collagen I ($R=0.37$, $p=0.23$) and collagen VI ($R=0.27$, $p=0.38$)

immunostaining (not shown). No correlation was found between miR-29c and COL1A1 ($R = 0.18$, $p = 0.55$) or COL6A1 ($R= 0.03$, $p = 0.90$) transcript levels, or between miR-29c and connective tissue extent evaluated by collagen I ($R=-0.36$, $p=0.22$) and collagen VI ($R=0.16$, $p=0.58$) immunostaining in muscle (not shown).

In fibroblasts not treated with TGF-β1, miR-21 expression levels were significantly higher in DMD fibroblasts (1.86 ± 0.37; $p<0.05$) than control fibroblasts (expressed as 1). No differences in miR-29a (0.95 ± 0.32, $p=0.94$) or miR-29c (0.74 ± 0.18, $p=0.08$) expression were found in DMD compared to control fibroblasts (Fig. 1H).

After TGF-β1 treatment miR-21 expression was significantly higher (2.11 ± 0.08, $p<0.001$), and miR-29a (0.59 ± 0.13, $p< 0.05$) and miR-29c (0.64 ± 0.06, $p<0.05$) expression significantly lower, in DMD fibroblasts compared to similarly treated control fibroblasts (Fig. 1I). There were no significant differences between treated and untreated control fibroblasts or between treated and untreated DMD fibroblasts.

As regards myoblasts not treated with TGF-β1, miR-21 (0.62 ± 0.23, $p<0.05$), miR-29a (0.46 ± 0.09, $p<0.001$) and miR-29c (0.48 ± 0.19, $p < 0.05$) levels were significantly lower in DMD myoblasts than in controls (expressed as 1)

(Fig. 1J).

After TGF-β1 treatment, mR-21 expression (1.1 ± 0.37, p = 0.67) and miR-29a (0.52±0.33, p=0.06) in DMD myoblasts were no longer significantly lower than in controls, while miR-29c levels (0.45 ± 0.21, p< 0.05) in DMD myoblasts remained significantly lower than those in controls (Fig. 1K). There were no significant differences between treated and untreated control fibroblasts or between treated and untreated DMD myoblasts.

3.2. MiR-21 targets were downregulated in DMD fibroblasts; and miR-29 targets were upregulated in DMD myoblasts

Search in the TargetScan or in microRNA database (www.targetscan.org and http://www.microrna.org), detected putative miR-21 or miR-29 binding sites in the untranslated regions of all the following target genes: PTEN and SPRY-1, both targets of miR-21; COL3A1, FBN1 and YY1, all targets of miR-29. These molecules have also been shown to be targets of miR-21 or miR-29, respectively, by 3′-UTR luciferase assay [28, 43, 44].

In DMD fibroblasts not treated with TGF-β1, levels of PTEN (0.60 ± 0.17, p<0.05) and SPRY-1 (0.69 ± 0.06,

p<0.001) transcripts were significantly lower than in controls (expressed as 1), while levels of COL1A1 (1.96 ± 0.35; p<0.05) and COL6A1 (1.85 ± 0.64; p<0.05) were significantly higher than in control fibroblasts (expressed as 1) (Fig. 2A). After TGF-β1 treatment, the levels of these transcripts in DMD fibroblasts did not change significantly compared to levels in untreated DMD fibroblasts (not shown).

In DMD myoblasts not treated with TGF-β1, COL1A1 (1.63 ± 0.34, p<0.05) and COL6A1 (1.76 ± 0.35, p<0.05) transcripts were significantly higher than those in untreated control myoblasts (Fig. 2B). Levels of COL3A1, FBN1, and YY1, were also significantly higher in untreated DMD myoblasts than untreated controls (expressed as 1) (COL3A1: 2.09 ± 0.51, p< 0.05; FBN1: 1.68 ± 0.36, p< 0.05; YY1: 1.63 ± 0.15, p< 0.001) (Fig. 2B). Following TGF-β1 treatment, levels of these transcripts in DMD myoblasts did not change significantly compared to those in untreated DMD myoblasts (not shown).

3.3. Transfection of miR-21 inhibitor and miR-29 mimic respectively lowered and increased miRNA levels

To further explore the effects of miRNAs in fibroblasts and myoblasts, the cells were transiently transfected with either miR-21 inhibitor or miR-29 mimics. Transfection efficiency was evaluated measuring miRNA levels by RT-PCR.

Forty-eight hours after transfection, miR-21 levelswere significantly lower in inhibitor-transfected DMD fibroblasts than scrambled transfected DMD fibroblasts: 0.38 ± 0.03 vs. 1.86 ± 0.37 ($p< 0.05$) (Fig. 3A).

Forty-eight hours after transfection, miR-29a and miR-29c levels were significantly higher in mimic-transfected DMD myoblasts, than scrambled-transfected DMD myoblasts. Specifically, after miR-29a mimicking both miR-29a (13.18 ± 0.56 vs. 0.46 ± 0.11; $p<0.001$) and miR-29c (24.71 ± 6.21 vs. 0.46 ± 0.11; $p<0.05$) were increased, and after miR-29c mimicking both miR-29a (6.74 ± 0.24 vs. 0.48 ± 0.18; $p<0.001$) and miR-29c (37.48 ± 1.99 vs. 0.48 ± 0.18; $p<0.001$) were increased. The effects of both miR-29a and miR-29c mimics together on transcription levels of miR-29a and miR-29c were also assessed. No significant differences in transcription levels of miR-29a and miR-29c after double transfection compared to single transfection were observed (miR-29a: 10.43 ± 1.8; miR-29c: 37.14 ± 6.00) (Fig. 3B).

3.4. MiR-21 inhibitor and miR-29 mimic transfection modulate target transcripts

In DMD fibroblasts, decreasing miR-21 levels by miR-21 inhibitor transfection was sufficient to induce upregulation of miR-21 target transcripts and downregulation of fibrosis related transcripts compared to scrambled-transfected DMD fibroblasts. Specifically, miR-21 silencing significantly

increased PTEN mRNA (2.01±0.69 vs. 0.6±0.17; $p<0.05$) and SPRY-1 mRNA (1.50 ± 0.23 vs. 0.69 ± 0.06; $p<0.05$); and significantly decreased COL1A1 mRNA (0.40 ± 0.20 vs. 1.96 ± 0.35; $p<0.05$) and COL6A1 mRNA (0.60 ± 0.27 vs. 1.85 ± 0.64; $p<0.05$) compared to scrambled-transfected DMD fibroblasts (Fig. 4A).

In DMD myoblasts, increasing miR-29 levels by transfection with miR-29a and miR-29c mimics induced downregulation of miR-29 targets.

Thus, after miR-29a mimicking, COL3A1 transcript levels were 0.52 ± 0.23 vs. 2.09 ± 0.51 in scrambled-transfected DMD myoblasts ($p<0.05$); FBN1 levels were 0.44±0.29 vs. 1.63±0.36 ($p<0.005$); and YY1 levels were 0.51 ± 0.37 vs. 1.68 ± 0.15 ($p<0.05$). After miR-29c mimicking COL3A1 levels were 0.25 ± 0.26 vs. 2.09 ± 0.51 ($p<0.05$); FBN1 levels were 0.70 ± 0.23 vs. 1.63 ± 0.36 ($p<0.05$); and YY1

levels were 1.08 ± 0.23 vs. 1.68 ± 0.15 ($p<0.05$). After co-transfection of miR-29a and miR-29c, COL3A1 levels were 0.35 ± 0.27 vs. 2.09 ± 0.51 ($p<0.05$); FBN1 levels were 0.51 ± 0.28 vs. 1.63 ± 0.36 ($p<0.05$); and YY1 levels were 0.66 ± 0.27 vs. 1.68 ± 0.15 ($p<0.05$).

Results using double miR-29 transfection did not differ from those obtained with single transfection (Fig. 4B).

COL1A1 and COL6A1 transcript levels were also evaluated in DMD myoblasts before and after miR-29 mimicking. In all conditions tested (miR-29a, miR-29c, miR-29a plus miR-29c), both COL1A1 and COL6A1 mRNA levels were significantly lower than in scrambled-transfected DMD myoblasts. Thus, after miR-29a mimic, COL1A1 was 0.27 ± 0.11 vs. 1.63 ± 0.34 ($p<0.001$); COL6A1 was 0.88 ± 0.08 vs. 1.76 ± 0.35 ($p<0.001$). After miR-29c mimic, COL1A1 was 0.39 ± 0.23 vs. 1.63 ± 0.34 ($p<0.05$); and COL6A1 was 0.57 ± 0.16 vs. 1.76 ± 0.35 ($p<0.001$).

After co-transfection of miR-29a and miR-29c, COL1A1 was 0.39 ± 0.30 vs. 1.63 ± 0.34 ($p<0.05$); and COL6A1 was 0.58 ± 0.06 vs. 1.76 ± 0.35 ($p<0.001$). Results using double miR-29 transfection did not differ from those obtained with single transfection (Fig. 4C).

3.5. MiR-21 inhibitor and miR-29 mimic transfection modulated protein expression

PTEN was not detected by immunocytochemistry in scrambled transfected DMD fibroblasts in basal conditions, but was expressed in the cytosol after miR-21 inhibition. Both collagen I and collagen VI immunostaining was clearly reduced in inhibitor-transfected compared to scrambled-transfected DMD fibroblasts (Fig. 5A). Collagen I and collagen VI immunostaining was also clearly reduced in DMD myoblasts after miR-29a and miR-29c mimicking, compared to scrambled transfected DMD myoblasts (Fig. 5B).

To determine whether PTEN is post-transcriptionally inhibited by miR-21, PTEN protein expression was further assessed in DMD fibroblasts by Western blot. A marked increase in PTEN protein after DMD fibroblast transfection with miR-21 inhibitor was found compared to scrambled-transfected DMD fibroblasts, showing that PTEN is a direct

target of miR-21 (Fig. 5C). Since PTEN is a negative regulator of the

Akt/PI3-kinase pathway, Akt/PI3K downstream signalling was also evaluated: it was found that phosphorylated-Akt (Ser473) was reduced after miR-21 silencing in DMD

fibroblasts (Fig. 5C). Akt/PI3K signalling has also been implicated in collagen production [24], so collagen I expression in DMD fibroblast supernatants was evaluated. MiR-21 inhibition induced a decrease in collagen I expression compared to DMD scrambled-transfected fibroblasts (Fig. 5C). Spry-1 expression was also increased in DMD fibroblasts after miR-21 inhibition (Fig. 5C).

3.6. MiR-21 inhibitor and miR-29 mimic transfection modulated soluble collagen production

Under basal conditions, soluble collagen production was significantly greater in the culture medium of DMD fibroblasts than in medium of control fibroblasts (237.71±12.88 μg/ml vs. 135.53±1.49 μg/ml; $p<0.05$).

TGF-β1 treatment induced a further significant increase in soluble collagen production in DMD fibroblasts only (385.83 ± 38.47 μg/ml, $p<0.05$).

MiR-21 silencing induced a significant reduction in soluble collagen production both in DMD(35.94±10.69 μg/ml; $p<0.001$) and control fibroblasts (44.41 ± 19.25 μg/ml; $p<0.05$) compared to medium from scrambled-transfected cells (Fig. 6A).

Under basal conditions soluble collagen production was significantly higher in culture medium of DMD myoblasts than control myoblast medium (131.73 ± 18.91 µg/ml vs. 37.02 ± 0.92 µg/ml; $p<0.05$). TGF-β1 treatment had no significant effects. Only transfection of control myoblasts with miR-29c mimic induced a significant reduction in soluble collagen production compared to scrambled-transfected control myoblasts (19.89 ± 4.66 µg/ml vs. 37.02 ± 0.92 µg/ml; $p<0.05$). In DMD myoblasts, by contrast, significant reductions in collagen production occurred after miR-29a (55.63 ± 13.56 µg/ml; $p<0.05$), miR-29c (67.46 ± 7.23 µg/ml, $p<0.05$) and miR-29a plus miR-29c mimic transfection (48.77 ± 6.58 µg/ml; $p<0.05$) compared to scrambled transfected myoblasts (131.73 ± 40.12 µg/ml) (Fig. 6B).

3.7. PAI-1/plasmin were downregulated by miR-21 inhibition in DMD fibroblasts

Transcript levels of PAI-1were significantly higher in DMD fibroblasts (2.19 ± 0.12) than control fibroblasts ($p<0.001$), and increased further after TGF-β1 treatment (2.42±0.22, $p<0.001$). No significant difference between basal DMD fibroblasts (not treated with TGF-β1) and TGF-β1-treated fibroblastswas observed. PAI-1 transcript levels were

significantly lower in DMD fibroblasts after miR-21 silencing compared to control fibroblasts (0.34 ± 0.27 vs. 2.19 ± 0.12; $p<0.05$; Fig. 7A).

PAI-1 protein was expressed in a punctate pattern in the nucleus and cytoplasm of DMD fibroblasts in basal conditions; after miR-21 silencing positivity decreased in both compartments (Fig. 7B).

PAI-1 production was significantly higher in basal conditions in DMD fibroblasts (965.08 ± 37.82 pg/ml) than control fibroblasts (261.53 ± 53.99 pg/ml; $p<0.05$). TGF-β1 treatment induced a significant increase in PAI-1 production both in DMD (4638.11 ± 143 pg/ml; $p<0.05$) and control (3602.75 ± 297 pg/ml; $p<0.05$) fibroblasts, compared to untreated cells. MiR-21 silencing in DMD fibroblasts significantly reduced PAI-1 production (437.88 ± 132 pg/ml vs. 965.08 ± 37.82; $p<0.001$) compared to DMD fibroblasts under basal conditions (Fig. 7C).

The enzymatic activity of plasmin was significantly lower in DMD fibroblast culture medium than control fibroblast medium (3.37 ± 0.46 ng substrate/min vs. 10.29 ± 4.58; $p<0.05$). Plasmin activity significantly increased in DMD fibroblast medium after miR-21 inhibition (7.47 ± 0.76 ng substrate/min; $p<0.001$) compared to untransfected DMD fibroblasts (Fig. 7D).

3.8. AntagomiR-21 treatment reduced muscle fibrosis in mdx mouse diaphragm

Histological evaluation of diaphragm muscle of *mdx* mice treated with antagomiR-21 showed that the morphology was better organized than scramble-treated diaphragms (Figs. 8A, B).

Numbers of acid phosphatase positive cells did not differ significantly between, respectively, highly or mildly inflamed regions of muscles from antagomiR-21-treated, and highly or mildly inflamed regions of muscles from scramble-treated mice (not shown). Assessment of miR-21 targets in diaphragm showed that PTEN (2.25±0.81; $p<0.01$) and SPRY-1 (1.61±0.82; $p<0.05$) transcript levels were significantly higher in antagomiR-21-treated compared to scramble-treated diaphragms (expressed as 1) (Fig. 8E). Immunostaining of diaphragm showed that collagen I and collagen VI were present in the perimysium and endomysium and that areas of collagen I/collagen VI positivity (Figs. 8C,D) were significantly lower in antagomiR-21-treated (19.02 ± 2.71% area) than scramble-treated diaphragms (22.56 ± 4.41% area; $p<0.01$) (Fig. 8F).

Assessment of soluble collagens extracted from the diaphragm of treated and untreated animals revealed that

collagens were significantly reduced in antagomiR-21-treated than scramble-treated diaphragms (41.42 ± 5.04 vs. 48.8 ± 4.86 μg/mg of tissue; $p<0.05$) (Fig. 8G).

4. Discussion

Our extensive investigations of miR-21 and miR-29 on DMD muscle and muscle-derived cells, show that miR-21 is upregulated in DMD muscles and fibroblasts and miR-29 is downregulated in DMD muscles and myoblasts, with corresponding profibrotic alterations in target transcript and protein expression.

Our miRNA inhibition and mimicking experiments directly implicate miR-21 and miR-29 in fibrosis-related alterations of target transcript and protein expression, and in increased production of ECM proteins and other profibrotic molecules. Overall our data show that these miRNAs have fundamental but opposing roles in regulating fibrosis in skeletal muscle (Fig. 9).

4.1. MiR-21 upregulation and its implications

We found that miR-21 was upregulated in DMD muscle, and that levels correlated directly with COL1A1 and COL6A1 transcript levels (markers of fibrosis, [61]) and also age (marker of disease progression [18]).

MiR-21 upregulation in DMD muscle and fibroblasts, together with upregulation of collagen, downregulation of known miR-21 targets involved in fibrogenesis, and interaction with TGF-β1, all strongly implicate this miRNA as a major player in DMD fibrosis. We also found that miR-21 is upregulated in highly fibrotic muscle biopsies from MDC1A patients, implying that miR-21 is involved in muscle fibrosis in general.

These findings are fully consistent with recent data showing that miR-21 is upregulated in fibrosis of lung, heart, liver and kidney [6, 12, 23, 32], while increased levels of miR-21 in fibroblasts have been found in several other conditions. Thus, Thum et al. [43] showed that miR-21 was weakly expressed in normal myocardium, but after infarction miR-21 levels increased in cardiac fibroblasts, in direct correlation with increased atrial collagen content and reduced SPRY-1 expression.

Roy et al. [38] found increased miR-21 levels in murine

cardiac fibroblasts during heart remodelling after induced myocardial infarction, and identified PTEN as a direct target of miR-21. In liver fibrosis, miR-21 is also upregulated and has been shown to activate stellate cells via PTEN/Akt signalling. Stellate cells are liver-specific and play fundamental roles in several biological and pathological processes including fibrogenesis [50].

The results of our miR-21-silencing experiments in DMD fibroblasts provide further evidence of miR-21 involvement in DMD fibrosis, since silencing resulted in upregulation of PTEN and SPRY-1 indicating that their downregulation is due to miR-21.

PTEN is a key regulator of the cell cycle, cell motility and apoptosis [51]. During normal tissue repair, PTEN upregulation due to ECM contraction induces inhibition of the Akt/PI3-kinase pathway and triggers fibroblast apoptosis and termination of the repair process [31]. In fibrotic conditions, reduction of PTEN expression increases Akt/PI3-kinase signalling and hence fibroblast proliferation and viability, thereby favouring increased fibrosis [33]. In DMD fibroblasts we found that miR-21 upregulation was associated with reduced PTEN expression (transcript and protein) and Akt pathway activation (Western blot of phosphorylated Akt), while miR-21 silencing rescued

PTEN and reduced Akt activation.

We also found that miR-21 silencing reduced collagen I protein expression, probably in relation to reduced Akt activation. Lu et al. [24] demonstrated that in human lung fibroblasts the Akt/PI3K pathway is involved in collagen production and fibroblast proliferation, whilemore recently He et al. [17] demonstrated that PTEN overexpression in lung fibroblasts suppresses collagen I production by inhibiting the Akt/PI3K pathway.

Bujor et al. [7] also found that activated Akt has profibrotic effects in dermal fibroblasts, promoting collagen synthesis

and reducing MMP-1 activity.

As regards SPRY-1 transcripts, their expression is reduced in failing heart, resulting in increased levels of extracellular signal-regulated kinases (ERK), which contribute to fibroblast survival and to interstitial fibrosis [43]. So, reduced expression of this target for miR-21 appears to promote fibrosis and is also consistent with our previous finding that the ERK pathway is upregulated in the same cells [54]. We also found that miR-21 inhibition in DMD fibroblasts induced increased expression of SPRY-1 protein.

4.2. MiR-21 and TGF-β1

TGF-β1 has an established role in fibrosis. Increased levels of TGF-β1 in DMD muscle had been reported previously by our group and others [4, 15, 26, 57]. In the present study we found that treatment of fibroblasts with TGF-β1 resulted in increased miR-21 levels. This is interesting in light of previous studies [6,53] showing that miR-21 downregulation inhibits TGF-β1-induced transdifferentiation of fibroblasts to myofibroblasts, while miR-21 upregulation promotes transdifferentiation. Myofibroblasts are principally responsible for increased collagen synthesis in DMD and other fibrotic conditions [29].

4.3. The PAI-1/plasmin system

In view of our finding [54, 55] that muscle-derived fibroblasts from DMD patients are fibrogenic, we investigated the PAI-1/plasmin system in fibroblasts. This system, in addition to being a negative regulator of the proteolytic activity of plasmin, is also involved in fibrosis and the regulation of miR-21 biogenesis [3]. We found significantly upregulated PAI-1 transcript and protein levels in DMD fibroblasts – further increased by TGF-β1

treatment – with consequent significant reduction in plasmin activity, suggesting that PAI-1 is directly involved in altered ECM homeostasis in DMD. PAI-1 is also linked to miR-21, since we found that miR-21 inhibition in DMD fibroblasts caused a significant reduction in PAI-1 mRNA levels and a significant increase in plasmin activity.

4.4. MiR-21 downregulation as anti-fibrotic therapy

Our findings therefore suggest miR-21 inhibition as a possible approach to reducing fibrosis, since inhibition not only has an antifibrotic effect on known target transcripts, but also an antifibrotic regulatory action on the PAI-1/plasmin system. Previous data also indicate that miR-21 inhibition can reduce fibrosis. Thus in a mouse cardiac hypertrophy model, miR-21 silencing inhibited interstitial fibrosis [43]; miR-21 antisense probes diminished the severity of induced lung fibrosis in mice and attenuated the pro-fibrogenic activity of TGF-β1 in fibroblasts [23]; and antagomiR-21 injection prevented fibrosis in a mouse model of heart infarction [1]. Our experiments on *mdx* mice showed that antagomiR-21 treatment effectively reduced not only levels of target transcripts but also extent of fibrosis and soluble collagen production.

These effects were evident only a month after treatment at lowest dose reported effective in the literature [14, 25, 35]. Thus miR-21 silencing shows promise as an anti-fibrosis therapy. Other miRNAs have been shown to be important modulators of the dystrophic phenotype. For example, Cordani et al. [8] recently showed that nitric oxide-induced upregulation of miR-27 was able to inhibit adipogenesis, which is an integral part of the fibrotic process.

4.5. MiR-29 downregulation and its implications

The miR-29 family comprises miR-29a, miR-29b and miR-29c that have similar sequences, expression patterns and functions [21]. MiR-29s are known to suppress fibrosis by suppressing the expression of various ECM components [19]. Reduced miR-29 expression has been implicated in the development of fibrosis in liver, kidney, lung and heart [16].

Our findings showing that miR-29a and miR-29c expression is reduced in DMD muscle biopsies and myoblasts (and also in highly fibrotic muscle biopsies from MDC1A patients), and that miR-29a and miR-29c mimicking in DMD myoblasts results in modulation of target transcripts involved in fibrosis [44], suggest that

miR-29 upregulation may be a useful mitigation strategy in advanced disease when myoblasts are producing greater quantities of ECM components (normally fibroblasts are the main producers of ECM components).

As well as acting as an anti-fibrogenic regulator, miR-29 also promotes myogenesis by directly inhibiting YY1, a negative regulator of muscle genes [46]. Thus, muscle regeneration inhibited by upregulation of YY1 was reversed by miR-29 upregulation [49].

Our findings that miR-29 downregulation and YY1 upregulation in DMD myoblasts in basal conditions were reversed after miR-29 mimicking, are in agreement with those of Wang et al. [49].

5. Conclusions

Ardite et al. [3] showed that miR-21 is involved in DMD fibrosis, while Wang et al. [47] showed that miR-29 is involved in fibrosis in the *mdx* mouse.

Our data amplify these findings by showing that miR-21 is upregulated in DMD muscles and fibroblasts andmiR-29 is downregulated in DMD muscles and myoblasts, with corresponding profibrotic alterations in target transcript and

protein expression.

Importantly we also show that miR-21 inhibition and miR-29 mimicking in fibrogenic and myogenic cells from DMD patients directly implicate miR-21 and miR-29 in profibrotic alterations of target transcript and protein expression, as well as the increased production of several ECM proteins. Taken together these findings show that miR-21 and miR-29 have fundamental but opposing roles in regulating fibrosis in skeletal muscle.

Finally our studies on *mdx* mice indicate that miR-21 inhibition has promise as an agent for contrasting muscle fibrosis.

In general miRNA modulators can be administered easily, have long duration of action

(up to 6 weeks in mice), are well tolerated, modulate miRNAs in most organs [34] and have more selective actions than the various pleiotropic molecules proposed as anti-fibrotic agents so far [2, 45, 60]. Effective miRNA mimics have become available for whole animal use only very recently.

Montgomery et al. [30] in their study have shown that miR-29 mimics decrease collagen expression and block and reverse bleomycin-induced pulmonary fibrosis. Our study

suggests that a combination of miR-21 inhibition and miR-29 upregulation could be a more effective strategy for treating muscle fibrosis.

Acknowledgements

This work was supported by institutional funds from the Italian Ministry of Health.

The authors gratefully acknowledge EuroBioBank (www.eurobiobank.org) and the Telethon Network of Genetic Biobanks (GTB12001F, www.biobanknetwork.org) for providing biological samples, and thank Don Ward for help with the English.

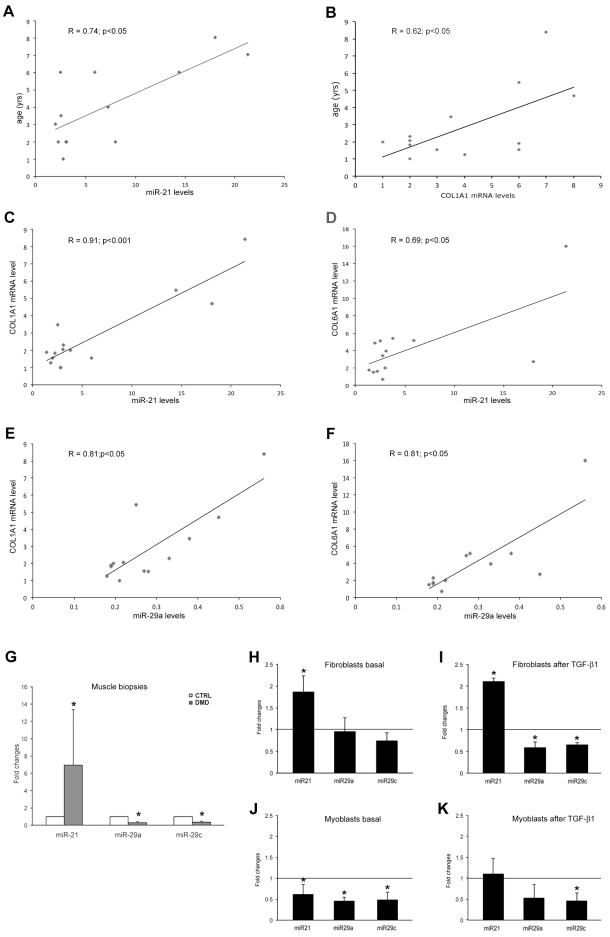

Fig. 1. MiRNA expression in cell cultures and muscle biopsies. Pearson's linear regression analysis showing: (A) positive correlation between miR-21 and patient age; (B) positive correlation between COLA1A transcript levels and patient age; (C) positive correlation between miR-21 and COL1A1 transcript levels; (D) positive correlation between miR-21 and COL6A1 transcripts; (E) positive correlation between miR-29a and COL1A1; and (F) positive correlation between miR-29a and COL6A1. (G) MiR-21, miR-29a and miR-29c levels in DMD and age-matched control muscle (data from 14 patients and 11 controls) as determined by real time PCR. (H) MiR-21, miR-29a and miR-29c levels in DMD fibroblasts in basal conditions and after TGF-β1 treatment. Fold changes are relative to miR-21 or miR-29 levels (expressed as 1) in control fibroblasts. (I) MiR-21, miR-29a and miR-29c levels in DMD myoblasts in basal conditions and after TGF-β1 treatment. Fold changes are relative to miR-21 or miR-29 levels (expressed as 1) in control myoblasts. MiR-21 and miR-29 levels were normalized to miR-U6B expression levels and are presented as means ± standard deviation (data from three duplicated experiments for three cell lines of each cell type).

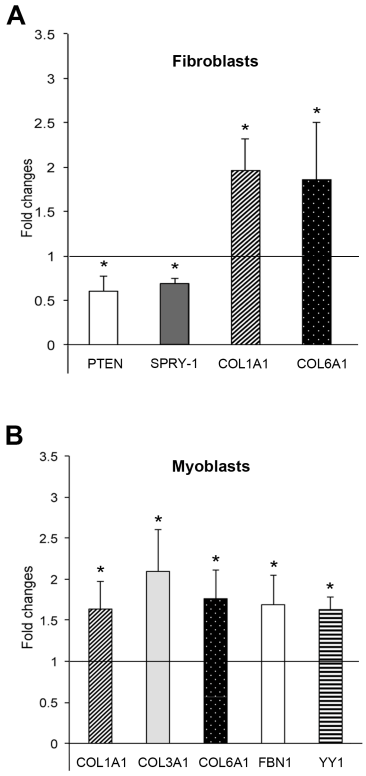

Fig. 2. Expression of target transcripts and fibrosis related genes in cell cultures showing that miR-21 targets are downregulated in DMD fibroblasts; and miR-29 targets are upregulated in DMD myoblasts. (A) Expression of miR-21 target transcripts PTEN and SPRY-1, and of COL1A1 and COL6A1 in DMD fibroblasts in basal conditions. Fold changes are relative to target transcript levels (expressed as 1) in age-matched control fibroblasts. (B) Expression of miR-29 target transcripts COL3A1, FBN1 and YY1, and of COL1A1 and COL6A1, in DMD myoblasts in basal conditions. Fold changes are relative to target transcript levels (expressed as 1) in control myoblasts. Target transcript expression levels are normalized to those of β-actin and presented as means ± standard deviations (data from three duplicated experiments for three cell lines of each cell type).

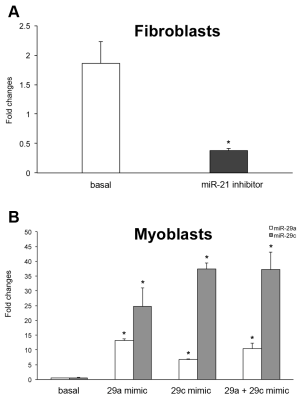

Fig. 3. Transfection of miR-21 inhibitor in DMD fibroblasts and miR-29 mimic in DMD myoblasts respectively lowers and increases miRNA levels. (A) Significant reduction in miR-21 levels after miR-21 inhibition in DMD fibroblasts (0.38 ± 0.03 vs. 1.86 ± 0.37; $p<0.05$) compared to scrambled-transfected DMD myoblasts. (B) Significant increases in miR-29a (13.18 ± 0.56 vs. 0.46 ± 0.11; $p<0.001$) and miR-29c (24.71 ± 6.21 vs. 0.46 ± 0.11; $p<0.05$) after transfection of miR-29a mimic, miR-29c mimic or both compared to scrambled-transfected DMD myoblasts. MiR-21 and miR-29 levels were normalized to those of miR-U6B and are presented as means ± standard deviations of data from three duplicated experiments for three cell lines of each cell type.

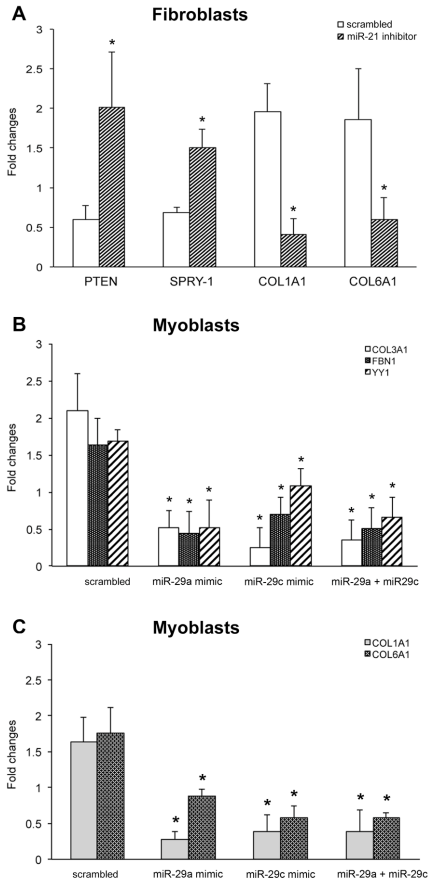

Fig. 4. Effects on target transcripts and fibrosis related genes of miR-21 inhibition in DMD fibroblasts and miR-29 mimicking in DMD myoblasts. (A) Expression levels of miR-21 target transcripts PTEN and SPRY-1, and of COL1A1 and COL6A1 in DMD fibroblasts after miR-21 inhibition relative to expression levels in DMD fibroblasts after transfection with scrambled miRNA. (B) Expression levels of miR-29 target transcripts COL3A1, FBN1 and YY1 in DMD myoblasts after miR-29 mimicking relative to expression levels in DMD myoblasts after transfection with scrambled miRNA. (C) Expression levels of COL1A1 and COL6A1 in DMD myoblasts after miR-29 mimicking. In all cases target transcript levels were normalized to β-actin expression levels and data are presented as means ± standard deviations (data from three duplicated experiments for three cell lines of each cell type).

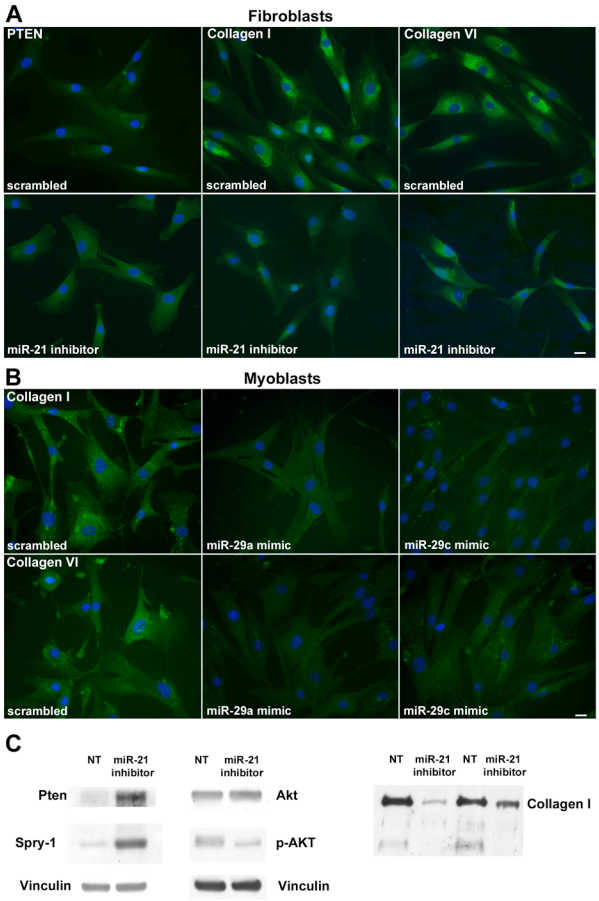

Fig. 5. Immunolocalization of target proteins after miR-21 inhibition in fibroblasts and miR-29 mimicking in myoblasts. (A) In DMD fibroblasts PTEN (Alexa Fluor 488 dye, green) positivity is present in the cytosol after transfection with miR-21 inhibitor, but is not present in DMD fibroblasts transfected with scrambled miRNA. Nuclei stained with DAPI (blue). Collagen I and collagen VI (Alexa Fluor 488 dye, green) positivity is lower in DMD fibroblasts transfected with miR-21 inhibitor than fibroblasts transfected with scrambled miRNA. Scale bar = 20 μm. (B) Staining for collagen I and collagen VI (Alexa Fluor 488 dye, green) is lower in DMD myoblasts after miR-29 mimicking, than staining in DMD myoblasts transfected with scrambled miRNA. Nuclei stained with DAPI (blue). Scale bar = 20 μm.

(C) Representative Western blots of DMD fibroblast cell extracts showing increased expression of PTEN and Spry-1 proteins and decreased expression of phosphorylated Akt; and of fibroblast cell culture supernatants showing collagen I decrease after miR-21 inhibition. NT= not treated.

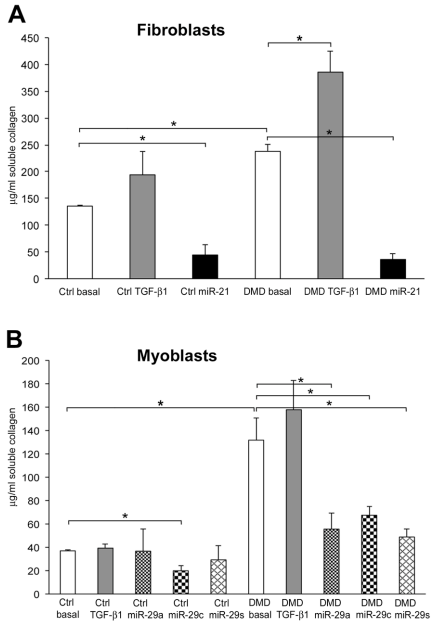

Fig. 6. MiR-21 inhibitor and miR-29 mimic transfection modulate soluble collagen production. (A) Collagen production in culture medium from control and DMD fibroblasts in basal conditions, after TGF-β1 treatment, and after miR-21 inhibition. (B) Collagen production in culture medium from control and DMD myoblasts in basal conditions, after TGF-β1 treatment, and after miR-29 mimicking (data from three duplicated experiments for three cell lines of each cell type). Soluble collagen in the supernatants was normalized to total protein content.

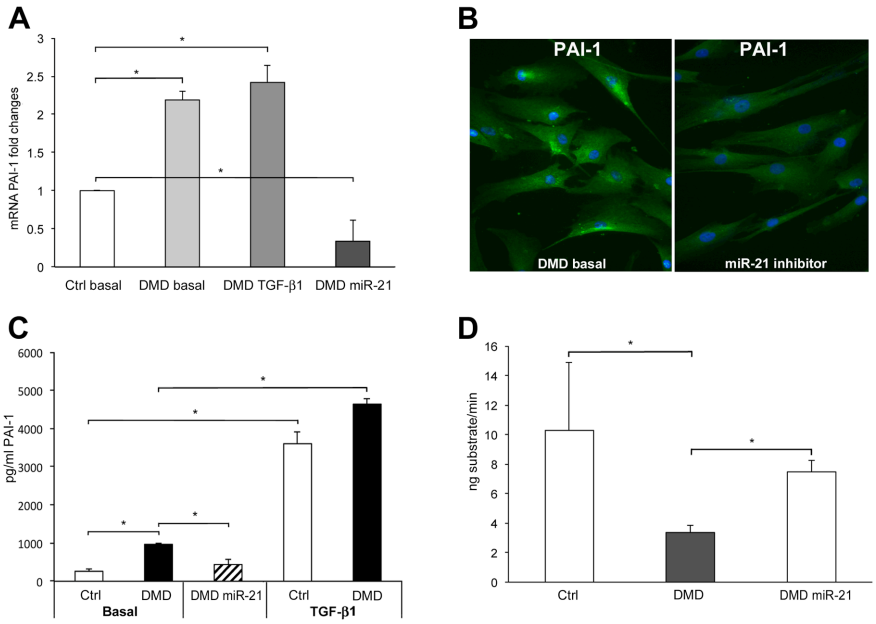

Fig. 7. PAI-1/plasmin are downregulated by miR-21 inhibition in DMD fibroblasts. (A) Expression levels of PAI-1 transcripts in DMD fibroblasts in basal conditions, after TGF-β1 treatment and after miR-21 inhibition. Fold changes are relative to PAI-1 levels (expressed as 1) in control fibroblasts, and are normalized to β-actin expression presented as means ± standard deviation (data from three duplicated experiments for three cell lines of each cell type). (B) PAI-1 protein (Alexa Fluor 488 dye, green) is evident as punctate positivity in the nucleus and cytoplasm of DMD fibroblasts in basal conditions. After miR-21 silencing positivity is reduced in both nucleus and cytoplasm. Nuclei stained with DAPI (blue). Scale bar = 20 μm. (C) PAI-1 protein levels determined by ELISA in medium from control and DMD fibroblasts in basal conditions and after TGF-β1 treatment (data from two duplicated experiments for three cell lines of each cell type), and after miR-21 inhibition (data from two duplicated experiments for three cell lines of each cell type). (D) Quantification of plasmin activity in supernatants from control and DMD fibroblasts in basal conditions and from DMD fibroblasts after miR-21 inhibition. (data from two duplicated experiments for three cell lines of each cell type).

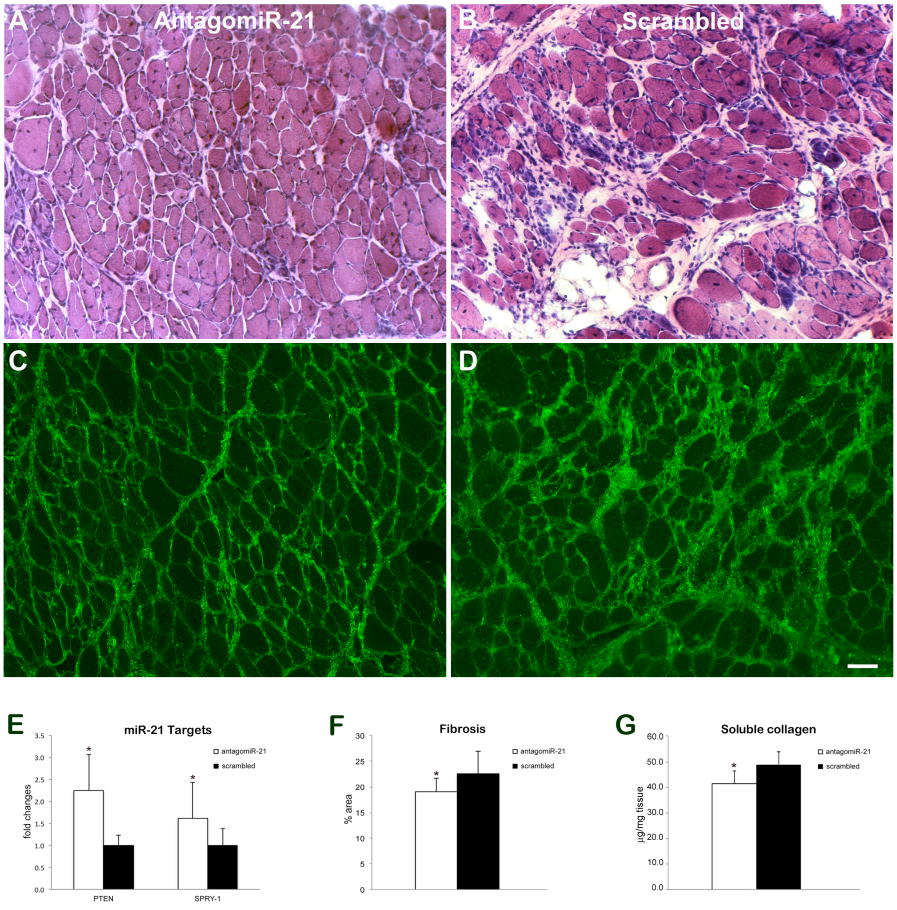

Fig. 8. AntagomiR-21 treatment reduces muscle fibrosis in *mdx* mouse diaphragm. H&E stained sections of diaphragm from an antagomiR-21-treated (A) and a scramble-treated (B) mouse, showing that histopathologic features are less severe in the former. Immunostaining of collagen I and VI on sections of diaphragm from an antagomiR-21-treated (C) and a scramble-treated mouse (D) showing decreased fibrosis in the former. Scale bar= 50 µm. (E) Transcript quantitation of miR-21 targets PTEN and SPRY-1, (F) quantitation of fibrosis and (G) soluble collagen determination in antagomiR-21 and scramble-treated mice. Levels of PTEN and SPRY-1 are significantly greater, and fibrosis is significantly reduced in antagomiR-21 treated diaphragm.

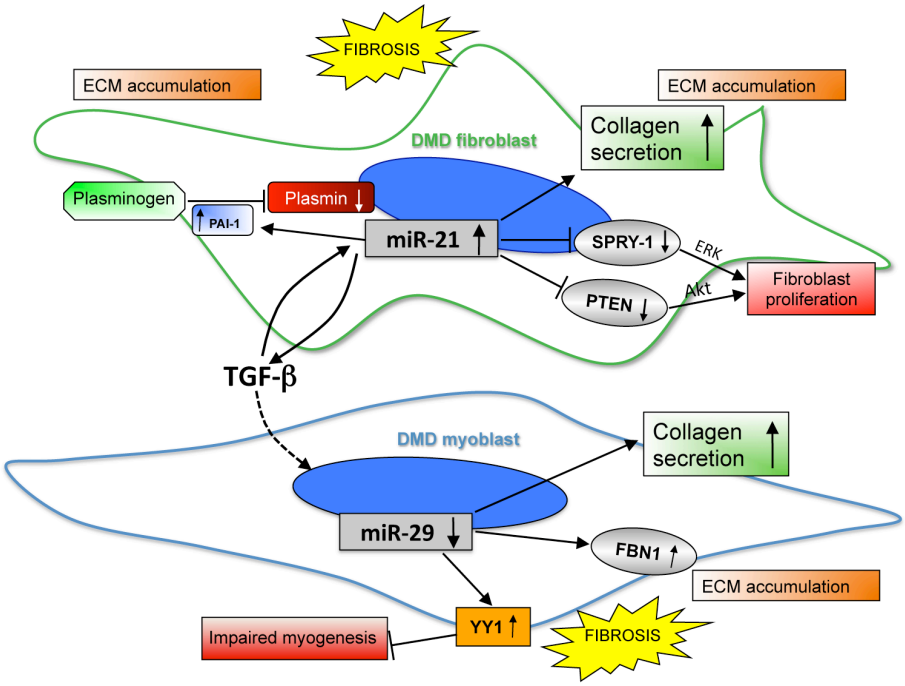

Fig. 9. Scheme summarizing our findings on influences of miR-21 and miR-29 on fibrotic mechanisms in DMD fibroblasts and myoblasts. ↑: upregulation, ↓: downregulation, ⊥: inhibition.

REFERENCES

[1] O. Adam, B. Löhfelm, T. Thum, S.K. Gupta, S.L. Puhl, H.J. Schäfers, et al., Role of miR-21 in the pathogenesis of atrial fibrosis, Basic Res. Cardiol. 107 (2012) 278.

[2] F. Aoki, I. Kojima, Therapeutic potential of follistatin to promote tissue regeneration and prevent tissue fibrosis, Endocr. J . 54 (2007) 849–854.

[3] E. Ardite, E. Perdiguero, B. Vidal, S. Gutarra, A.L. Serrano, P. Muñoz-Cánoves, PAI-1-regulated miR-21 defines a novel age-associated fibrogenic pathway in muscular dystrophy, J. Cell Biol. 196 (2012) 163–175.

[4] P. Bernasconi, E. Torchiana, P. Confalonieri, R. Brugnoni, R. Barresi, M. Mora, et al., Expression of transforming growth factor-beta 1 in dystrophic patient muscles correlates with fibrosis. Pathogenetic role of a fibrogenic cytokine, J. Clin. Invest. 96 (1995) 1137–1144.

[5] T. Bowen, R.H. Jenkins, D.J. Fraser, MicroRNAs, transforming growth factor beta-1, and tissue fibrosis, J. Pathol. 229 (2013) 274–285.

[6] H. Brønnum, D.C. Andersen, M. Schneider, M.B. Sandberg, T. Eskildsen, S.B. Nielsen, et al., MiR-21 promotes fibrogenic epithelial-to-mesenchymal transition of epicardial mesothelial cells involving Programmed Cell Death 4 and Sprouty-1, PLoS One 8 (2013) e56280.

[7] A.M. Bujor, J. Pannu, S. Bu, E.A. Smith, R.C. Muise-Helmericks, M. Trojanowska, Akt blockade downregulates collagen and upregulates MMP1 in human dermal fibroblasts, J. Invest. Dermatol. 128 (2008) 1906–1914.

[8] N. Cordani, V. Pisa, L. Pozzi, C. Sciorati, E. Clementi, Nitric oxide controls fat deposition in dystrophic skeletal muscle by regulating fibro-adipogenic precursor differentiation, Stem Cells 32 (2014) 874–885.

[9] L. Cushing, P.P. Kuang, J. Qian, F. Shao, J.Wu, F. Little, et al.,

MiR-29 is a major regulator of genes associated with pulmonary fibrosis, Am. J. Respir. Cell Mol. Biol. 45 (2011) 287–294.

[10] A.Desmoulière, A. Geinoz, F.Gabbiani, G. Gabbiani, Transforming growth factor-beta 1 induces alpha-smooth muscle actin expression in granulation tissue myofibroblasts and in quiescent and growing cultured fibroblasts, J. Cell Biol. 122 (1993) 103–111.

[11] C.M. Deveaud, E.J.Macarak, U. Kucich, D.H. Ewalt,W.R. Abrams, P.S. Howard, Molecular analysis of collagens in bladder fibrosis, J. Urol. 160 (1998) 1518–1527.

[12] F. Glowacki, G. Savary, V. Gnemmi, D. Buob, C. Van der Hauwaert, J.M. Lo-Guidice, et al., Increased circulating miR-21 levels are associated with kidney fibrosis, PLoS One 8 (2013) e58014.

[13] S. Gibertini, S. Zanotti, P. Savadori, M. Curcio, S. Saredi, F. Salerno, et al., Fibrosis and inflammation are greater in muscles of beta-sarcoglycan-null mouse than *mdx* mouse, Cell Tissue Res. 356 (2014) 427–443.

[14] C.E. Grueter, E. van Rooij, B.A. Johnson, S.M. DeLeon, L.B. Sutherland, et al., A cardiac microRNA governs systemic energy homeostasis by regulation of MED13, Cell 149 (2012) 671–683.

[15] J.N. Haslett, D. Sanoudou, A.T. Kho, R.R. Bennett, S.A. Greenberg, I.S. Kohane, et al., Gene expression comparison of biopsies from Duchenne muscular dystrophy (DMD) and normal skeletal muscle, Proc. Natl. Acad. Sci. U. S. A. 99 (2002) 15000–15005.

[16] Y. He, C. Huang, X. Lin, J. Li,MicroR-29 family, a crucial therapeutic target for fibrosis diseases, Biochimie 95 (2013) 1355–1359.

[17] Z. He, Y. Deng, W. Li, Y. Chen, S. Xing, X. Zhao, et al., Overexpression of PTEN suppresses lipopolysaccharide-induced lung fibroblast proliferation, differentiation and collagen secretion through inhibition of the PI3-K-Akt-GSK3 beta pathway, Cell Biosci. 4 (2014) 2.

[18] E.K. Henricson, R.T. Abresch, A. Cnaan, F. Hu, T.Duong, A. Arrieta, et al., The cooperative international neuromuscular research group Duchenne natural history study: glucocorticoid treatment preserves clinically meaningful functional milestones and reduces rate of disease progression as measured by manual muscle testing and other commonly used clinical trial outcome measures, Muscle Nerve 48 (2013) 55–67.

[19] D. Hubmacher, S.S. Apte, The biology of the extracellular matrix: novel insights. Curr Opin Rheumatol 2013; 25: 65–70.

[20] A.E. Kossakowska, D.R. Edwards, S.S. Lee, L.S. Urbanski, A.L. Stabbler, C.L. Zhang, et al., Altered balance between matrixmetalloproteinases and their inhibitors in experimental biliary fibrosis, Am. J. Pathol. 153 (1998) 1895–1902.

[21] A.J. Kriegel, Y. Liu, Y. Fang, X. Ding,M. Liang, ThemiR-29 family: genomics, cell biology, and relevance to renal and cardiovascular injury, Physiol. Genomics 44 (2012) 237–244.

[22] Y.Y. Li, C.F. McTiernan, A.M. Feldman, Interplay of matrix metalloproteinases, tissue inhibitors of metalloproteinases and their regulators in cardiac matrix remodeling, Cardiovasc. Res. 46 (2000) 214–224.

[23] G. Liu, A. Friggeri, Y. Yang, J. Milosevic, Q. Ding, V.J. Thannickal, et al., MiR-21 mediates fibrogenic activation of pulmonary fibroblasts and lung fibrosis, J. Exp.Med. 207 (2010) 1589–1597.

[24] Y. Lu,N. Azad, L.Wang, A.K. Iyer, V. Castranova, B.H. Jiang, et al., Phosphatidylinositol-3-kinase/akt regulates bleomycin-induced fibroblast proliferation and collagen production, Am. J. Respir. Cell Mol. Biol. 42 (2010) 432–441.

[25] L. Maegdefessel, J. Azuma, R. Toh, A. Deng, D.R. Merk, A. Raiesdana, et al., MicroRNA- 21 blocks abdominal aortic aneurysm development and nicotine-augmented expansion, Sci. Transl. Med. 4 (2012) 122ra22.

[26] C.J. Mann, E. Perdiguero, Y. Kharraz, S. Aguilar, P. Pessina, A.L. Serrano, et al., Aberrant repair and fibrosis development in

skeletal muscle, Skelet. Muscle 1 (2011) 21.

[27] P.P. Medina, M. Nolde, F.J. Slack, OncomiR addiction in an in vivo model of microRNA-21-induced pre-B-cell lymphoma, Nature 467 (2010) 86–90.

[28] F. Meng, R. Henson, H. Wehbe-Janek, K. Ghoshal, S.T. Jacob, T. Patel, MicroRNA-21 regulates expression of the PTEN tumor suppressor gene in human hepatocellular cancer, Gastroenterology 133 (2007) 647–658.

[29] L. Micallef, N. Vedrenne, F. Billet, B. Coulomb, I.A. Darby, A. Desmoulière, The myofibroblast, multiple origins for major roles in normal and pathological tissue repair, Fibrogenesis Tissue Repair (Suppl. 1) (2012) S5.

[30] R.L. Montgomery, G. Yu, P.A. Latimer, C. Stack, K. Robinson, C.M. Dalby, et al., MicroRNA mimicry blocks pulmonary fibrosis, EMBO Mol. Med. 6 (2014) 1347–1356.

[31] R.S. Nho, H. Xia, D. Diebold, J. Kahm, J. Kleidon, E. White, et al., PTEN regulates fibroblast elimination during collagen matrix contraction, J. Biol. Chem. 281 (2006) 33291–33301.

[32] A. Noetel, M. Kwiecinski, N. Elfimova, J. Huang, M. Odenthal, MicroRNA are central players in anti- and profibrotic gene regulation during liver fibrosis, Front. Physiol. 3 (2012) 49, http://dx.doi.org/10.3389/fphys.2012.00049.

[33] S.K. Parapuram, X. Shi-wen, C. Elliott, I.D. Welch, H. Jones, M. Baron, et al., Loss of PTEN expression by dermal fibroblasts causes skin fibrosis, J. Invest. Dermatol. 131 (2011) 1996–2003.

[34] V. Patel, L. Noureddine, MicroRNAs and fibrosis, Curr. Opin. Nephrol. Hypertens. 21 (2012) 410–416.

[35] N. Pencheva, H. Tran, C. Buss, D. Huh, M. Drobnjak, K. Busam, S.F. Tavazoie, Convergent multi-miRNA targeting of ApoE drives LRP1/LRP8-dependent melanoma metastasis and angiogenesis, Cell 151 (2012) 1068–1082.

[36] M.W. Pfaffl, A new mathematical model for relative quantification in real-time RTPCR, Nucleic Acids Res. 29 (2001) e45.

[37] C. Roderburg, G.W. Urban, K. Bettermann, M. Vucur, H. Zimmermann, S. Schmidt, et al., Micro-RNA profiling reveals a role for miR-29 in human and murine liver fibrosis, Hepatology 53 (2011) 209–218.

[38] S. Roy, S. Khanna, S.R. Hussain, S. Biswas, A. Azad, C. Rink, et al., MicroRNA expression in response to murine myocardial infarction: miR-21 regulates fibroblast metalloprotease-2 via phosphatase and tensin homologue, Cardiovasc. Res. 82 (2009) 21–29.

[39] H.W. Schnaper, J.B. Kopp, A.C. Poncelet, S.C. Hubchak, W.G. Stetler-Stevenson, P.E. Klotman, et al., Increased expression of extracellular matrix proteins and decreased expression of matrix proteases after serial passage of glomerular mesangial cells, J. Cell Sci. 109 (1996) 2521–2528.

[40] M. Selman, T.E. King, A. Pardo, Idiopathic pulmonary fibrosis: prevailing and evolving hypotheses about its pathogenesis and implications for therapy, Ann. Intern. Med. 134 (2001) 136–151.

[41] H.R. Stephens, V.C. Duance, M.J. Dunn, A.J. Bailey, V. Dubowitz, Collagen types in neuromuscular diseases, J. Neurol. Sci. 53 (1982) 45–62.

[42] M.C. Tamby, Y. Chanseaud, L. Guillevin, L. Mouthon, New insights into the pathogenesis of systemic sclerosis, Autoimmun. Rev. 2 (2003) 152–157.

[43] T. Thum, C. Gross, J. Fiedler, T. Fischer, S. Kissler, M. Bussen, et al., MicroRNA-21 contributes to myocardial disease by stimulating MAP kinase signalling in fibroblasts, Nature 456 (2008) 980–984.

[44] E. Van Rooij, L.B. Sutherland, J.E. Thatcher, J.M. DiMaio, R.H. Naseem, W.S. Marshall, et al., Dysregulation of microRNAs after myocardial infarction reveals a role of miR-29 in cardiac fibrosis, Proc. Natl. Acad. Sci. U. S. A. 105 (2008) 13027–13032.

[45] J. Varga, B. Pasche, Transforming growth factor beta as a therapeutic target in systemic sclerosis, Nat. Rev. Rheumatol. 5 (2009) 200–206.

[46] H.Wang, R. Garzon, H. Sun, K.J. Ladner, R. Singh, J. Dahlman, et al., NF-kappaB-YY1-miR-29 regulatory circuitry in skeletal myogenesis and rhabdomyosarcoma, Cancer Cell 14 (2008) 369–381.

[47] L. Wang, L. Zhou, P. Jiang, L. Lu, X. Chen, H. Lan, et al., Loss of miR-29 in myoblasts contributes to dystrophic muscle pathogenesis, Mol. Ther. 20 (2012) 1222–1233.

[48] T.Wang, Y. Feng, H. Sun, L. Zhang, L. Hao, C. Shi, et al., MiR-21 regulates skin wound healing by targeting multiple aspects of the healing process, Am. J. Pathol. 181 (2012) 1911–1920.

[49] X.H. Wang, Z. Hu, J.D. Klein, L. Zhang, F. Fang, W.E. Mitch, Decreased miR-29 suppresses myogenesis in CKD, J. Am. Soc. Nephrol. 22 (2011) 2068–2076.

[50] J. Wei, L. Feng, Z. Li, G. Xu, X. Fan, MicroRNA-21 activates hepatic stellate cells via PTEN/Akt signaling, Biomed. Pharmacother. 67 (2013) 387–392.

[51] K.M. Yamada, M. Araki, Tumor suppressor PTEN: modulator of cell signaling, growth, migration and apoptosis, J. Cell Sci. 114 (2001) 2375–2382.

[52] X. Yang, J. Wang, S.L. Guo, K.J. Fan, J. Li, Y.L. Wang, et al., MiR-21 promotes keratinocyte migration and re-epithelialization during wound healing, Int. J. Biol. Sci. 7 (2011) 685–690.

[53] Q. Yao, S. Cao, C. Li, A. Mengesha, B. Kong, M. Wei, Micro-RNA-21 regulates TGF-β-induced myofibroblast differentiation by targeting PDCD4 in tumor–stroma interaction, Int. J. Cancer 128 (2011) 1783–1792.

[54] S. Zanotti, S. Gibertini, C. Bragato, R. Mantegazza, L. Morandi, M. Mora, Fibroblasts from the muscles of Duchenne muscular dystrophy patients are resistant to cell detachment apoptosis, Exp. Cell Res. 317 (2011) 2536–2547.

[55] S. Zanotti, S. Gibertini, M. Mora, Altered production of extra-cellular matrix components by muscle-derived Duchenne muscular dystrophy fibroblasts before and after TGF-beta 1 treatment, Cell Tissue Res. 339 (2010) 397–410.

[56] S. Zanotti, S. Gibertini, P. Savadori, R. Mantegazza, M. Mora, Duchennemuscular dystrophy fibroblast nodules: a cell-based assay for screening anti-fibrotic agents, Cell Tissue Res. 352 (2013) 659–670.

[57] S. Zanotti, T. Negri, C. Cappelletti, P. Bernasconi, E. Canioni, C. Di Blasi, et al., Decorin and biglycan expression is differentially altered in several muscular dystrophies, Brain 128 (2005) 2546–2555.

[58] S. Zanotti, S. Saredi, A. Ruggieri, M. Fabbri, F. Blasevich, S. Romaggi, et al., Altered extracellular matrix transcript expression and protein modulation in primary Duchenne muscular dystrophy myotubes, Matrix Biol. 26 (2007) 615–624.

[59] L. Zhou, L. Wang, L. Lu, P. Jiang, H. Sun, H.Wang, Inhibition of miR-29 by TGF-beta-Smad3 signaling through dual mechanisms promotes transdifferentiation of mouse myoblasts into myofibroblasts, PLoS One 7 (2012) e33766.

[60] J. Zhu, Y. Li,W. Shen, C. Qiao, F. Ambrosio, M. Lavasani, et al., Relationships between transforming growth factor-beta1, myostatin, and decorin: implications for skeletal muscle fibrosis, J. Biol. Chem. 282 (2007) 25852–25863.

[61] S. Zanotti, S. Gibertini, C. Di Blasi, C. Cappelletti, P. Bernasconi, R. Mantegazza, et al., Osteopontin is highly expressed in severely dystrophic muscle and seems to play a role in muscle regeneration and fibrosis, Histopathology 59 (2011) 1215–1228.

Chapter 4:

Summary, Conclusion and Future perspectives

In skeletal and cardiac muscle a large protein complex called dystrophin-glycoprotein complex (DGC) forms a structural link between the extracellular matrix and the cytoskeleton. (1, 2)

Protection of the sarcolemma from repetitive stress occurring during muscle contraction depends primarily on the stability of this complex.

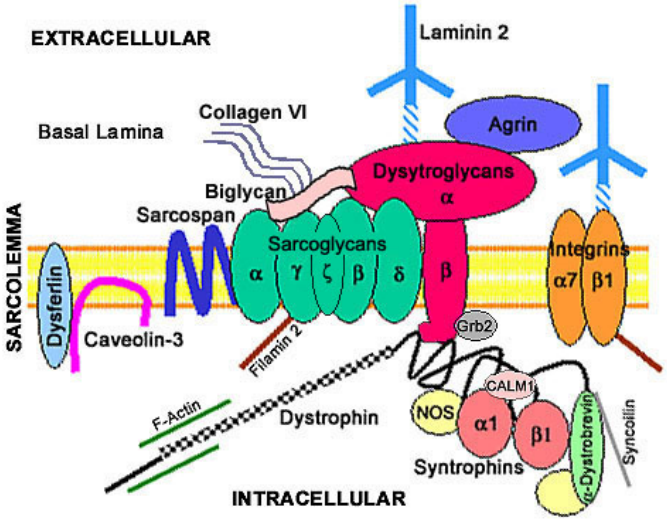

Fig.1 Dystrophin-glycoprotein complex

Dystrophin is the protein defective in Duchenne muscular dystrophy (DMD). (3)

Some of the dystrophin-associated proteins are integral membrane proteins (2) such as sarcoglycans, a group of single pass transmembrane proteins that form a stable tetrameric complex.

The link between β-dystroglycan, α-dystroglycan and dystrophin is strengthened by sarcoglycan complex.

Indeed mutations in the genes encoding for sarcoglycan proteins cause the loss of the entire sarcoglycan complex. These mutations result in forms of limb-girdle muscular dystrophy (LGMD) in humans and mice. (4)

A marked reduction of the DGC occurs in DMD patients and in other dystrophies (1, 5), where the disruption of the link between the actin-based subsarcolemmal cytoskeleton and the extracellular matrix (6) induces dystrophic muscle fibers to be more susceptible to necrosis.

The link's integrity is a fundamental requirement for sarcolemma stability. Its loss leads to an impairment of muscle fibers' resistance to mechanical contraction.

Physiological muscle regeneration can be divided in three sequential but overlapping stages:

1) the inflammatory response, in which neutrophils migrating to the injury site promote inflammation by releasing cytokines that can attract and activate additional inflammatory cells. Macrophages invade damaged muscle fibers and phagocytize debris. Then an increase in a M2 subpopulation of macrophages induces muscle regeneration (7, 8)

2) the activation, differentiation, and fusion of satellite cells;

3) newly formed myofibers mature and restore tissue architecture.

The new fibers are discernible thanks to a small caliber and central myonucleous. (9)

In muscular dystrophies, where DGC is lost, the continuous fibers rupture cannot be fully compensated by satellite cell proliferation because muscle tissue has only limited recovery potential.

Inflammatory repeated processes following muscular necrosis lead to fibrotic remodelling and finally to adipocite replacement.

In the muscular dystrophies the proliferation of connective tissue is considered to be a secondary phenomenon but the increase of in collagenous connective tissue could be a significant co-determining factor.

Fibrosis is the most consistent pathological change suffered by muscle tissue and it could be considered as a central element in the dystrophic process, leading to a loss of tissue organisation. Fibrosis can impair function and cause chronic diseases also in a large numbers of organs and tissues.

The abnormal activation of fibroblasts and excessive accumulation of collagens and other extracellular matrix (ECM) components characterize the interstitial fibrosis. (10)

Chemotaxis and mechanical stimuli initiate the production of fibrous tissue, in which fibroblast and myofibroblasts are

the main players and most abundant type of cells. Myofibroblasts derive principally from activation of fibroblasts (process termed transactivation) through various stimulators. One of them is the transforming growth factor-β1 (TGF-β1) which, beside being able to transactivate fibroblasts, it is also able to regulate expression of other mediators. (11)

Normally fibroblasts and myofibroblasts are present only during the time of tissue repair but in muscular dystrophies (and in the other fibrotic chronic pathologies) they are persistently recruited and activated due to constant myofibre breakdown.

The aberrant production of ECM proteins by myofibroblasts during muscle fiber necrosis also inhibits the normal regeneration process. The principal collagens involved in fibrotic process are collagen I, III and VI. (12, 13, 14) Natural and engineered mouse models of many muscular dystrophies are available. (15)

The *mdx* mouse, lacking dystrophin, is the most used model for Duchenne muscular dystrophy (DMD).

Mdx has mild clinical features in limb muscles and shows significant regeneration with little fibrosis compared to human patients. (16)

Instead the diaphragm muscle exhibits progressive damage with connective tissue proliferation and significant increase in TGF-β1 expression.

Because of the mild phenotype of *mdx* model to study in depth thefibrotic process we have chosen the *Sgcb-null* mouse.

In this model the β-sarcoglycan gene is knocked down leading to a disruption of the sarcoglycan and dystroglycan complexes in skeletal, cardiac, and smooth muscle with severe muscular dystrophy, cardiomyopathy, and vascular abnormalities. (17)

The first part of this thesis is aimed at characterizing the progression of muscle fibrosis in this model and comparing it to age-matched *mdx* mice.

Collagens I and VI are major components of connective tissue in DMD and CMD. (13, 18, 19)

Moreover collagen III is critical for collagen I fibrillogenesis (20) and decorin regulates collagen fibril formation and organisation by interacting with collagens I and VI via different binding sites. (21, 22)

Decorin also orchestrates multiple signalling pathways, is a crucial regulator of the inflammatory response and it is a natural inhibitor of TGF-β1, as it binds the cytokine with high affinity preventing its interaction with pro-fibrotic receptors. (23)

To describe the progression of ECM component deposition and of the events which intervene in the fibrotic process we have performed histological and immunofluorescence studies on *Sgcb-null* and *mdx* quadriceps and diaphragm muscles at different age.

Both *Sgcb-null* mouse's diaphragm and quadriceps display early (already at 4 weeks) signs of muscle damage, such as degenerating and regenerating fibres (present at all ages, but diminishing with increasing age) and extensive increase in centronucleated fibres between 2 and 8 weeks. Connective tissue proliferation is generally greater in *Sgcb-null* mice than in *mdx* and is mainly evident in quadriceps.

The amount of all analyzed collagens (Collagen type I, III and VI) remains stable with age in the *mdx* mouse, while in the Sgcb-null mouse it increases steadily throughout life.

We also find significantly increased decorin protein levels in both *Sgcb-null* quadriceps and diaphragm being significantly higher in *Sgcb-null* quadriceps than in *mdx*.

Collagen transcript trends are similar to those of the corresponding proteins and decorin transcripts are variably expressed in quadriceps and diaphragm, with low levels generally present during major muscle remodelling (8-26 weeks).

This trend is in accordance with the reduced levels of decorin mRNA that we found in a previous study in DMD and MDC1A. (24)

As mentioned before, TGF-β1 is a key player in the physiopathology of tissue repair, and we assess that TGF-β1 transcript is variably increased in the *Sgcb-null* mouse, in accordance with the findings of Andreetta et al. (2006) who found an increase in TGF-β1 transcript in diaphragm at 24 weeks, followed by a decrease. (25)

Quantitation of TGF-β1 immunoblot bands shows great variability and in general no significant differences between the two models.

Moreover we perform a macrophages count, whose role in fibrosis is depending on their subtype. (7, 8)

In regions of mild inflammation of quadriceps we find a significantly higher levels of macrophages in *Sgcb-null* mice than in similar regions of *mdx* quadriceps. However, further studies are required to identify macrophage subtypes.

Another important player in the fibrotic process is osteopontin, a pleiotropic extracellular protein that intervenes in physiological process such as regulation of immune functions (26), vascular remodelling, wound repair and developmental processes (27), and in pathological

conditions such as tissue injury, infection, autoimmune disease, tumour growth (28) and fibrosis modulating immune cell subsets and intramuscular TGF-β. (29)

We observe an increase in osteopontin transcript levels in highly inflamed micro-dissected areas in the *Sgcb-null* mouse quadriceps at 12 weeks, compared to the *mdx*.

In the first part of this thesis the major interesting observation is that *Sgcb-null* mouse develops severe and progressive fibrosis of limb muscles at an early stage, and that fibrosis is greater than in the *mdx* model.
A possible explanation of this significant difference could be the fact that in *mdx* there is a sub-physiological sarcoglycan expression (30) that could be a protective element from mechanical-induced injury. Conversely in *Sgcb-null* mouse, the sarcoglycan complexes are completely disrupted (17) and therefore such protection is lacking.
Moreover another explanation of this difference could be the abnormally leaky vascular walls present in *Sgcb-null* mice (17) but not in *mdx*. The leaky walls may worsen fibrosis by allowing increased numbers of circulating macrophages to reach the muscle.

Early involvement of quadriceps in *Sgcb-null* model renders it more suitable for investigating the fibrotic process and for testing anti-fibrotic drugs.
The growing comprehension of molecular dynamics underlying inflammation, myofibroblast proliferation, tissue contracture and fibrosis will help in the development of future antifibrotic therapy approaches.

The second goal of this thesis was to test an anti-fibrotic molecule that has shown effective activity in *in vitro* experiments.
We performed a pilot study in a small group of *mdx* mice.
Although we have established that Sgcb-null model is more representative of human condition, in this pilot study for practical needs we have decided to use *mdx* mice because more readily available.

We focus on investigating the role of microRNAs (miRNAs) in TGFβ-dependent fibrosis formation.
MiRNAs are short, non-coding RNA nucleotides that play a major role in post-transcriptional regulation of gene expression. They can inhibit the translation of their target genes by various and redundant mechanisms, such as directly binding to the target mRNAs by either perfect or imperfect base-pairing that leads to mRNA degradation and/or translational repression. (31)

Recent findings have revealed the involvement of miRNAs in the regulation of numerous biological and pathological processes.

MiR-21, in particular, is highly upregulated during tissue injury and contributes to tissue fibrosis in heart (32), kidney (33) and liver. (34)

MiR-21 expression could be enhanced by TGF-β with a mechanism that involves the formation of a microprocessor complex containing Smad proteins. (34)

Ardite and co-worker have demonstrated that dysregulation in miR-21 results in PTEN-AKT-dependent fibroblast proliferation, altered collagen metabolism and disease aggravation. (35)

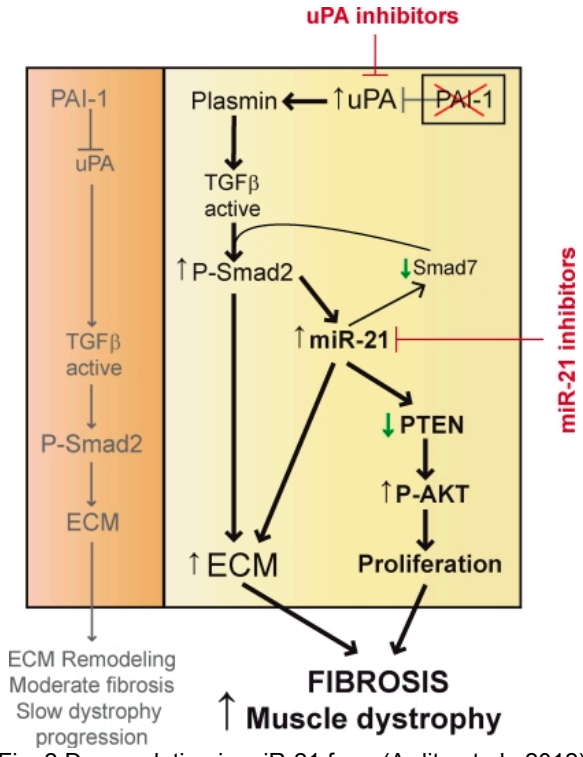

Fig. 2 Dysregulation in miR-21 from (Ardite et al., 2012)

In cultered miRNA-transfected myocardial cells Xu and co-workers have demonstrated that the overexpression of miR-21 was associated with a decrease in SPRY1 protein expression and an increase of the MAPK protein expression. The 3'UTR of SPRY1 mRNA contains a predicted miRNA-binding site for miRNA-21, thus SPRY1 is a direct target of miRNA-21.

PTEN and SPRY-1 have been predicted to be miR-21 targets also with the TargetScan or microRNA database.

SPRY can regulate the expression of the collagen genes and regulates cell growth, differentiation, transformation,

proliferation, cell survival and apoptosis. (36)

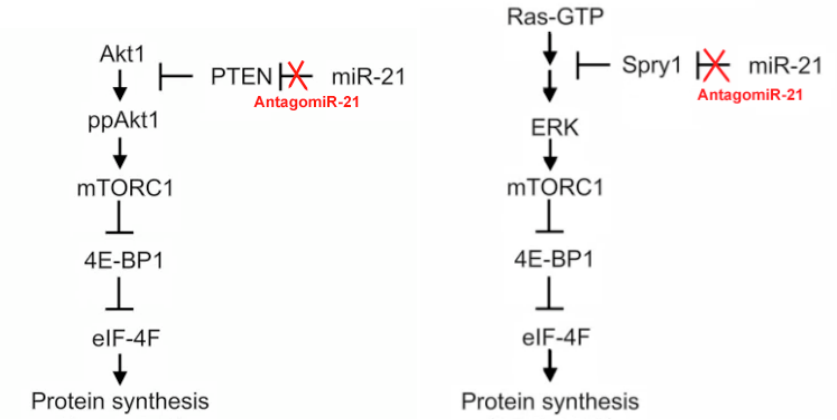

Fig. 3 antagomiR-21's mechanism of actions

In DMD muscle and DMD-derived fibroblast we found an increase of miR-21, moreover in DMD fibroblasts we observed a reduction of SPRY-1 and PTEN expression (transcript and protein) with consequent Akt and ERK pathways activation.

In DMD fibroblasts we performed an analysis of the expression levels of miR-21 targets after transfecting the cells with miR-21 inhibitor.

MiR-21 silencing in DMD fibroblasts induced a significant increase of PTEN and SPRY-1 expression (transcript and protein) as well as a decrease of COL1A1 and COL6A1 transcripts. MiR-21 inhibition also decreased collagen I protein level. Our miR-21-silencing *in vitro* experiments in DMD fibroblasts suggested a miR-21 involvement in DMD fibrosis.

To confirm the involvement of miR-21 in the fibrosis process we inhibited his expression in a small group of *mdx* mice.

In order to silence miR-21 we inject intraperitoneally antagomiR-21 or scrambled (as negative control) which are locked nucleic acid oligonucleotides.

Histological evaluation of diaphragm muscles showed that the morphology was better conserved in antagomiR-21-treated than in scramble-treated animals.

Furthermore we found significantly higher PTEN and SPRY-1 transcript levels and significantly lower collagen I and collagen VI protein levels in antagomiR-21-treated than scramble-treated diaphragms, thus demonstrating that antagomiR-21 treatment effectively reduced levels of target transcripts but also extent of fibrosis.

We observed these positive effects even with a short treatment at the lowest dose reported to be effective in the literature. (37, 38)

The therapeutic use of synthetic oligonucleotides to inhibit or enhance the expression of a specific miRNA is a promising approach for many diseases.

In particular, antagonize miRNAs with antagomiR is an ideal therapeutic strategy, since these inhibitors are single strand oligonucleotide which are complementary to a mature miRNA, easily administered, with a long duration of

action (up to 6 weeks in mice), well tolerated, and with the potencial to modulate miRNAs activity in most organs. (39)

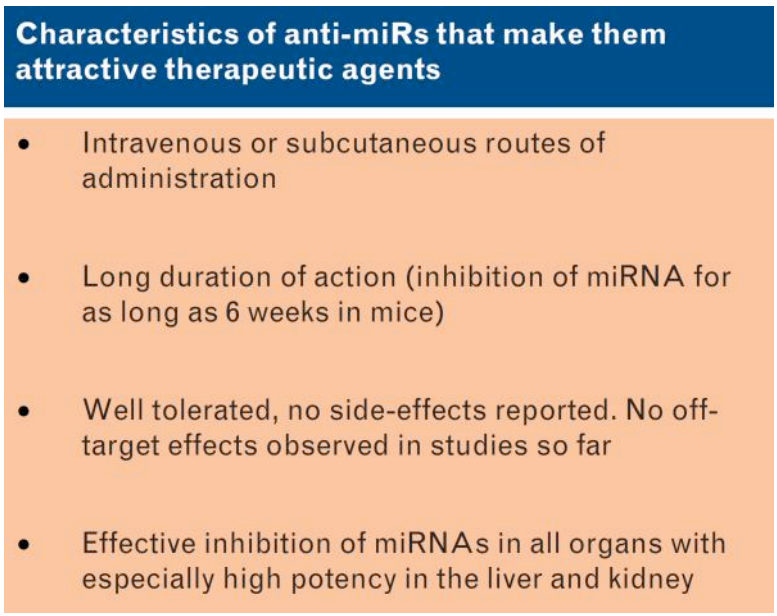

Fig.4 anti-miR characteristic

Conversely, miRNA-mimics are duplex oligonucleotides with an identical sequence to that one of a mature miRNA. Duplex oligonucleotides are more difficult to administer because they have to be integrated in the DNA to elicit they activity.

The miR-29 family is a group of three miRNAs with similar sequences, expression patterns and functions which comprises miR-29a, miR-29b and miR-29c. MiR-29s are encoded by two gene clusters. (40)

Recent studies showed that the miR-29 family participates in the development of liver fibrosis, renal fibrosis, pulmonary fibrosis, cardiac fibrosis. (41, 42)

Concerning its value as therapeutic agent, a recent paper from Montgomery et al. (43) reported an *in vivo* treatment with a modified, more stable, miR-29 mimics. In this study these researchers injected mir-29 mimic in an induced-model of pulmonary fibrosis. The treatment was able to increase miRNA's level for several days without observable side effects and indicate miR-29 to be a potent therapeutic miRNA as treatment for pulmonary fibrosis.

Wang and co-workers have found a downregulation of miR-29 in *mdx* muscles while its overexpression lead to an inhibition of collagens' expression, implying that collagens are target of miR-29. (44)

We found in DMD muscles and DMD-derived myoblasts lower levels of miR-29a and miR-29c than in control muscles and a significant inverse correlation between miR-29a level and COL1A1 and COL6A1 transcript levels. Moreover DMD myoblasts trasfected with miR-29a and miR-29c mimics showed a downregulation of miR-29 targets (transcript and protein levels) suggesting that miR-29 upregulation could be an interesting strategy to reduce the production of ECM components by myoblasts in advanced stages of the disease.

At the moment there is no definitive cure for muscular dystrophies. Most clinical trials, employing different therapeutic strategies to correct the primary cause, are

under study.

These strategies involved cell therapy (myoblast transplantation and stem cell therapy), gene replacement therapy, utrophin upregulation and mutation-specific approaches (exon skipping and suppression of premature termination codons).

The major limitation to the cell therapy is the incapacity of myoblasts vehiculated through intravenous or intraperitoneal injections to replace dystrophic muscle (45), this compels the use of intramuscular injection leading to a fusion of myoblasts mainly around the site of injection, thus resulting only in a little zone of muscle growth and recovery. (46, 47)

Moreover local injection makes treatment of diaphragm (hardly accessible muscle) virtually impossible.

The strategy of direct gene replacement is limited by the large size (14 kb) of the dystrophin gene.

To overcome this size issue, delivery of mini- and microdystrophin genes have been attempted. Pichavant and co-workers demonstrated an effective delivery of minidystrophin genes with adeno-associated virus (AAV) in mice and dogs. (48) Unfortunately intramuscular injections of AAV2 into DMD patients did not restore dystrophin expression because of immunological system. (49)

Another approach was the delivery of the utrophin's gene (a dystrophin-related protein ubiquitously expressed).
Overexpression of utrophin transgene in the *mdx* mouse has been shown to prevent the dystrophic phenotype (50) even though Li and co-workers have demonstrated that utrophin overexpression failed to protect *mdx* muscle from exercise-associated injury because its inability to anchor nNOS to the sarcolemma. (51)

The suppression of premature termination codons can be achieved with high concentrations of aminoglycoside antibiotics (such as Gentamicin). This treatment could lead to reduce the efficiency of translation termination by a mechanism that alters this ribosomal proofreading process. (52)
A trial in DMD patients showed that gentamicin could significantly increase dystrophin expression in skeletal muscle and decrease levels of creatine kinase, however one of the patients developed an immune response to the newly expressed dystrophin protein. (53)
Moreover treatment with gentamicin leads to a lack of potency and possible toxic effects (54) suggesting that the use of different compounds to elicit the same activity, but without side effects, such as PTC124 must be investigated.

A promising approach is the exon skipping methodology based on sterical block or alteration of mRNA structure.
The rational of this procedure is that the controlled alteration of the slicing events could induce a functional dystrophin (even though with altered structure) in skeletal muscle.
A treatment in cells and in *mdx* mice with this approach showed an improvement of the disease phenotype. (55)

Until a strong efficient strategy to contrast the primary cause will not be discover, the main goal still remains to reduce the secondary effect of lacking dystrophin or other DGC components.

First of all, the reduction of fibrosis, by improving the functionality of muscle, including those involved in cardio-respiratory task, will have a strong effect on patients' quality of life.
Moreover, increasing our knowledge on the mechanisms that lead to fibrosis is a fundamental step in the research for novel therapeutic targets.
Furthermore the fibrosis reduction could enhance the gene delivery approach thanks to the improvement of its diffusion in the muscle tissue.

Our future purpose is to investigate the role of the different subtypes of macrophages in the disease process, to

understand their specific role in the fibrosis. This might help finding a way to increase the subtype-induced repair mechanism.

Additionally, we would like to repeat our pilot treatment with antagomiR-21 in *Sgcb-null* mice and perform a miR-29 mimic strategy alone or in combination with miR-21 inhibition.

Beside this, we are performing on *Sgcb-null* and *mdx* mice a treatment with spironolactone, a selective antagonist of aldosterone.
We are doing this treatment both in early and late stages of the disease since our aim is to be able to have a rescue of the fibrotic phenotype even in those patients already showing the muscle impairment.

REFERENCES:

1. Ervasti JM, Ohlendieck K, Kahl SD, Gaver MG, Campbell KP - Deficiency of a glycoprotein component of the dystrophin complex in dystrophic muscle - Nature - 1990

2. Ervasti JM, Campbell KP - Membrane organization of the dystrophin-glycoprotein complex - Cell. 1991

3. Hoffman EP, Brown RH Jr, Kunkel LM - Dystrophin: the protein product of the Duchenne muscular dystrophy locus - Cell - 1987

4. Ozawa E, Mizuno Y, Hagiwara Y, Sasaoka T, Yoshida M - Molecular and cell biology of the sarcoglycan complex - Muscle Nerve - 2005

5. Ozawa E, Noguchi S, Mizuno Y, Hagiwara Y, Yoshida M - From dystrophinopathy to sarcoglycanopathy: evolution of a concept of muscular dystrophy - Muscle Nerve - 1998

6. Ervasti JM, Campbell KP - A role for the dystrophin-glycoprotein complex as a transmembrane linker between laminin and actin - J Cell Biol - 1993

7. Villalta SA, Nguyen HX, Deng B, Gotoh T, Tidball JG - Shifts in macrophage phenotypes and macrophage competition for arginine metabolism affect the severity of muscle pathology in muscular dystrophy - Hum Mol Genet - 2009

8. Mann CJ, Perdiguero E, Kharraz Y, Aguilar S, Pessina P, Serrano AL, Muñoz-Cánoves P - Aberrant repair and fibrosis development in skeletal muscle - Skelet Muscle - 2011

9. Dubowitz V - Muscle biopsy--technical and diagnostic aspects - Ann Clin Res - 1974

10. Nakatsuji S, Yamate J, Sakuma S - Macrophages, myofibroblasts, and extracellular matrix accumulation in

interstitial fibrosis of chronic progressive nephropathy in aged rats - Vet Pathol - 1998

11. Henry G, Garner WL - Inflammatory mediators in wound healing - Surg Clin North Am - 2003

12. Stephens HR, Duance VC, Dunn MJ, Bailey AJ, Dubowitz V - Collagen types in neuromuscular diseases - J Neurol Sci - 1982

13. Hantaï D, Labat-Robert J, Grimaud JA, Fardeau M - Fibronectin, laminin, type I, III and IV collagens in Duchenne's muscular dystrophy, congenital muscular dystrophies and congenital myopathies: an immunocytochemical study - Connect Tissue Res - 1985

14. Goldspink G, Fernandes K, Williams PE, Wells DJ - Age-related changes in collagen gene expression in the muscles of *mdx* dystrophic and normal mice - Neuromuscul Disord - 1994

15. Durbeej M, Campbell KP - Muscular dystrophies involving the dystrophin-glycoprotein complex: an overview of current mouse models - Curr Opin Genet Dev - 2002

16. Dangain J, Vrbova G - Muscle development in *mdx* mutant mice - Muscle Nerve - 1984

17. Durbeej M, Cohn RD, Hrstka RF, Moore SA, Allamand V, Davidson BL, Williamson RA, Campbell KP - Disruption of the beta-sarcoglycan gene reveals pathogenetic complexity of limb-girdle muscular dystrophy type 2E - Mol Cell - 2000

18. Zanotti S, Saredi S, Ruggieri A, Fabbri M, Blasevich F, Romaggi S, Morandi L, Mora M - Altered extracellular matrix transcript expression and protein modulation in primary Duchenne muscular dystrophy myotubes - Matrix Biol. 2007

19. Zanotti S, Gibertini S, Di Blasi C, Cappelletti C, Bernasconi P, Mantegazza R, Morandi L, Mora M - Osteopontin is highly expressed in severely dystrophic muscle and seems to play a

role in muscle regeneration and fibrosis - Histopathology - 2011

20. Liu X, Wu H, Byrne M, Krane S, Jaenisch R - Type III collagen is crucial for collagen I fibrillogenesis and for normal cardiovascular development - Proc Natl Acad Sci USA - 1997

21. Nareyeck G, Seidler DG, Troyer D, Rauterberg J, Kresse H, Schönherr E - Differential interactions of decorin and decorin mutants with type I and type VI collagens - Eur J Biochem. 2004

22. Reed CC, Iozzo RV - The role of decorin in collagen fibrillogenesis and skin homeostasis - Glycoconj J. 2002

23. Baghy K, Iozzo RV, Kovalszky I - Decorin-TGFβ axis in hepatic fibrosis and cirrhosis - J Histochem Cytochem - 2012

24. Zanotti S, Negri T, Cappelletti C, Bernasconi P, Canioni E, Di Blasi C, Pegoraro E, Angelini C, Ciscato P, Prelle A, Mantegazza R, Morandi L, Mora M - Decorin and biglycan expression is differentially altered in several muscular dystrophies - Brain. 2005

25. Andreetta F, Bernasconi P, Baggi F, Ferro P, Oliva L, Arnoldi E, Cornelio F, Mantegazza R, Confalonieri P - Immunomodulation of TGF-beta 1 in *mdx* mouse inhibits connective tissue proliferation in diaphragm but increases inflammatory response: implications for antifibrotic therapy - J Neuroimmunol. 2006

26. Lund SA, Giachelli CM, Scatena M - The role of osteopontin in inflammatory processes - J Cell Commun Signal - 2009

27. Denhardt DT, Noda M, O'Regan AW, Pavlin D, Berman JS - Osteopontin as a means to cope with environmental insults: regulation of inflammation, tissue remodeling, and cell survival - J Clin Invest - 2001

28. Anborgh PH, Mutrie JC, Tuck AB, Chambers AF - Role of the metastasis-promoting protein osteopontin in the tumour

microenvironment - J Cell Mol Med - 2010

29. Vetrone SA, Montecino-Rodriguez E, Kudryashova E, Kramerova I, Hoffman EP, Liu SD, Miceli MC, Spencer MJ - Osteopontin promotes fibrosis in dystrophic mouse muscle by modulating immune cell subsets and intramuscular TGF-beta - J Clin Invest - 2009

30. Li D, Long C, Yue Y, Duan D - Sub-physiological sarcoglycan expression contributes to compensatory muscle protection in *mdx* mice - Hum Mol Genet. 2009

31. Bartel DP - MicroRNAs: genomics, biogenesis, mechanism, and function - Cell - 2004

32. Brønnum H, Andersen DC, Schneider M, Sandberg MB, Eskildsen T, Nielsen SB, Kalluri R, Sheikh SP - miR-21 promotes fibrogenic epithelial-to-mesenchymal transition of epicardial mesothelial cells involving Programmed Cell Death 4 and Sprouty-1 - PLoS One - 2013

33. Glowacki F, Savary G, Gnemmi V, Buob D, Van der Hauwaert C, Lo-Guidice JM, Bouyé S, Hazzan M, Pottier N, Perrais M, Aubert S, Cauffiez C - Increased circulating miR-21 levels are associated with kidney fibrosis - PLoS One - 2013

34. Noetel A, Kwiecinski M, Elfimova N, Huang J, Odenthal M - microRNA are Central Players in Anti- and Profibrotic Gene Regulation during Liver Fibrosis - Front Physiol - 2012

35. Ardite E, Perdiguero E, Vidal B, Gutarra S, Serrano AL, Muñoz-Cánoves P - PAI-1-regulated miR-21 defines a novel age-associated fibrogenic pathway in muscular dystrophy - J Cell Biol - 2012

36. Xu HF, Ding YJ, Zhang Z1, Wang ZF, Luo CL, Li BX, Shen YW, Tao LY, Zhao ZQ - MicroRNA-21 regulation of the progression of viral myocarditis to dilated cardiomyopathy - Mol Med Rep - 2014

37. Grueter CE, van Rooij E, Johnson BA, DeLeon SM, Sutherland LB, Qi X, Gautron L, Elmquist JK, Bassel-Duby R, Olson EN - A cardiac microRNA governs systemic energy homeostasis by regulation of MED13 - Cell - 2012

38. Maegdefessel L, Azuma J, Toh R, Deng A, Merk DR, Raiesdana A, Leeper NJ, Raaz U, Schoelmerich AM, McConnell MV, Dalman RL, Spin JM, Tsao PS - MicroRNA-21 blocks abdominal aortic aneurysm development and nicotine-augmented expansion - Sci Transl Med - 2012

39. Patel V, Noureddine L - MicroRNAs and fibrosis - Curr Opin Nephrol Hypertens - 2012

40. Kriegel AJ, Liu Y, Fang Y, Ding X, Liang M - The miR-29 family: genomics, cell biology, and relevance to renal and cardiovascular injury - Physiol Genomics - 2012

41. Cushing L, Kuang PP, Qian J, Shao F, Wu J, Little F, Thannickal VJ, Cardoso WV, Lü J - miR-29 is a major regulator of genes associated with pulmonary fibrosis - Am J Respir Cell Mol Biol - 2011

42. He Y, Huang C, Lin X, Li J - MicroRNA-29 family, a crucial therapeutic target for fibrosis diseases - Biochimie - 2013

43. Montgomery RL, Yu G, Latimer PA, Stack C, Robinson K, Dalby CM, Kaminski N, van Rooij E - MicroRNA mimicry blocks pulmonary fibrosis - EMBO Mol Med - 2014

44. Wang L, Zhou L, Jiang P, Lu L, Chen X, Lan H, Guttridge DC, Sun H, Wang H - Loss of miR-29 in myoblasts contributes to dystrophic muscle pathogenesis - Mol Ther - 2012

45. Partridge TA - Invited review: myoblast transfer: a possible therapy for inherited myopathies? - Muscle Nerve - 1991

46. El Fahime E, Torrente Y, Caron NJ, Bresolin MD, Tremblay JP -

In vivo migration of transplanted myoblasts requires matrix metalloproteinase activity - Exp Cell Res - 2000

47. El Fahime E, Mills P, Lafreniere JF, Torrente Y, Tremblay JP - The urokinase plasminogen activator: an interesting way to improve myoblast migration following their transplantation - Exp Cell Res - 2002

48. Pichavant C, Chapdelaine P, Cerri DG, Dominique JC, Quenneville SP, Skuk D, Kornegay JN, Bizario JC, Xiao X, Tremblay JP - Expression of dog microdystrophin in mouse and dog muscles by gene therapy - Mol Ther - 2010

49. Mendell JR, Campbell K, Rodino-Klapac L, Sahenk Z, Shilling C, Lewis S, Bowles D, Gray S, Li C, Galloway G, Malik V, Coley B, Clark KR, Li J, Xiao X, Samulski J, McPhee SW, Samulski RJ, Walker CM - Dystrophin immunity in Duchenne's muscular dystrophy - N Engl J Med - 2010

50. Tinsley JM, Potter AC, Phelps SR, Fisher R, Trickett JI, Davies KE - Amelioration of the dystrophic phenotype of *mdx* mice using a truncated utrophin transgene - Nature - 1996

51. Li D, Bareja A, Judge L, Yue Y, Lai Y, Fairclough R, Davies KE, Chamberlain JS, Duan D - Sarcolemmal nNOS anchoring reveals a qualitative difference between dystrophin and utrophin - J Cell Sci - 2010

52. Manuvakhova M, Keeling K, Bedwell DM - Aminoglycoside antibiotics mediate context-dependent suppression of termination codons in a mammalian translation system - RNA - 2000

53. Malik V, Rodino-Klapac LR, Viollet L, Wall C, King W, Al-Dahhak R, Lewis S, Shilling CJ, Kota J, Serrano-Munuera C, Hayes J, Mahan JD, Campbell KJ, Banwell B, Dasouki M, Watts V, Sivakumar K, Bien-Willner R, Flanigan KM, Sahenk Z, Barohn RJ, Walker CM, Mendell JR - Gentamicin-induced readthrough of stop codons in Duchenne muscular dystrophy -

Ann Neurol - 2010

54. Welch EM, Barton ER, Zhuo J, Tomizawa Y, Friesen WJ, Trifillis P, Paushkin S, Patel M, Trotta CR, Hwang S, Wilde RG, Karp G, Takasugi J, Chen G, Jones S, Ren H, Moon YC, Corson D, Turpoff AA, Campbell JA, Conn MM, Khan A, Almstead NG, Hedrick J, Mollin A, Risher N, Weetall M, Yeh S, Branstrom AA, Colacino JM, Babiak J, Ju WD, Hirawat S, Northcutt VJ, Miller LL, Spatrick P, He F, Kawana M, Feng H, Jacobson A, Peltz SW, Sweeney HL - PTC124 targets genetic disorders caused by nonsense mutations - Nature - 2007

55. Alter J, Lou F, Rabinowitz A, Yin H, Rosenfeld J, Wilton SD, Partridge TA, Lu QL - Systemic delivery of morpholino oligonucleotide restores dystrophin expression bodywide and improves dystrophic pathology - Nat Med - 2006